Comprehensive Summaries of Uppsala Dissertations
from the Faculty of Science and Technology 934

Optical Efficiency of Low-Concentrating Solar Energy Systems with Parabolic Reflectors

BY

MARIA BROGREN

ACTA UNIVERSITATIS UPSALIENSIS
UPPSALA 2004

Dissertation presented at Uppsala University to be publicly examined in Polhemsalen, Ångströmlaboratoriet, Uppsala, Friday, February 27, 2004 at 09:30 for the degree of Doctor of Philosophy. The examination will be conducted in English.

Abstract

Brogren, M. 2004. Optical Efficiency of Low-Concentrating Solar Energy Systems with Parabolic Reflectors. Acta Universitatis Upsaliensis. *Comprehensive Summaries of Uppsala Dissertations from the Faculty of Science and Technology* 934. 160 pp. Uppsala. ISBN 91-554-5867-X

Solar electricity is a promising energy technology for the future, and by using reflectors for concentrating solar radiation onto photovoltaic cells, the cost per produced kWh can be significantly reduced. The optical efficiency of a concentrating system determines the fraction of the incident energy that is transferred to the cells and depends on the optical properties of the system components. In this thesis, low-concentrating photovoltaic and photovoltaic-thermal systems with two-dimensional parabolic reflectors were studied and optimised, and a new biaxial model for the incidence angle dependence of the optical efficiency was proposed.

Concentration of light generally results in high cell temperatures, and the uneven irradiance distribution on cells with parabolic reflectors leads to high local currents and temperatures, which reduce fill-factor and voltage. Cooling the cells by means of water increases the voltage and makes it possible to utilize the thermal energy. The performance of a 4X concentrating photovoltaic-thermal system was evaluated. If operated at 50°C, this system would produce 250 $kWh_{electrical}$ and 800 $kWh_{thermal}$ per m^2 cell area and year. Optical performance can be increased by 20% by using better reflectors and anti-reflectance glazing.

Low-concentrating photovoltaic systems for façade-integration were studied and optimised for maximum annual electricity production. The optimisation was based on measured short-circuit currents versus solar altitude. Measurements were performed outdoors and in a solar simulator. It was found that the use of 3X parabolic reflectors increases the annual electricity production by more than 40%. High solar reflectance is crucial to system performance but by using a low-angle scattering reflector, the fill-factor and power are increased due to a more even irradiance on the modules.

Long-term system performance depends on the durability of the components. The optical properties and degradation of reflector materials were assessed using spectrophotometry, angular resolved scatterometry, Fresnel modelling, optical microscopy, and surface profilometry before and after ageing. The degradation of reflectors was found to be strongly dependent on material composition and environmental conditions. Back surface mirrors, all-metal reflectors, and polymer-metal laminates degraded in different ways, and therefore accelerated ageing must be tailored for testing of different types of reflector materials. However, new types of reflector laminates showed a potential for increasing the cost-effectiveness of low-concentrating solar energy systems.

Keywords: Photovoltaic cells, Photovoltaic-thermal systems, Parabolic reflectors, Optical properties, Reflector materials, Optical efficiency, Accelerated ageing, Outdoor ageing, Building-integrated photovoltaics

Maria Brogren, Department of Engineering Sciences, Box 534, Uppsala University, SE-751 21 Uppsala, Sweden

ISSN 1104-232X
ISBN 91-554-5867-X
urn:nbn:se:uu:diva-3988 (http://urn.kb.se/resolve?urn=urn:nbn:se:uu:diva-3988)

To Anders

This thesis is based on work conducted within the interdisciplinary graduate school Energy Systems. The national Energy Systems Programme aims at creating competence in solving complex energy problems by combining technical and social sciences. The research programme analyses processes for the conversion, transmission and utilisation of energy, combined together in order to fulfil specific needs.

The research groups that participate in the Energy Systems Programme are the Division of Solid State Physics at Uppsala University, the Division of Energy Systems at Linköping Institute of Technology, the Department of Technology and Social Change at Linköping University, the Department of Heat and Power Technology at Chalmers Institute of Technology in Göteborg as well as the Division of Energy Processes and the Department of Industrial Information and Control Systems at the Royal Institute of Technology in Stockholm.

www.liu.se/energi

Preface

Most of the work presented in this thesis was carried out between July 1999 and January 2004 at the division of Solid State Physics at Uppsala University under the leadership of Prof. Claes-Göran Granqvist and under the auspices of the Energy Systems Program, which is financed by the Swedish Foundation for Strategic Research, the Swedish Energy Agency, and Swedish industry. It is in Uppsala that I have performed the major part of my research on the optical efficiency of solar concentrators and I would like to express my gratitude to my superb supervisor Prof. Arne Roos for sharing his expertise in solar energy materials and optical measurements with me, and for not complaining about the number of pages of this thesis. I also wish to acknowledge my former supervisor Dr. Ewa Wäckelgård.

Experiments on photovoltaic and photovoltaic-thermal systems were performed at Vattenfall Utveckling AB in Älvkarleby, who also supplied experimental backup and ideas for the appended papers. Other experiments were conducted at the Division of Energy and Building Design at Lund Institute of Technology. At these institutions, I mainly worked with my co-supervisor Prof. Björn Karlsson and I would like to acknowledge him for fruitful collaboration.

During my time as a graduate student, I have worked with solar energy systems on three different system levels:

1. *Optical characterisation and evaluation of materials* for use in photovoltaic and photovoltaic-thermal systems. This included spectral measurements on reflectors, solar cells and glazings in order to determine their optical properties, as well as modelling the optical properties and characterising the surfaces of reflector materials using various methods. Furthermore, reflector samples were aged in a climatic test chamber or outdoors and the degradation of their optical properties was studied.

2. *Analysis of technical systems*. Results from the optical measurements were used in calculations of the optical efficiency of solar energy systems and the calculations were compared with outdoor measurements of the performance of prototype systems. In these analyses, photovoltaic cells with

reflectors, glazings and, in some cases, active cooling by means of water, were studied as a system and the electricity and heat production were assessed. Ray-tracing and solar simulator measurements of the optical efficiency of systems with differently shaped reflectors of various materials were also performed.

3. *Socio-technical systems analysis*. In interdisciplinary work, which is not presented in this thesis, photovoltaic systems were studied as building components and as a means of coming closer to ecologically sustainable living. An investigation of the level of knowledge and acceptance among users and other actors (inhabitants, installers, building companies, architects, utility companies, etc.) was performed and an analysis of economical, aesthetic, environmental, and electricity production aspects was made. A socio-technical systems approach was used since the system in which solar energy technologies are to be embedded must be seen to be, not only technical, but also socio-technical and socio-cultural [1]. The objectives of the study were to predict the results of implementing photovoltaics in a residential area in Stockholm and to assess the obstacles for building-integration of photovoltaic systems. The study is reported elsewhere [i–iii].

The research presented in this summary and in the appended papers is part of my examination in Engineering Sciences with specialisation in Solid State Physics. My work at the division of Solid State Physics has included studies on the first two system levels discussed above. It has focused on reflector materials, concentrating optics, and cooling for increasing the electrical output from solar cells.

I have also had the privilege of participating in the research school of the national, interdisciplinary Energy Systems Programme. Some of the work that was performed within the framework of the Energy Systems Programme does not straightforwardly fit in under the rather narrow title of this thesis but, nevertheless, it has provided me with knowledge that I have found very valuable in my work on the thesis. This work included studies of the deregulation of the Swedish electricity system [v], studies of photovoltaic systems as socio-technical systems [i–iv], as well as building-integration aspects of photovoltaic systems [i, ii, ix, x]. I would like to acknowledge my Energy Systems colleagues for scientific input, inspiration, and friendship. I would especially like to mention Anna Green. Other sources of inspiration during the course of this work have been Prof. Dean Abrahamson, Dr. Björn Sandén, Prof. Christian Azar, and Dr. Tomas Kåberger. My former supervisor Prof. Lars Ingelstam is acknowledged for comments on my papers and for interesting discussions.

Part of the OptiCAD modelling that is presented in Paper IV was carried out at the Fraunhofer-Institut für Solare Energiesysteme in Freiburg. Christopher Bühler and his colleagues at Fraunhofer-ISE are acknowledged for assistance with OptiCAD and for making my stay in Freiburg pleasant as well as rewarding.

Elforsk AB, Liljewalch's foundation, and J. Gust. Richert's foundation are acknowledged for financial support that made it possible for me to present my work at several photovoltaics conferences. Part of the work was carried out in association with the Swedish Energy Agency's solar heating programme (FUD) and the International Energy Agency's Solar Heating and Cooling Proramme's Task 27.

I would like to acknowledge Dr. Per Nostell (co-author of Paper I), Peter Krohn, Håkan Håkansson (Paper IV), Jacob Jonsson, Jonas Malmström, and Dr. Peter Hansson for valuable assistance. Dr. Mats Rönnelid is acknowledged for providing solar energy expertise and for commenting on my licentiate thesis. Helena Gajbert is acknowledged for co-authoring Paper V and for help with MINSUN calculations. Anna Helgesson is acknowledged for co-authoring Papers VI and VIII. Anna Werner is acknowledged for co-authoring Paper VII and for rides between Uppsala and Stockholm. I also enjoyed working with Johan Wennerberg (co-author of Paper III), who was great company in South Korea. In addition, I would like to thank the present and former members of the Solid State Physics group for creating a friendly atmosphere.

I would like to acknowledge professors Arne Roos, Björn Karlsson, Claes-Göran Granqvist, Lars Ingelstam, and Carl-Gustaf Ribbing, as well as colleagues within the Energy Systems Programme who have read and commented on earlier versions of this summary. However, the responsibility for any errors in this thesis is solely mine.

Finally, I wish to thank my family for always being there whenever I need them and for making my life richer. I love you all. I dedicate this thesis to Anders, who is the most intense yet softest sunshine of my life.

Stockholm, January 2004,

Maria Brogren

Contents

List of Papers

This summary is an introduction to, and is partly based on, the following appended papers, which are referred to in the text by their Roman numerals:

I M. Brogren, P. Nostell, and B. Karlsson, *Optical efficiency of a PV-thermal hybrid CPC module for high latitudes*, Solar Energy, 69 suppl. (1–6) 2000, p. 173–185.

II B. Karlsson, M. Brogren, S. Larsson, L. Svensson, B. Hellström, and Y. Safir, *A large bifacial photovoltaic-thermal low-concentrating module*, Proceedings of the 17th European Photovoltaic Solar Energy Conference and Exhibition, Munich, Germany, 22–26 October, 2001.

III M. Brogren, J. Wennerberg, R. Kapper, and B. Karlsson, *Design of concentrating elements with CIS thin-film solar cells for facade integration*, Solar Energy Materials and Solar Cells, 75 (3–4) 2003, p. 567–575.

IV M. Brogren, B. Karlsson, and H. Håkansson, *Design and modelling of low-concentrating photovoltaic solar energy systems and investigation of irradiation distribution on modules in such systems*, Proceedings of the 17th European Photovoltaic Solar Energy Conference and Exhibition, Munich, Germany, 22–26 October, 2001.

V H. Gajbert, M. Brogren, and B. Karlsson, *Optimisation of reflector and module geometries for static, low-concentrating facade-integrated photovoltaic systems*. Submitted to Solar Energy.

VI M. Brogren, A. Helgesson, A. Roos, J. Nilsson, and B. Karlsson, *Biaxial model for the incidence angle dependence of the optical efficiency of photovoltaic and solar thermal systems with asymmetric reflectors*. In manuscript.

VII M. Brogren, B. Karlsson, A. Roos, and A. Werner, *Analysis of the effects of outdoor and accelerated ageing on the optical properties of reflector materials for solar energy applications*. Submitted to Solar Energy Materials and Solar Cells.

VIII M. Brogren, A. Helgesson, B. Karlsson, J. Nilsson, and A. Roos, *Optical properties, durability, and system aspects of a new aluminium-polymer-laminated steel reflector for solar concentrators*. Accepted for publication in Solar Energy Materials and Solar Cells.

IX M. Brogren, A. Roos, and B. Karlsson, *Reflector materials for two-dimensional low-concentrating photovoltaic systems – The effect of specular versus diffuse reflectance on module efficiency*. Submitted to Solar Energy.

Publications concerning socio-technical aspects of energy systems, building-integration of photovoltaic systems, concentrating solar energy systems, or optical properties of materials, which are not included in the thesis:

i M. Brogren and A. Green, *Hammarby Sjöstad – an interdisciplinary case study of the integration of photovoltaics in a new ecologically sustainable residential area in Stockholm*, Solar Energy Materials and Solar Cells, 75 (3–4) 2003, p. 761–765.

ii M. Brogren and A. Green, *Solel i bostadshus – vägen till ett ekologiskt hållbart boende?,* Program Energisystem, Arbetsnotat Nr 17, ISSN 1403-8307, 2001 (in Swedish).

iii A. Green and M. Brogren, *Svårt att nå uthålligt boende i Hammarby Sjöstad*, PLAN Tidskrift för samhällsplanering, Nr. 3, 2002 (in Swedish).

iv B. Andersson, M. Brogren, and T. Kåberger, *El och värme från solen*, IVA, Energimyndigheten, 2003 (in Swedish).

v M. Brogren and D. Sundgren, *Avreglering och omstrukturering av det svenska elsystemet*, in Program Energisystem, Arbetsnotat Nr 15. Ed. M. Söderström, ISSN 1403-8307, 2001 (in Swedish).

vi M. Brogren, *Low-Concentrating Photovoltaic Systems with Parabolic reflectors*, Licentiate thesis from Uppsala University, ISSN 038887, UPTEC 01 006 Lic, 2001.

vii M. Brogren, M. Rönnelid, and B. Karlsson, *PV-Thermal Hybrid Low Concentrating CPC Module*, Proceedings of the 16th European Photovoltaic Solar Energy Conference and Exhibition, Glasgow, United Kingdom, 1–5 May, 2000.

viii M. Brogren and B. Karlsson, *Low-Concentrating Water-Cooled PV-Thermal Hybrid Systems for High Latitudes*, 29th IEEE PVSC, New Orleans, USA, 20–24 May, 2002.

ix M. Brogren, B. Karlsson, A. Werner, and A. Roos, *Design and evaluation of low-concentrating, stationary, parabolic concentrators for wall-integration of water-cooled photovoltaic-thermal hybrid modules at high latitudes*, Proceedings of PV for Europe, Rome, Italy, 22–25 October, 2002.

x H. Gajbert, M. Brogren, and B. Karlsson, *Optimisation of reflector and module geometries for stationary, low-concentrating facade-integrated photovoltaic systems*. Proceedings of Eurosun 2003, Göteborg, Sweden, 14–19 June, 2003.

xi M. Brogren, A. Helgesson, and B. Karlsson, *Incidence angle dependence of the performance of photovoltaic modules with east-west aligned reflectors: a computational model*, Proceedings of Eurosun 2003, Göteborg, Sweden, 14–19 June, 2003.

xii M. Brogren, G. Harding, R. Karmhag, G. A. Niklasson, C.-G. Ribbing, L. Stenmark, *$Ti_xAl_yN_z$ coatings for thermal control of spacecraft*, Proceedings of the EOS/SPIE Symposium on Optical Systems Design and Production, Berlin, Germany, 25–28 May, 1999.

xiii M. Brogren, G. Harding, R. Karmhag, C.-G. Ribbing, G. A. Niklasson, L. Stenmark, *Ti_xAl_y nitride coatings for temperature control of spacecraft*, Thin Solid Films, 370, 2000, p. 268–277.

1. Introduction

Solar cells generate electricity from sunlight. Considering that the "fuel" is free, the question may arise; Why are not solar cells more commonly used? The answer is simple. The cells are expensive. However, there are a number of remedies to that obstacle. This thesis deals with two of those remedies; concentration of solar radiation and electrical-thermal cogeneration.

The electrical current that is produced in a solar cell is, in principle, proportional to the solar radiation intensity on the surface of the cell. Solar concentrators are a means to increase the irradiance on the cell surface, and thus the electricity production. Hence, the overall motivation for research on concentrating systems is the potential for a reduced cost of solar electricity due to a smaller cell area needed for generation of a given amount of power.

When a solar cell is exposed to concentrated sunlight, its temperature is increased. A high cell temperature reduces the cell efficiency and the generated power is decreased. In this way, some of the benefit of concentrating the sunlight may be lost. The simple, straightforward remedy to this problem is to cool the solar cells. The cooling can be passive, by means of cooling fins, or active, by means of a cooling medium. If water is used as a coolant, the thermal energy can be utilised for heating.

1.1. Objectives of this work

The overall aim of the work presented in this thesis was to investigate the possibilities to increase the efficiency of solar energy systems, and thereby reducing the cost of the electricity or heat that is produced. Attention was also given to the long-term durability and robustness of the systems. The basic hypothesis was that the use of durable, low-cost reflectors for increasing the electrical output from solar cells can make solar electricity come closer to cost-competitiveness in two niche markets: building-integrated photovoltaics (BIPV) and small-scale combined heat and power systems. In order to facilitate rapid diffusion and widespread use of solar energy technologies, the systems should also be easy to install, operate and maintain. Cost-competitiveness and increasing demand of solar energy

technologies will increase production volumes, which will reduce costs, and thus a positive loop will be created.

In order to improve the performance of solar concentrators for increasing the production of electrical and thermal energy at a low extra cost, various low-concentrating photovoltaic and photovoltaic-thermal cogeneration systems with different geometries and different types of reflectors were evaluated with respect to their optical and energy conversion efficiency.

To assure good performance and long technical lifetime of a concentrating system, the solar reflectance of the reflectors must be high and long-term stable. Therefore, different types of reflector materials were analysed in this work, and the optical properties and degradation of the reflecting surfaces were assessed.

During the work, focus has shifted from evaluation of the performance of concentrating solar cogeneration systems to analysis of the optical properties of reflector materials. The shift of focus is motivated by the need to assess long-term system performance and possibilities of optimising the optical efficiency or reducing costs by using new types of reflector materials. The overall aim has, however, remained the same: To contribute to the improvement of solar energy technology.

1.2. Outline of this thesis

This introductory chapter presents the objectives of the work that has been performed. It also gives the outline of this thesis and a very brief summary of the contents of the nine appended papers. **Chapter 2** puts the work on concentrating photovoltaic systems and reflector materials in a broader perspective. The need to get the global energy system onto a more sustainable track is discussed. An introduction to photovoltaics, its history and applications, as well as the cost of solar electricity, is also provided in this chapter.

The properties of electromagnetic radiation are summarized in **Chapter 3**. The aim is to provide the reader with a theoretical background that facilitates the understanding of the performance of the solar energy materials and the concentrating photovoltaic systems that are studied in this thesis.

Chapter 4 discusses the available solar resource and **Chapter 5** describes three technologies for solar energy conversion, focusing on solar cells and photovoltaic-thermal cogeneration systems and only briefly describing some

properties of solar thermal collectors. Concentrating optics, especially parabolic reflectors, are discussed in **Chapter 6**.

Chapter 7 describes the methods, measurement techniques, and instruments that were used in this work. Some of the concentrating systems were studied using the ray-tracing program OptiCAD. The program MINSUN was used for calculating the annual electricity production of various concentrating systems. These programs, as well as general aspects of modelling and simulation as a tool for the analysis of concentrating systems, are discussed. Optical modelling of thin films, which was used to study the reflectance of reflector materials, is also briefly described in this chapter.

Results of optical measurements on system components are presented in **Chapter 8**. Some results of the evaluations of different prototypes of concentrating photovoltaic and photovoltaic-thermal systems are presented in **Chapter 9**. Analysis of the optical efficiency of different concentrating systems and results of ray-tracing are presented in **Chapter 10**, which also describes a new model for assessing the incidence angle dependence of concentrators, which was developed and validated during the course of this work. A few suggestions for improvement of the optical and electrical performance of concentrating photovoltaic systems are made in Chapters 8–10.

In **Chapter 11**, the specific conditions for photovoltaic modules in parabolic concentrators are elaborated, i.e. high, non-uniform illumination and high temperatures. The advantages of diffuse versus specular solar reflectors for low-concentrating systems are pointed out, as well as the difficulties of interpreting the results from accelerated ageing tests. The future potential for photovoltaic-thermal and building-integrated photovoltaic systems is discussed and a concept for a solar building is proposed.

Some concluding remarks are made in **Chapter 12**, as well as a few suggestions on further work that could be undertaken in this and related fields in order to improve performance and facilitate a broader market penetration of low-concentrating photovoltaic systems.

Chapter 13 is a short summary in Swedish, which gives an overview of the background, objectives, and main conclusions of the thesis.

1.3. Content of the appended papers

In **Paper I,** the optical efficiency, as well as the annual electrical and thermal output, of a water-cooled photovoltaic-thermal cogeneration system with non-tracking 4X concentrating compound parabolic concentrators was investigated. It was found that the cells in the concentrating system generate 2.5 times as much electricity as cells without concentrators and a significant amount of heat that can be utilised. **Paper II** describes the design and performance of a bifacial combined photovoltaic module and thermal absorber for use in concentrating photovoltaic-thermal systems.

An increasingly common way of reducing the cost of photovoltaic electricity and the ground area needed for the installations is to use photovoltaic modules as combined building material and electricity generators. Integration of photovoltaic systems in vertical facades is particularly appropriate at high latitudes, due to the low solar height. Therefore, low-concentrating photovoltaic modules for wall-integration, which include thin film or crystalline silicon modules, parabolic over edge reflectors of aluminium, and thermal insulation, were evaluated and their geometry was optimised. This work was reported in **Papers III, IV, and V**.

In order to facilitate evaluation and optimisation of the optical efficiency of concentrating systems with cylindrical geometries, a new biaxial model for the incidence angle dependence of the optical efficiency of such systems was presented and validated in **Paper VI**.

The initial optical properties of various types of reflector materials and their degradation during outdoor and accelerated ageing were studied in **Paper VII**. In **Paper VIII**, the properties of a new laminated polymer-aluminium-steel reflector material were analysed. The possibility of exchanging standard specular anodised aluminium reflectors for less expensive laminated rolled aluminium, which has more favourable optical properties for use in low-concentration systems, was explored in **Paper IX**. The work reported in these papers included ageing tests, outdoor as well as in a climatic test chamber, measurements of optical properties, and evaluation of the effect of the choice of reflector material on electricity production when the material is used in a concentrating photovoltaic system.

2. Background

This chapter provides a broad background to the thesis and a motivation for the work that is presented. Global energy supply and use, the problems with today's energy system as well as the potential for solar energy to fulfil a major part of the future energy demand are discussed. The development of the market for photovoltaics is given special attention.

2.1. Global energy use and environmental problems

Industrialisation has meant a lot to mankind in terms of welfare, and so have the centralised production of heat and electricity that is associated with industrialisation. Energy is usually acknowledged to be a mainstay of an industrial society, and in the industrialised countries, unlimited supply of electricity, from two (or three) holes in the wall, is taken for granted. Today, most of the electricity is produced in steam cycles, which are utilizing fossil fuels. A lot of thermal energy, in the forms of domestic hot water, district heating and process steam, is also produced using fossil fuels. Currently, oil provides more than 35% of the global primary energy; coal and natural gas add 23% and 21%, respectively [2, 3]. Figure 1 shows the global use of primary energy sources in 1999. The total primary energy use amounted to approximately $1.1 \cdot 10^{15}$ Wh in 1999 and this figure is believed to increase to $1.8 \cdot 10^{15}$ Wh in 2030 [4, 5].

There are some severe problems with today's energy conversion technologies that have not been dealt with satisfactorily. A fundamental problem is that the sources that constitute the bulk of the primary energy supply are limited. On a local and regional scale, there are environmental problems at sites of extraction of primary energy sources, emissions of particles and toxic gases from conversion plants, and waste products that have to be disposed of or stored safely. Acidification is only one of the critical regional problems that follow from the combustion of fossil fuels.

On the global level, there is one problem that has drawn a lot of attention during the last decades. Global warming, due to a build-up in the atmosphere

of greenhouse gases that originate from combustion of fossil fuels, has been predicted by many scientists [6].

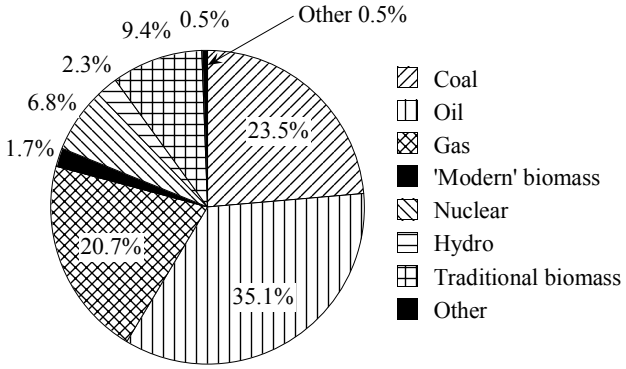

Figure 1: The global use of primary energy sources in 1999, by energy source [3].

The greenhouse gases are, for example, carbon dioxide (CO_2), methane, nitrous oxide, and halocarbons. These gases are essential to life on Earth, as they absorb infrared radiation emitted from Earth and radiate some of it back towards its surface. Without the greenhouse effect, the mean temperature on Earth would be -18°C instead of the actual +15°C. The greenhouse gases also help stabilising the climate. However, a small increase in the amount of greenhouse gases may result in an altered radiation balance.

According to the Intergovernmental Panel on Climate Change (IPCC)[1], 75% of the prime anthropogenic greenhouse gas, CO_2, is produced by the combustion of fossil fuels. The atmospheric concentration of CO_2 has risen from a stable 280 ppm level before mankind started to use fossil fuels around 1860 to the present level of 370 ppm [8]. Today, the industrialised countries emit roughly ten times more CO_2 per capita than the developing countries. If the atmospheric CO_2 concentration is to be stabilised at levels that are considered safe[2] and that are discussed in for example the Kyoto agreements, per capita CO_2 emissions should be reduced to levels below those prevailing in the developing countries. A major changeover of the global energy system is needed to achieve these reductions, and there is little doubt that the treat of

[1] The role of the IPCC is to assess the scientific, technical and socio-economic information relevant for the understanding of the risk of human-induced climate change. It bases its assessments mainly on published and peer reviewed scientific technical literature [7].
[2] 450 ppm (parts per million) is a level that is often cited as a “safe” maximum [9], but we do not know what is the right level, and decisions will have to be made under uncertainty and adjusted as scientific understanding develops.

global warming will be the most decisive force influencing the development of new and improved energy technologies [10].

2.1.1 Energy usage and energy-efficiency

Due to its high exergy content, electricity is the most versatile and useful form of energy. The United Nation's Development Programme's World Energy Assessment introduces the concept of the energy ladder [2]. At higher levels (or steps on the ladder) of societal development, when the basic energy needs in form of fuels for cooking, heating, and lighting are supplied, the demand for electricity for lighting and communication increases. In the industrialised countries, about two thirds of the generated electricity is used in residential and commercial buildings and about one third is used in industrial processes [11]. However, electricity is widely used for purposes which do not necessarily require electricity, such as domestic hot water and heating. Furthermore, electricity is increasingly used for air conditioning and as the demand of indoor climatic comfort follows the increasing incomes in countries like China, even more electricity will be used for air-conditioning. A part of this cooling-demand could be met by using solar-control windows, more efficient appliances, and better insulated buildings. The electricity that is used for heating could be reduced by similar measures, such as low-emittance coated windows, triple glazings, and better insulation. However, in order to meet the Kyoto agreements, in addition to increased energy-efficiency, the electricity and heat generated in power plants which utilise coal or other fossil fuels have to be replaced by electricity and heat from renewable energy sources.[3]

2.1.2 Renewable energy

The term renewable energy refers to energy sources based on the Sun (and the Earth and the Moon) and having a short time of renewability[4]. Renewable energy sources can be roughly divided into biomass, wind energy, hydropower (including conventional hydro, tidal, and wave power), geothermal energy, and solar energy [12, 13]. The use of non-fuel renewable energy (such as wind and hydro power and solar energy) and the combustion of renewable fuels (for example biomass) do not contribute to an increase of carbon dioxide in the atmosphere, as long as the biomass is replanted.

Since the oil crisis in the 1970s, considerable interest has been taken in the area of renewable energy. Differences between renewable and non-

[3] Or the CO_2 has to be captured and safely stored.
[4] The "short" time span is not well defined. In Sweden, it is often discussed if turf, which has a time of renewability of a couple of hundred years, is renewable or not.

renewable energy sources, except for their inherent difference regarding CO_2 emissions, are for example that renewable energy sources more often than non-renewable sources are locally available, and therefore they do not need transportation networks for the fuels as required for conventional energy sources. In addition, renewable energy sources are generally less pollutant than other forms of energy and less hazardous [12].

In 2000, 6% of all energy utilised in the fifteen European Union member countries came from renewable sources. Sweden had the highest share of renewables (31%), mainly due to the large fraction of hydro power in the electricity supply, while the United Kingdom had the lowest (1%) [13].

2.2. Introduction to photovoltaics

One of the options available for future CO_2-lean electricity supply is direct conversion of sunlight to electricity in photovoltaic solar cells. The principle function of a solar cell is rather simple: when a solar cell is illuminated, a current is produced. The physical mechanisms that govern the functioning of solar cells are described in section 5.2.

Even though photovoltaics and other solar energy technologies do not show impressive figures on the supply side of the global energy balance today, solar energy has an enormous potential. The annual amount of solar energy that reaches the Earth is $1.5 \cdot 10^{21}$ Wh, which is approximately 15 000 times greater than the present total use of primary energy [3, 4, 14]. However, the relatively low power density is an obstacle for solar energy compared to conventional fuel combustion. On an average land area on the Earth, at noon and under clear sky conditions, approximately 1 kW/m^2 of energy from solar radiation is available for conversion into electrical power or heat. With a typical conversion efficiency of 10% for a standard photovoltaic system, this corresponds to an electrical power of 100 W/m^2.

2.2.1 Applications

Photovoltaic cells are the smallest units of a photovoltaic system. The maximum voltage of a single silicon cell is 0.5–0.6 V, which is too low for most applications. Therefore, several cells are connected in series to form modules. Figure 2 shows different types of photovoltaic modules. A module is usually an essentially plane, encapsulated assembly of solar cells and ancillary parts, such as interconnections, terminals, and protective devices (such as diodes), of convenient size for handling. The structural (load carrying) part of a module can either be the top layer (in a superstrate

configuration) or the back layer (for a substrate configuration). Photovoltaic modules require little maintenance, and while system lifetime have increased to 20–30 years, recent advances in manufacturing have reduced the total energy payback-time[5] to 2.5–5 years.

Figure 2: Various types of photovoltaic modules, including mono-crystalline silicon (the two modules to the left in the back row), poly-crystalline silicon (the module in the middle of the front row and the two rightmost in the back row), and thin film modules (the two small modules in the front row). Photo: M. Brogren.

A disadvantage for solar energy, besides the low energy density, is that the supply varies over time, with the celestial movement of the Earth and with the weather conditions. Due to the intermittent nature of solar radiation, photovoltaic systems have to include energy storage in order to be able to provide uninterrupted supply of electricity. Photovoltaic systems can be either grid-connected or stand-alone systems. Stand-alone systems include photovoltaic modules, energy storage (e.g. batteries) and other equipment, such as a charge controller, a DC/AC inverter, and tracking and monitoring equipment, collectively called balance-of-system components. In a grid-connected system, the grid acts like a battery with a virtually unlimited storage capacity. Therefore the total efficiency of a grid-connected photovoltaic system is higher than the efficiency of a stand-alone system, in which the batteries will sometimes be fully loaded, and the generated electricity can not be utilised.

[5] The energy payback-time is the time it takes for a photovoltaic module to produce as much electricity as was consumed during its manufacturing.

Photovoltaic systems are already in widespread use for telecommunications and navigation aids, such as buoys and repeater stations in remote areas. A low loss-of-load probability, i.e. the probability that the electricity supply is interrupted, is essential in these kinds of applications. In places with little wintertime irradiation, like northern Sweden, this requires large photovoltaic modules and battery capacity. Photovoltaics are also used for corrosion protection of pipelines and transmission lines by providing a cathodic voltage. Figure 3 shows another niche application for photovoltaics. Although the parking ticket machine in the photograph is at a distance of no more than two metres from the electric grid, it is cost-effective to utilise a photovoltaic module and a battery to power the ticket machine instead of connecting it to the grid.

Figure 3: Photovoltaic module that supplies electricity to a parking ticket machine in Berlin, Germany. Photo: M. Brogren.

In many developing countries, where the electricity grid is largely confined to the main urban areas, and where a substantial proportion of the rural population does not have access to most basic energy services, photovoltaics is widely regarded as the best and least expensive means of providing many of the energy services that are lacking [15]. Photovoltaic modules can be used for lighting (for homes, schools, and health centres to enable education and income generation activities to continue after dark), solar home systems (to provide power for domestic lighting and other DC appliances such as TVs, radios, sewing machines, etc), refrigeration systems (to preserve

vaccines, blood, and other consumables vital to healthcare programmes), and pumping systems (to supply water to villages, for land irrigation, or for livestock watering).

Incorporation into rooftops and facades of buildings is anticipated to be the main application for photovoltaics in many industrialized countries. The main advantage of building-integration is that various costs, such as purchase of land and building components as well as transmission and distribution costs can be avoided either wholly or partially. In the future, it is expected that module cost reductions will encourage larger deployment in these market segments and that decentralised grid-connected photovoltaic systems, either integrated into buildings and other structures or ground-based, which provide grid support and peak power will be more common applications of photovoltaics.

In conclusion, the majority of grid-connected applications are found in industrialized countries, while stand-alone applications mainly relate to rural areas and developing countries [15].

2.2.2 History of photovoltaics

The history of photovoltaics dates back to 1839, when the French physicist Edmond Becquerel first observed the photovoltaic effect. In 1886, the American Charles Fitts constructed a selenium photovoltaic cell that converted visible light into electricity with an efficiency of 1% [16]. In the 1930s, the theory was developed for the electrical properties of silicon and other crystalline semi-conductors. Primitive photovoltaic cells were developed using selenium but these cells were expensive and the conversion efficiency was still only 1%.

In the early 1950s, the Czochralski method for production of high-purity crystalline silicon was developed, and in 1954, scientists at Bell Laboratories in search of a practical way to generate electricity for telephone systems in rural areas far from the power lines, produced a silicon photovoltaic cell with 6% efficiency [17]. Soon the efficiency was raised to 11% and it was realized that solar cells could have numerous practical applications. There was another reason for optimism as well: the material that was used, silicon, is the second most abundant element on Earth, comprising 29% of its crust [113].

The 1950s were an unfavourable time, however, to develop an energy technology based on photovoltaics. The price of oil was less than $2 per barrel and large fossil-fuelled power plants were being built. Moreover, in

1954, construction began on the world's first commercial nuclear reactor [18]. Nuclear power was envisioned as a source of electricity "too cheap to meter" and in many countries, the government's energy funds were devoted to that technology. Photovoltaic researchers faced an unsettling economic reality. Silicon cells developed in the 1950s were extremely expensive, with costs as high as $600 per watt (compared to $5 today), and funding for research to reduce the cost was not available in an era with falling electricity prices and little concern about the environment.

The space programmes rescued photovoltaics from the technological scrap heap. When scientists went searching for a long-lasting, lightweight power source for satellites, costs were largely irrelevant and photovoltaic cells, which could take advantage of the continuous sunlight in space, were their choice. During the middle of the 20th century, the development of photovoltaic cells was therefore a direct result of the race to explore space. In 1957, the Russians, and in 1958, the Americans, launched their first solar powered satellites [19]. Today, solar cells power virtually all satellites.

Achievements in solar cell research during the peak years of the space programmes included a major increase in efficiency and reduction in cost. However, the space-related photovoltaics market levelled off and photovoltaic cell production decreased. Since the 1970s, the interest in photovoltaics has largely been coupled to the uncertainty of the supply of fossil fuels and to the concern for the environment. During the first oil crisis in 1973–74, the need for alternative energy sources promoted great interest in the photovoltaics industry and research and development programmes in Europe, Japan, and the United States expanded. In the 1980s there was a relative disinterest in solar power, while the Gulf war of 1990 again sparked an interest in non-fossil fuel energy alternatives. Since the beginning of the 1990s, the annual growth of the global solar cell market has been 20–40%, and production can barely keep up with demand. In 1999, the cumulative worldwide installed solar cell capacity reached 1 000 MW and it is believed to have reached 2 000 MW in 2002.[6] By the end of 2002, a cumulative total of about 1 300 MW of photovoltaic capacity had been installed in the twenty member countries of the International Energy Agency's Photovoltaic Power Systems Programme (IEA-PVPS). This capacity can be compared with the maximum power of the largest Swedish nuclear reactor F3 of 1 155 MW. Since 1999, the twenty IEA-PVPS countries have accounted for more than 90% of global solar cell production and around 80% of this production has been installed in the IEA-PVPS member countries [20]. Figure 4 shows the global annually installed and cumulative photovoltaic capacity during the period 1980–2002 as well as the development of the module prices.

[6] Data are not readily available for developing countries.

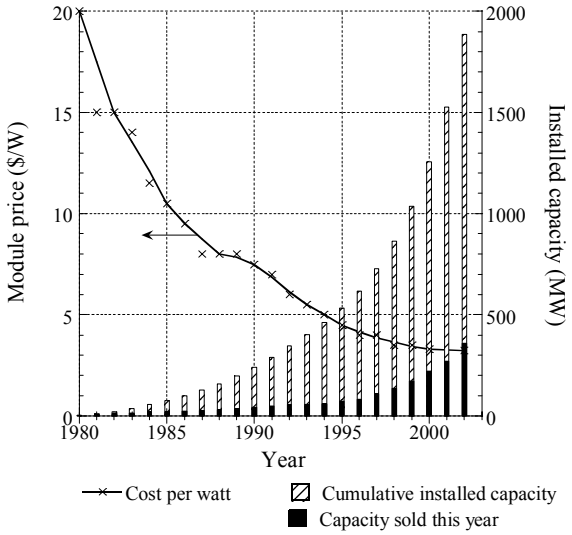

Figure 4: The development of the worldwide market for photovoltaics during 1980–2002: Module prices, annually installed rated capacity, and cumulative capacity [21, 22].

2.2.3 Cost of solar electricity

During the past 25 years, there have been a number of significant advances in solar energy technologies, which have made some applications cost-competitive in comparison with conventional energy sources. Passive solar heating is a standard feature in modern, energy-efficient homes in cold but relatively sunny parts of the world, such as Scandinavia, Germany, and Canada. Solar water heating systems are reliable, efficient and long lasting. Solar thermal power systems, which produce electricity from solar energy by using thermal absorbers to produce heat, which is converted into steam that drives a generator, has been demonstrated successfully at a level of hundreds of megawatts [23, 24], and the technology for solar photovoltaic conversion has matured markedly. Photovoltaic systems now have an efficiency of 10–15% and the price of photovoltaic modules has fallen to less than 15% of the price 25 years ago. The module price development is shown in Figure 4 above. In 1978, the total sale of photovoltaic modules was 1 MW at a cost of about €30–50/W [19, 21]. Today, turn-key photovoltaic systems, including balance-of-system components, cost €5–12/W, resulting in life-cycle costs for photovoltaic electricity of €0.20–1.00/kWh, depending on module technology and the annual irradiation at the site of installation. Therefore, photovoltaics are already cost-effective in many stand-alone applications, e.g. for rural electrification and for powering telecommunication systems, all over the world. Still, however, the large initial investments needed for photovoltaics

and the subsequently long payback time continue to compose an impediment to investment in photovoltaics, especially in developing countries.

Due to the high cost per kWh produced, solar photovoltaic and solar thermal electricity are still not cost-competitive on the mass electricity market, where they have to compete with electricity produced in nuclear and conventional fossil-fuelled power plants.[7] However, the electricity retail prices vary significantly between the national markets and there are some countries with high electricity prices and high annual irradiation in which solar electricity is close to being cost-competitive today.

2.2.4 Future paths for photovoltaics

Photovoltaics can play an important role for satisfying the demand for electricity and at the same time secure a long-term stabilisation of the CO_2 concentration in the atmosphere, but equally important is the fact that for two billion people without access to electricity today, photovoltaics can provide a means for a better life [26]. Almost half a million families in the developing world are already using small, household solar photovoltaic systems to power fluorescent lamps, radio-cassette players, 12 volt black-and-white TVs, and other small appliances [27]. The numerous photovoltaic powered refrigerators and water pumping systems installed throughout Africa have proven the technology to be both reliable and suitable for such purposes [28]. There are several specific advantages of photovoltaics for rural electrification in developing countries. Photovoltaics are small-scale, modular, easy to transport and install and do not require an extensive infrastructure, thus suitable for remote areas. Photovoltaics are also more environmentally benign than most other energy technologies available for rural electrification, for example diesel generators or lead acid batteries, and the technology is competitive, on a cost per kWh basis, in comparison with the traditional alternatives.[8]

However, the lack of finance available for purchase of photovoltaic systems, either through cash sales or through affordable credit, is a problem for dissemination of the technology in developing countries. This is especially problematic in rural areas, where the population is often reliant upon subsistence agriculture and informal employment. As this demographic group represent the largest market for stand-alone photovoltaic power

[7] Alternatively, it could be argued that it is the prices of fossil (and fissile) fuels that are too low, i.e. that these fuels are not priced at their total costs because the negative externalities (such as environmental problems and health effects) are largely not included in the prices [25].

[8] World Bank surveys indicate that rural households in Africa often spend as much as $10 per month on kerosene and batteries.

systems, the problem of financing needs to be addressed in order to develop the potential market [29].

It is often argued that if photovoltaic electricity is going to play a more than marginal role in the industrialised parts of the world, for example in the European energy system, grid-connection is necessary because of the high losses and costs associated with other types of storage. Furthermore, in densely populated areas, where space is limited, building-integration of the photovoltaic modules is appropriate. Building-integrated photovoltaics (BIPV) make cost-savings possible because the modules can serve as a functioning part of the building envelope (as roof, facade, or windows) as well as an electricity-producing element. Thus the avoided costs of, for example, wall cladding can be deducted from the cost of the modules. Today, BIPV continue a steady advance on the building market as the price of photovoltaic modules drops. In addition, large BIPV programmes, such as the 100 000 solar roofs programme in Germany, and programmes in the USA, Japan, Italy, etc., have contributed to an increased production capacity and reduced module prices. Regarding BIPV, there are other significant obstacles than high costs, such as a lack of knowledge among utility companies, constructors (applicable for BIPV), municipalities and end users [i], which also have to be addressed.

For both stand-alone and grid-connected applications, system costs have to be reduced in order to increase the use of photovoltaic electricity. One measure to take is to develop new manufacturing techniques for making the photovoltaic module itself less expensive. However, today this is not enough, since the costs of installation and additional electrical equipment, such as inverters in the case of a grid-connected system, is a major part (often as large as 50–70%) of the total system cost. Another way of reducing the cost of photovoltaic electricity is to generate more electricity using the same module and balance of system components; and this is essentially what this thesis is about. Concentrating photovoltaic systems, which employ reflectors to concentrate sunlight on the photovoltaic cell and increase its output, have a high potential for cost reduction due to the reduced amount of expensive photovoltaic material that is needed to generate a given amount of power [30]. Concentrating photovoltaic systems are therefore considered as one of the most promising solar energy technologies.

3. Light and its interaction with matter

In this chapter, the properties of electromagnetic waves and their interaction with matter are summarised and the optical properties of materials are introduced. The aim is to provide the reader with a theoretical background that facilitates the understanding of the performance of the solar energy materials and the concentrating photovoltaic and photovoltaic-thermal systems that are studied in this thesis.

3.1. Electromagnetic waves

Maxwell's equations predict the behaviour of electromagnetic waves, i.e. fluctuations of electrical and magnetic fields in space. Maxwell also showed that optics, the study of visible light, is a branch of electromagnetism [31]. The propagation of electromagnetic radiation in a medium is governed by the wavelength dependent complex index of refraction,

$$N(\lambda) = n(\lambda) + ik(\lambda)\,, \tag{1}$$

where λ is the wavelength and the refractive index, n, describes the refraction of the electromagnetic wave, while the extinction coefficient, k, describes the damping of the amplitude of the wave. Although n and k are both wavelength dependent, they are often called optical constants.

From Maxwell's equations, which are found in most physics textbooks, an expression for the propagation of a plane harmonic wave, $\vec{E}$, in a homogeneous medium that is characterised by n and k, can be derived:

$$\vec{E} = E_0 \cdot \exp\left[i(\omega t - \tfrac{n}{c}\vec{r}\cdot\vec{s}) - \tfrac{k}{c}\omega\vec{r}\cdot\vec{s}\right]. \tag{2}$$

Here, E_0 is the amplitude of the wave at a reference point in the medium, normally just before the wave encounters the first interface, ω is the angular frequency, t denotes time, c is the velocity of light in vacuum, $\vec{r}$ is the position vector, and $\vec{s}$ is a unit vector in the direction of the wave propagation.

Electromagnetic radiation can also be described in terms of a stream of photons, which are mass-less particles, each travelling at the speed of light. Each photon corresponds to a quantum of energy and the only difference between the various types of electromagnetic radiation is the amount of energy found in each photon. The electromagnetic spectral variation can be expressed in terms of photon energy, frequency, or wavelength. In materials optics, the wavelengths of light are often given in nanometres, nm, which is the unit that is used in this thesis.

3.2. Blackbody radiation

All matter emits electromagnetic radiation [32]. An ideal blackbody is a hypothetical body that emits radiation only according to its temperature and absorbs all radiation that impinges on it. For a blackbody at a temperature, T, the intensity of the emitted radiation, I_{bb}, per unit surface area and unit wavelength (W/m^2, nm) is given by Planck's law [33]:

$$I_{bb}(\lambda, T) = \frac{2\pi hc^2}{\lambda^5 (e^{hc/\lambda k_B T} - 1)} \tag{3}$$

where h is the Planck constant, c is the speed of light, and k_B is the Boltzmann constant. Figure 5 shows emission spectra for blackbodies at different temperatures. It is worth noting that the scales on the y axes are considerably different. Wien's displacement law states that, for a blackbody at a thermodynamic temperature, T, the product of the temperature (in Kelvin) and the wavelength that corresponds to the maximum radiation of energy, λ_m, is constant. When temperature is decreased, the spectral energy distribution curve is increased in width and its maximum is displaced towards longer wavelengths. At room temperature, the peak is located at about 10 000 nm.

The spectral emittance, ε, of a body is defined as the ratio of the radiated power from the surface of the body at a given wavelength and temperature, to the radiated power of an ideal blackbody at the same wavelength and temperature. The emittance of an ideal blackbody is thus 1. For all other materials, $0<\varepsilon<1$. Metals have low emittance, while absorbing materials have high emittance, as we will see in the next section. The radiated power, P, per unit surface area is given by Stefan-Boltzmann's law:

$$P(T) = \varepsilon \sigma T^4, \tag{4}$$

where T is the temperature of the radiating body and σ is the Stefan-Boltzmann constant.

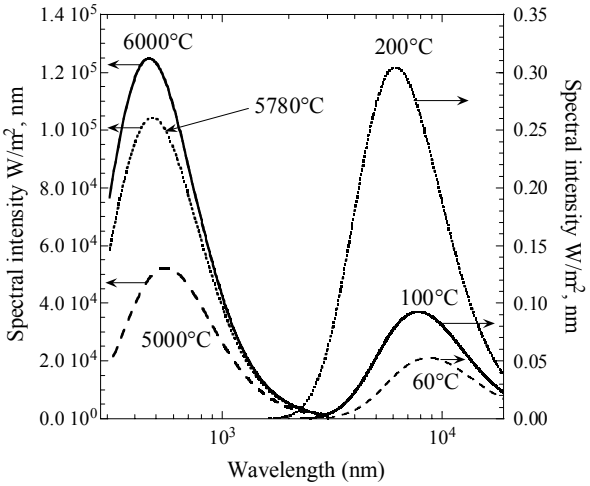

Figure 5: Calculated emission spectra for blackbodies at different temperatures. Note the different scales on the y axes.

3.3. Optical properties of materials

When electromagnetic radiation impinges on a material, it can be reflected, transmitted, or absorbed. The optical properties reflectance, ρ, transmittance, τ, and absorptance, α, of a material are defined as fractions of the incident radiation intensity, and thus dimensionless. The first law of thermodynamics gives that, for each wavelength, the sum of the energy that is reflected, transmitted, and absorbed must equal the incident energy:

$$\rho(\lambda) + \tau(\lambda) + \alpha(\lambda) = 1 . \tag{5}$$

The relationship

$$\varepsilon(\lambda) = \alpha(\lambda) \tag{6}$$

follows from energy conservation and is often referred to as Kirchhoff's law [32].

The optical properties of solar energy materials are essential for their function. For example, a solar thermal collector (see section 5.1) should

absorb as much as possible of the solar radiation that falls upon it. It should thus have unity absorption at solar wavelengths. However, if the collector was a blackbody, it would re-radiate the absorbed energy according to its temperature and much of the thermal energy would be lost to the ambient. Therefore, modern solar collectors contain thermal absorbers with selective surfaces, which have different optical properties for different wavelengths. The collector efficiency is increased by a high absorptance in the solar radiation part of the electromagnetic spectrum and a high reflectance, which, according to Equations 5 and 6 above, is equal to a low emittance, in the infrared part of the electromagnetic spectrum. The low thermal emittance reduces the fraction of thermal energy that is re-radiated from the absorber surface.

When light is incident on an interface between two different materials, it is refracted according to Snell's law:

$$N_1(\lambda)\sin\theta_1 = N_2(\lambda)\sin\theta_2 \tag{7}$$

where N_1 and N_2 are the complex indexes of refraction for the first and the second material, respectively, θ_1 is the angle of incidence, which is equal to the angle of the reflected light, and θ_2 is the angle at which the refracted light leaves on the other side of the interface, as shown in Figure 6.

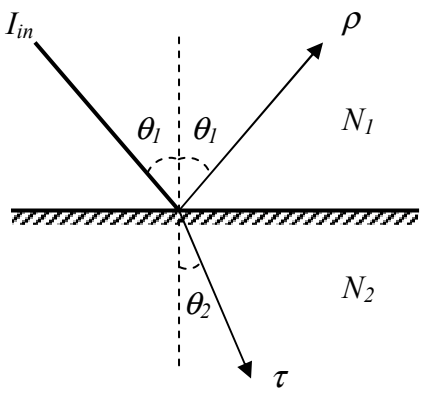

Figure 6: Visualisation of Snell's law, which relates the complex indices of refraction for the first and second material, N_1 and N_2, to the angle of incidence, θ_1, and the angle at which the refracted light leaves on the other side of the interface, θ_2. I_{in} is the incident intensity, ρ is the reflected intensity, and τ is the intensity that is transmitted trough the interface.

Light can be polarised parallel to the plane of incidence (*p*-polarised) or perpendicular to the plane of incidence (*s*-polarised[9]). Fresnel's equations relate the complex amplitudes, $\mathfrak{R}$ and $\mathfrak{I}$, of the reflected and transmitted electromagnetic fields at an interface to the complex amplitude of the incident field, I. At non-normal angles of incidence, the wavelength dependent transmitted intensity and the wavelength dependent reflected intensity are different for the different polarisation states and the two states have to be treated separately:

$$r_p = \frac{\mathfrak{R}_p}{\mathrm{I}_p} = \frac{N_2 \cos\theta_1 - N_1 \cos\theta_2}{N_2 \cos\theta_1 + N_1 \cos\theta_2} \tag{8}$$

$$r_s = \frac{\mathfrak{R}_s}{\mathrm{I}_s} = \frac{N_1 \cos\theta_1 - N_2 \cos\theta_2}{N_1 \cos\theta_1 + N_2 \cos\theta_2} \tag{9}$$

$$t_p = \frac{\mathfrak{I}_p}{\mathrm{I}_p} = \frac{2N_1 \cos\theta_2}{N_2 \cos\theta_1 + N_1 \cos\theta_2} \tag{10}$$

$$t_s = \frac{\mathfrak{I}_s}{\mathrm{I}_s} = \frac{2N_2 \cos\theta_2}{N_1 \cos\theta_1 + N_2 \cos\theta_2} \tag{11}$$

A similar set of equations can be derived for a stack of thin films on a substrate.

The measurable angle and wavelength dependent intensities, ρ and τ, of the reflected and transmitted radiation, in terms of fractions of the intensity of the incident radiation, are given by

$$\rho_{s,p} = \left| r_{s,p} \right|^2 \tag{12}$$

$$\tau_{s,p} = \left| t_{s,p} \right|^2 \tag{13}$$

where the subscripts *s* and *p* denote the different polarisation states. The unpolarised reflectance and transmittance are then calculated as the arithmetic mean of the values for the polarised states:

$$\rho = \frac{\rho_s + \rho_p}{2} = \frac{\left| r_p \right|^2 + \left| r_s \right|^2}{2} \tag{14}$$

$$\tau = \frac{\tau_s + \tau_p}{2} = \frac{\left| t_p \right|^2 + \left| t_s \right|^2}{2} \tag{15}$$

[9] s=senkrecht (German)

The laws of reflection and refraction are deduced assuming material homogeneity over lengths that are long in comparison with a wavelength. Therefore, measured optical properties of a material can be regarded as averages. Furthermore, a reflected light beam is the summation of all scattered components that are similar in direction, phase, and frequency [34].

4. The solar energy resource

This chapter discusses the solar energy resource and the properties of solar radiation to which the properties of the materials and systems for utilisation of solar energy should be matched.

4.1. Solar radiation on Earth

The Sun can be approximated by a blackbody with a temperature of about 5780°C that radiates hemispherically into space according to this temperature. The solar constant is defined as the power received on a unit area perpendicular to the solar position vector, which is located in free space at the Earth's mean distance from the Sun. The solar "constant" varies by ±3.4% on an annual basis, but the value 1 353 W/m^2 is often found in the literature [33].

When sunlight passes through the atmosphere on its way to Earth, it is reduced from the level outside the Earth's atmosphere (the extraterrestrial solar radiation) by about 30%. The attenuation is caused by Rayleigh scattering by molecules in the atmosphere, scattering by aerosols and dust particles, and absorption by atmospheric gases, such as oxygen, ozone, water vapour, and carbon dioxide. After scattering and absorption followed by partial re-radiation into space, approximately 1 000 W/m^2 reaches the ground under clear weather conditions. However, this amount varies greatly from one point in time to another due to the atmospheric conditions and the movement of the Earth with respect to the Sun [35].

The term air mass (AM), which is often used in the field of solar energy, is defined as the ratio of the path length of the radiation trough the atmosphere at a given solar zenith angle, θ_Z, to the path length when the sun is directly overhead. The solar zenith angle is the angle between the ground normal and the solar position vector. Figure 7 shows the definition of the solar zenith angle and the air mass number, m. The air mass number is given by

$$m = \frac{1}{\cos(\theta_Z)} . \tag{16}$$

The International Organization for Standardization's AM1.5 solar spectrum [36] is often used for rating of photovoltaic cells and other solar energy components for terrestrial applications and it is obtained at θ_Z=48.2°. Air mass zero (AM0) refers to the absence of atmospheric attenuation [37]. While the intensity of solar radiation is about 1.35 kW/m^2 at AM0 outside the atmosphere, it is 0.96 kW/m^2 at AM1.5.

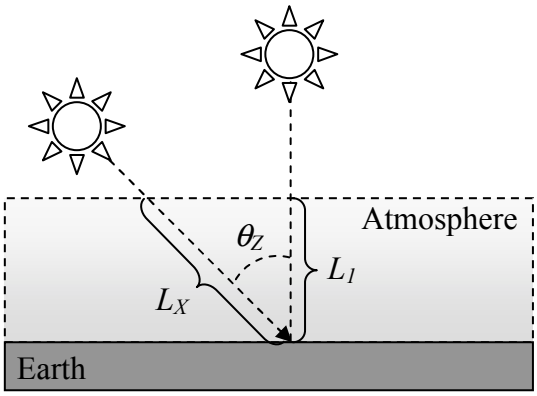

Figure 7: Definitions of the solar zenith angle and the air mass (AM). AM1 is defined as the air mass at the path length L_1 through the atmosphere. The air mass number for the path length L_X is 1/cos(θ_Z), where θ_Z is the solar zenith angle.

In order to determine how a photovoltaic system will operate at a given geographic location, the solar resource at the location must be characterized. The total irradiation, G_{tot}, is the amount of energy that is contained in the sunlight that strikes a unit surface over a specified period of time. The irradiance is the power of the sunlight that is incident on the surface. The total irradiance on the surface, I_{tot}, can be divided into the direct or beam radiation, I_b, which has travelled in a straight path directly from the sun, and the diffuse radiation, I_{diff}, which is received indirectly as a result of scattering due to clouds, fog, haze, dust or other substances in the atmosphere, as well as from the ground, buildings, and other surrounding objects, according to

$$I_{tot} = I_b + I_{diff} . \tag{17}$$

Figure 8 shows the extraterrestrial irradiance and the terrestrial total and direct irradiance spectra for AM1.5 [36]. The most important absorption bands of different atmospheric gases can be seen as dips in the terrestrial irradiance spectra. The normalized spectral sensitivity of the human eye is also shown in Figure 8. The human eye can detect photons with wavelengths between 380 and 780 nm (and does this most efficiently at 555 nm [38]).

This part of the solar spectrum is therefore called the visible. The solar radiation spectrum is often divided in three parts: the ultraviolet (λ<380 nm), the visible, and the infrared (λ>780 nm) [37, 39]. Sometimes the infrared is divided in near infrared and far infrared, where the latter refers to wavelengths longer than 3 000 nm. 99.5% of the solar irradiance that reaches the atmosphere has wavelengths shorter than 5 000 nm.

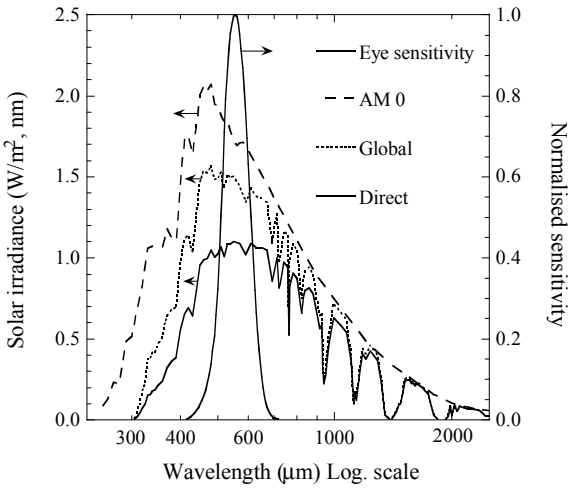

Figure 8: The solar spectrum AM0 (extraterrestrial irradiance), the direct and total AM1.5 spectra [36], and the normalized spectral sensitivity of the human eye.

4.2. Solar radiation on inclined surfaces

The position of the sun relative to an arbitrarily inclined surface can be described using different angles. The angle of incidence, θ_i, of the direct radiation on the surface is the angle between the solar position vector and the surface normal. This angle can be calculated using

$$\cos\theta_i = \cos\beta \sin\theta_H + \sin\beta \cos\theta_H \cos(\gamma_S - \gamma_P), \tag{18}$$

where β is the inclination of the surface with respect to the horizontal, γ_P is the azimuth of the plane, γ_S is the sun's azimuth from the south, and θ_H is the solar altitude angle. The angles are defined in Figure 9. The solar altitude angle is given by

$$\theta_H = 90° - \theta_Z, \tag{19}$$

where θ_Z is the zenith angle of the sun. For a calculation of the zenith angle and the sun's azimuth at any given time, the reader is referred to solar energy handbooks, for instance the books by Duffie and Beckman, and Meinel and Meinel [33, 40, 41].

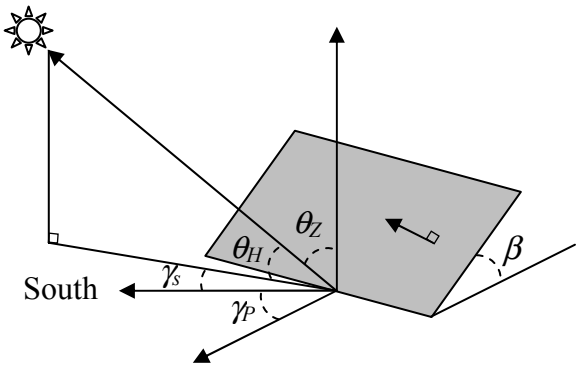

Figure 9: Plane inclined at an angle β and with an azimuth γ_P. θ_H is the solar altitude, θ_Z is the solar zenith angle, and γ_S is the sun's azimuth from the south.

The direct irradiance, I_b, on the surface can be expressed in terms of the solar radiation normal to the surface, $I_{b,n}$ and the angle of incidence, θ_i, using a cosine factor:

$$I_b = I_{b,n} \cos\theta_i \,. \tag{20}$$

4.2.1 Projection of radiation into different planes

The direct irradiance on a surface can be treated as a vector with two orthogonal components. If the surface faces south, it is convenient to divide the solar position vector in one component in the east-west direction and one component in the vertical plane P_{NS}, that is extended from north to south, as shown in Figure 10. The two orthogonal components can then be treated separately. The direct irradiance on a surface facing south is determined by the component in the P_{NS} plane only, since the component in the east-west direction, which is parallel to the receiving surface, will not contribute to the energy flux through the surface. Figure 10 also gives the definition of the south projection angle, θ_{NS}, which is the angle between the south horizon and the projection of the solar position vector in the north-south vertical plane [42]. The south projection angle determines the optimum inclination of a flat plate solar collector or photovoltaic module that faces south. The

minimum angle of incidence and maximum direct irradiance on a surface facing south is obtained if the surface is tilted to 90°-θ_{NS}.

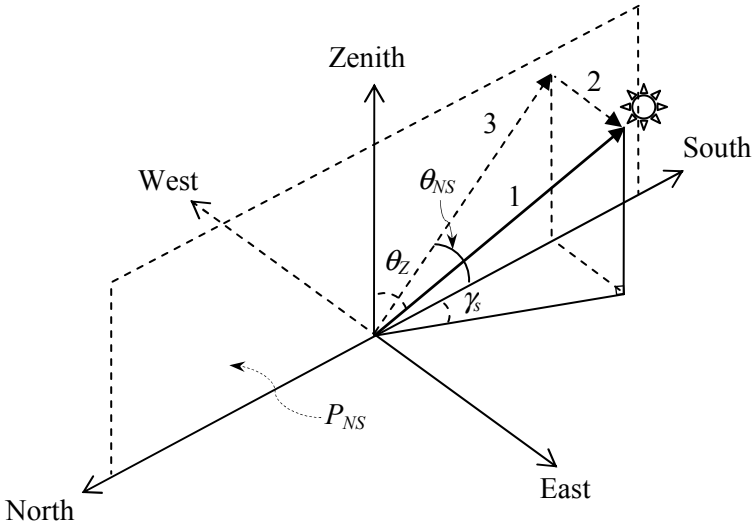

Figure 10: Definition of various angles. The solar position vector (1) can be divided in one component in the east-west direction (2) and one component in the north-south vertical P_{NS} plane (3). The south projection angle, θ_{NS}, is the angle between the south horizon and the projection of the solar position vector on the P_{NS} plane. θ_z is the solar zenith angle and γ_s is the solar azimuth angle [42].

Figure 11 shows the south projection angle in Stockholm (latitude 59.4°N) for different dates of the year. At the equinoxes, the south projection angle at a latitude θ_N is constant and equal to 90°-θ_N during the entire day. This means that during the equinoxes, the sun moves in an east-west plane that is normal to a module plane that is inclined at an angle 90°-θ_N. In summer, the south projection angle has a minimum at noon, which coincides with the solar altitude angle.

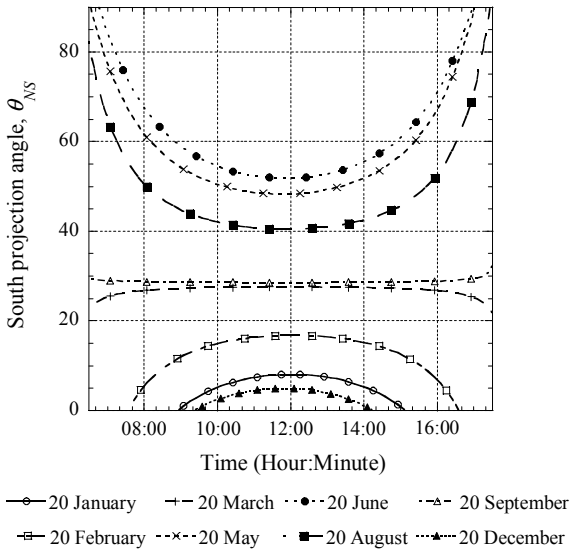

Figure 11: The south projection angle, θ_{NS}, in Stockholm (59.4°N), Sweden, shown for different dates of the year. Courtesy of A. Helgesson.

4.3. Irradiation at high latitudes

When photovoltaic modules are placed on the ground with an inclination of 30°–40° or integrated into inclined roofs, the solar irradiation at high solar altitudes gives a relatively higher contribution to the annually collected energy than the irradiation at low solar altitudes. The situation is different, however, when photovoltaic systems are integrated into vertical facades, since the irradiation at low solar heights gives a larger contribution to the collected energy on a facade. Therefore, integration of photovoltaic systems into vertical facades is more appropriate at high latitudes, for example in Sweden, than at lower latitudes, as a larger fraction of the annual irradiation is received at relatively low solar heights [42]. Figure 12 shows the total monthly irradiation on a horizontal plane and on a vertical wall that faces south, at three different sites on the northern hemisphere: Stockholm in Sweden, Madrid in Spain, and Accra in Ghana. The figure shows that the difference between the annual irradiation on the vertical wall, G_v, and on the horizontal, G_h, is negligible in Stockholm (G_v=959 kWh/m^2, G_h=978 kWh/m^2), while it is significant in Madrid (G_v=1 257 kWh/m^2, G_h=1 663 kWh/m^2) and in Accra (G_v=799 kWh/m^2, G_h=1 812 kWh/m^2). Furthermore, at high latitudes, integration of photovoltaic systems into facades reduces the variation in electricity production between the summer and the winter seasons.

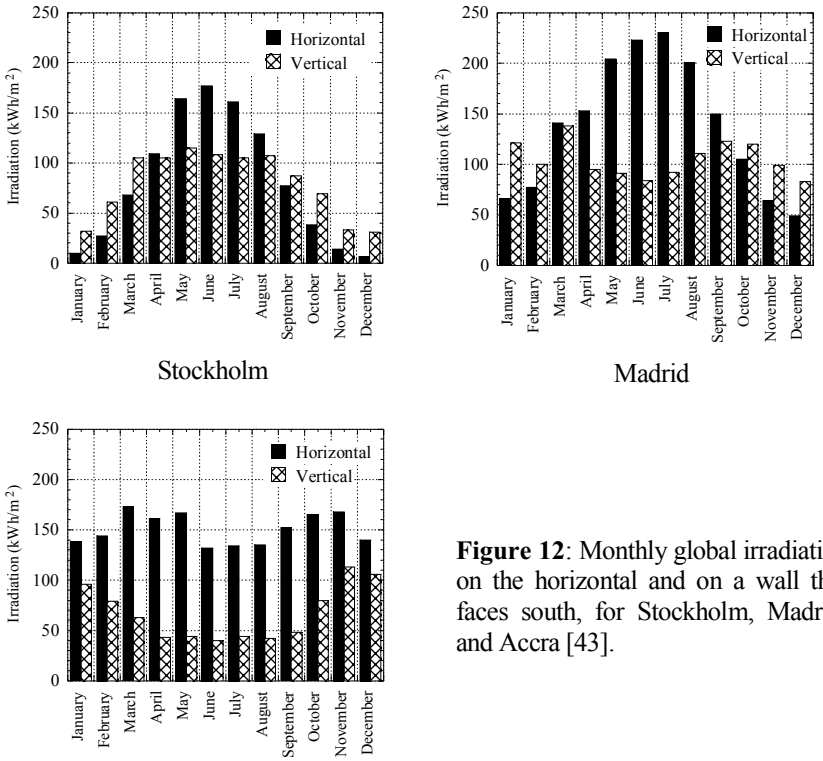

Figure 12: Monthly global irradiation on the horizontal and on a wall that faces south, for Stockholm, Madrid, and Accra [43].

In Stockholm, as well as on many other places at high latitudes, the direct irradiation is low for low south projection angles, i.e. during wintertime [42]. This makes it possible to design solar energy systems, which collect radiation that is incident in a rather narrow angular interval, without wasting a significant part of the annual irradiation. This is convenient when constructing low-concentrating photovoltaic and solar thermal systems as we shall see later, for example in section 6.4. In Figure 13, the projected annual irradiation on a wall in Stockholm that faces due south is shown as a function of the south projection angle, θ_{NS}. The diffuse irradiation was assumed to be isotropic in the calculations. It is shown that almost all direct irradiation is incident at $5° < \theta_{NS} < 60º$. A facade-integrated solar energy system could thus be designed to accept irradiation within this angular interval only. Figure 13 also shows that the irradiation distribution for Stockholm has a maximum for south projection angles of 50°–55°, which corresponds to the hours around noon during May–July. During these months, there is also irradiation incident at higher south projection angles (>65°), which is received during morning and afternoon hours [42].

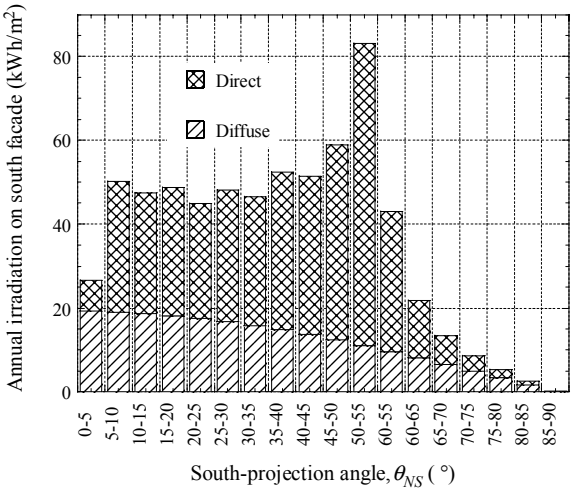

Figure 13: Calculated annual direct and diffuse irradiation on a south wall in Stockholm (mean values for 1983–1991), projected on the north-south vertical plane [44].

5. Technologies for conversion of solar energy

The energy contained in sunlight is critical to life on Earth and fundamental to human survival. It also provides for our comfort. The use of solar energy is usually identified in two contexts: passive solar energy systems, which use natural processes without mechanical equipment and or additional energy to operate (such as passive solar heating) and active solar energy systems, which utilise solar energy with the assistance of mechanical equipment or electronic hardware. Solar thermal collectors, photovoltaics and photovoltaic-thermal cogeneration systems count as active systems. The most significant difference between solar thermal and photovoltaic systems is that solar thermal systems produce heat and photovoltaic systems produce electricity. This chapter describes these two technologies, as well as their combination into photovoltaic-thermal systems.

5.1. Solar thermal collectors

Solar thermal collectors convert solar radiation to thermal energy. In a thermal collector, a liquid or gas is heated and pumped, or allowed to flow through thermal convection, around a circuit and used for domestic or industrial heating. Examples of solar collectors are the flat-plate collectors, in which the solar energy is absorbed by a spectrally selective surface that is covered by one or more glass plates or some other transparent material for reduction of convective heat losses. The glass that covers the absorber is often a glass with a low iron oxide content that is anti-reflectance treated for reduction of absorptive and reflective losses. Whatever glass and treatment of the glass that is used, the use of a cover glass reduces the transmittance of solar radiation to the absorber surface. Teflon films, which have low absorptance and reflectance, are sometimes used beneath a cover glass to reduce convective heat losses. However, Teflon films are not mechanically strong and cannot be used without an additional glazing. The choice of glazing for a solar collector is therefore a trade-off between low heat losses, high solar transmittance, and mechanical strength.

The spectrally selective surface should have high absorption at solar wavelengths and low thermal emittance, corresponding to a high reflectance

in the infrared, to suppress radiative heat losses. A figure of merit that is often used for solar absorber surfaces is the ratio of the solar weighted absorbtance to the thermal emittance, which is the spectral emittance weighted over the blackbody spectrum applicable for the operating temperature of the solar collector. For an entire solar collector, the optical efficiency, η_{opt}, can be formulated as

$$\eta_{opt} = T_{glass}\, A_{absorber} \tag{21}$$

where T_{glass} is the solar weighted transmittance (see section 7.1.2) of the glazing and $A_{absorber}$ is the solar weighted absorbtance of the absorber surface.

Tubes that are attached on the back of the absorber carry air, water, or some other medium to which the heat is transferred. The panel is thermally insulated at the back and can thus form part of the roof or the facade of a building.

More sophisticated collectors use vacuum tubes around the absorber surfaces to minimize radiative heat losses and/or reflectors to concentrate the irradiation on the absorber surface. The reflectors can be applied outside the glass cover, for example in the shape of planar booster reflectors (see section 6.1) [45, 46], or beneath the glass cover, as in the MaReCo collector [47-49]. In the case where external or internal reflectors are used, their solar weighted reflectance should be included in the expression for the optical efficiency.

A solar collector system often includes some form of heat storage, such as an accumulator tank; or an auxiliary heat source, for instance a pellet burner, for use when the sun is not shining. More advanced systems are combined heating and cooling devices that provide heat in the winter and air-conditioning in the summer.

5.2. Photovoltaic cells

The aim of this chapter is to facilitate the understanding of how photovoltaic cells function. A more thorough introduction to the subject is given for example in the textbooks by Kittel [50], and Ashcroft and Mermin [51].

5.2.1 Introduction to semiconductors

The semiconductor silicon is a group four element. It has valence four and the diamond crystal structure. In the diamond structure, each atom has four nearest neighbours and it shares one of its valence electrons with these

neighbours. This results in electron-pair bonds between the atoms. At absolute zero, the band structure of a semiconductor is similar to that of an insulator and it has an energy band gap between the valecnce and the conduction band. However, for a semiconductor, the band gap is small. For example, the band gap of intrincic silicon is 1.14 eV at 300 K [52]. As temperature is raised, thermal energy excites electrons from the valence band, across the band gap, to the conduction band. Conduction starts because of electrons in the conduction band and holes in the valence band, and resistivity decreases with increasing temperature. In silicon, the resistivity is still high at room temperature and it is not until well above room temperature that the resistivity falls sharply because of the increasing number of excited negative and positive charge carriers [53].

If a small number of impurity atoms are added to the semiconductor it is said to be doped. If the impurity atoms have valence five, the extra electron does not form an electron-pair bond and is rather loosely bound to the impurity atom. With a small addition of energy the extra electron can move through the crystal. Valence five atoms are called donor atoms since they donate an electron to the conduction band. If an impurity of valence three is used, there is one electron missing after formation of the electron-pairs. The empty electron state, or the acceptor state, has a slightly higher energy than the electrons in the valence band. All acceptor states are empty at absolute zero but a small amount of thermal energy excites electrons from the valence band to these states. Similarly, all donor states are filled at absolute zero, while all states in the conduction band are empty. When the temperature of a donor doped semiconductor is increased, the donor level electrons are excited to the conduction band and the resistivity falls. As the temperature is further increased and all donor level electrons have been excited to the conduction band, phonon scattering starts to increase the resistivity again.

Because donor impurities result in conduction due to negative donor electrons in the conduction band, donor doped semiconductors are called n-type. When valence three atoms are used as impurities, the acceptor levels accept electrons from the valence band, resulting in conduction by holes in the valence band. As holes are considered to be positive, as opposed to the negative electrons, acceptor doped semiconductors are called p-type. When n- and p-type semiconductor materials are brought in close contact or when valence five and valence three impurities are diffused into different parts of the semiconductor material, a p-n junction and a related depletion layer are formed. In the discussion of solar cell operation which follows, a p-n junction approach will be used.

5.2.2 Photoelectric conversion

A photovoltaic cell converts light into electric energy in the form of a direct current. Most photovoltaic cells are made of semiconductors. Certain semiconductors, including silicon, gallium arsenide, copper-indium-diselenide, and cadmium telluride, are well suited for photovoltaic conversion of solar radiation. In a typical photovoltaic cell, for example made from mono-crystalline silicon, light is absorbed near a p-n junction in the semiconductor. The n-type layer, which is to the front of the cell, is contacted by a transparent conducting oxide or a metal grid, which is designed to cover only a small fraction of the surface. The cell surface is often textured or an anti-reflective coating is deposited on the surface to minimise reflection losses, and a cover glass is employed for structural stability and to protect the device from degradation. The p-type layer below the junction is contacted at the back by a metallic contact that covers the complete back surface. Figure 14 shows a p-n junction solar cell. There are also solar cells, which utilise several junctions on top of each other.

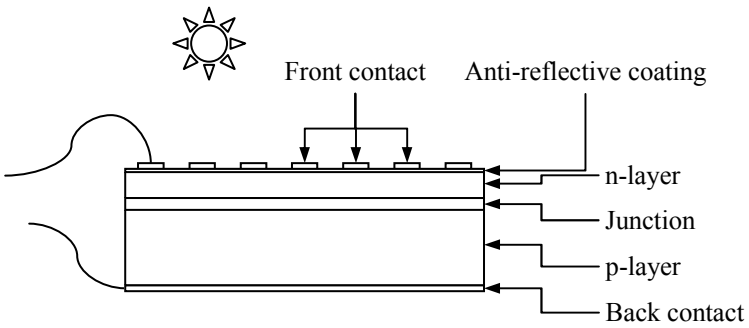

Figure 14: Schematic picture of a p-n-junction solar cell.

In the dark, the idealised p-n junction current, I, is given by the diode equation:

$$I = I_0\left(e^{\frac{q(V-IR_S)}{nk_BT}} - 1\right). \tag{22}$$

Here, I_0 is the reverse saturation current, q is the absolute value of the electronic charge, V is the voltage, R_S is the series resistance, n ($1<n<2$) is the diode's ideality factor, T is the cell temperature, and k_B is Boltzmann's constant [54]. The reverse saturation current and the ideality factor, are

determined by processes occurring at the p-n junction [55]. The series resistance of a photovoltaic cell or module is the parasitic resistance to current flow in a cell and is due to mechanisms such as resistance in the bulk of the semiconductor material, in the metallic contacts, and in the interconnections.

When a solar cell is exposed to sunlight, the part of the incident radiation which has photon energies above the band gap energy of the cell material will excite electrons to the conduction band and create electron-hole pairs. If, in their diffusion in the material, the generated excess minority carriers encounter the internal electric field of the junction depletion layer, they will be collected and swept across the p-n junction [56]. As charge separation continues, a voltage will build up across the depletion region if no external connections are made. The p-n junction then becomes forward biased and a diode injection current is produced. At steady-state, this induced current equals the light induced current and the open-circuit voltage, V_{OC}, condition will be established. When an external load is connected, current will flow and power will be delivered. The voltage across the cell will then be reduced from its open-circuit value. Under illumination, the produced current, I, is described by

$$I = I_L - I_0 \left(e^{\frac{q(V - I R_S)}{n k_B T}} - 1 \right), \tag{23}$$

where I_L is the light induced current. For an ideal cell, I_0 and n are independent of illumination. Note that, under illumination, the direction of the current is opposite to that of the saturation current. Figure 15 shows an equivalent circuit for a photovoltaic cell or module.

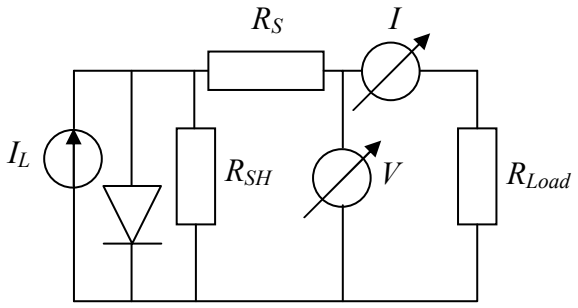

Figure 15: Equivalent circuit for a photovoltaic cell or module. I_L is the light induced current. R_{SH} is the shunt resistance, R_S is the series resistance, V is the output voltage, I is the output current, and R_{Load} is a resistive load [54].

The photovoltaic conversion efficiency, η_{PV}, is the ratio of the electrical power produced by a photovoltaic device to the irradiance on the device. The efficiency depends on materials properties, such as the band gap energy and on the spectral distribution of the incident light. The spectral quantum efficiency, *QE*, is the number of electrons that are delivered from the solar cell per incident photon [57]:

$$QE(\lambda) = \frac{n_{electron}}{n_{photon}(\lambda)}. \tag{24}$$

The relationship between the quantum efficiency and the measurable (in A/W) spectral response, *S*, is given by

$$S(\lambda) = \frac{q\lambda}{hc} QE(\lambda), \tag{25}$$

where q is the elementary charge, c is the speed of light, and h is Planck's constant. A typical silicon solar cell converts photons with wavelengths shorter than 1 200 nm into electricity and the response is highest at around 900 nm [I].

The open-circuit voltage, V_{OC}, is the maximum voltage possible across a photovoltaic cell or module; it is the voltage across the cell in sunlight when no current is flowing. For a silicon cell, this point is at a voltage of about 0.5–0.6 V, but there are semiconductor materials that can supply a voltage of almost 1 V [58]. The short-circuit current, I_{SC}, is the current flowing freely from a photovoltaic cell through an external circuit that has no resistance; the maximum current possible. Current-voltage curves are used to characterise photovoltaic cells and show the relationship between current and voltage of a photovoltaic device, as the load is increased from the short-circuit (maximum current) condition to the open-circuit (maximum voltage) condition. A typical current-voltage curve for a solar cell is shown in Figure 16. The maximum power point is the point on the current-voltage curve of a cell or a module under illumination where the product of current and voltage is at its maximum. The fill-factor, *FF*, is a key characteristic in evaluating cell performance: a high fill-factor is equal to a high quality cell, which has low internal losses (see section 5.2.3). The fill-factor is given by the ratio of a photovoltaic cell's actual maximum power, P_{max}, to its power if both current and voltage were at their maxima, according to

$$FF = \frac{P_{\max}}{V_{OC} I_{SC}}. \tag{26}$$

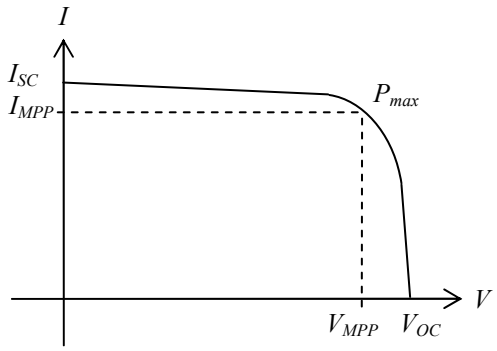

Figure 16: Typical current-voltage characteristic (current as a function of voltage) for a photovoltaic cell under illumination. I_{MPP} and V_{MPP} denote the current and voltage at the maximum power point, P_{max}.

In a rough approximation, the presence of a series resistance, R_S, in the cell or module reduces the maximum power according to [54]:

$$P_{\max} \approx I_{SC} V_{OC} \left(1 - R_S \frac{I_{SC}}{V_{OC}} \right). \tag{27}$$

Equation 27 indicates the importance of the series resistance. The problems with high R_S cells in concentrators were encountered during the work on several of the appended papers and are further discussed in section 11.1. For an ideal cell, the parallel shunt resistance across the junction, R_{SH}, is effectively infinite. In real life, both the series and the shunt resistances of a solar cell have to be taken into account. The non-infinite shunt resistance of a cell is due to p-n junction non-idealities and impurities near the junction, which cause partial shorting of the junction [54]. The R_S and R_{SH} affect the fill-factor and thus the maximum power. In presence of both series and shunt resistances, the current-voltage curve of a solar cell is given by

$$I = I_L - I_O \left[\exp\left(\frac{V + R_S I}{n k_B T / q} \right) - 1 \right] - \frac{V + R_S I}{R_{SH}}. \tag{28}$$

The conditions under which a cell or a module is typically tested in a laboratory are called standard test conditions. Under standard test conditions, the spectral distribution is the AM1.5 ISO standard, the irradiance on the cell is 1 000 W/m^2, and the cell temperature is kept at 25°C.

5.2.3 Loss mechanisms and effects of increased temperature

There are several loss mechanisms that apply to a solar cell and limit the charge separation and transport: reflection in the glass surface, shading by the front contact, reflection and absorption in the front contact, reflection in the cell surface, recombination, resistive losses, absorption in the back contact, etc. Recombination is when the created electron-hole pair does not reach the contacts, but recombine to its initial low energy states. There are several types of recombination: radiative recombination, band-to-band or Auger recombination, and recombination at defect levels in the semiconductor material. Defects can be impurity atoms or grain boundaries.

The operating conditions for a solar cell in a concentrating system are different from operation under standard test conditions. At high irradiance, high local charge concentrations in the photovoltaic cell lead to internal voltages due to series and contact resistances, which in turn cause parasitical losses. Furthermore, the non-unity electrical conversion efficiency leads to generation of thermal energy in the cell. An increased cell temperature leads to a reduction in open-circuit voltage, which is about -2 mV/°C for crystalline silicon cells [59]. High concentration implies high cell temperatures, which lead to a lower output voltage. Therefore, cooling often is applied to concentrating photovoltaic systems.

5.2.4 State-of-the-art of photovoltaics

Silicon is by far the most common material for production of photovoltaic cells, and crystalline silicon modules are the most developed and prevalent type in use today [60]. These include modules of mono-crystalline silicon, which has 35% of the global market, and poly-crystalline silicon, which has 48% of the market [61]. Crystalline silicon is either drawn or cast from molten silicon and sliced into its cell size [58]. Conventional crystalline silicon cells are typically 0.3–0.4 mm thick [62]. The cell thickness is determined by the absorption coefficient of the material and crystalline silicon cells have to be thick due to its rather poor absorption. Many semiconductors that are made from compounds have stronger absorption than silicon. This means that compound semiconductor cells can be made thin but still be efficient. Thin film cells are often made from a number of layers, which are typically a few microns or less in thickness and applied onto substrates of glass or metal using physical or chemical vapour deposition processes. Thin film cells include cells made from compounds like copper-indium-gallium-diselenide (CIGS) and cadmium telluride (CdTe), as well as amorphous silicon (α-Si) cells like the ones found in pocket calculators, which has 9% of the global market. Due to their low materials content, thin film cells are inherently

cheaper to produce than crystalline silicon cells, but they are not as efficient [63]. The lower efficiency is partly due to the fact that the thin film cell technologies are not as mature as the silicon technologies and that the compound materials that are used are complex, which makes it more difficult to understand the loss mechanisms. An advantage of compound material cells is the possibility of band gap engineering, i.e. to increase the conversion efficiency by changing the material composition [64]. A different type of thin film cells utilise ruthenium-based organic compounds that are coated onto titanium dioxide particles and immersed in an electrolyte [58].

5.3. Photovoltaic-thermal cogeneration systems

Most of the solar radiation that is absorbed by a solar cell is not converted into electricity. The ”excess” energy increases the temperature of the photovoltaic cell and reduces its efficiency. Cooling by means of natural or forced ventilation or circulation of a fluid cooling medium reduces the cell temperature. Cooling is often applied to concentrating photovoltaic systems, in which the irradiance on the cell surface is high [65]. An alternative to ordinary photovoltaic modules is to use photovoltaic-thermal modules, which are photovoltaic modules coupled to heat extraction devices [II]. Hence, these systems, in addition to converting sunlight into electricity, collect the residual thermal energy and delivers both heat and electricity in usable forms. Figure 17 shows a comparison between the three types of solar conversion techniques that are discussed in this chapter. In the future, solar thermal and solar electrical systems may compete for the same suitable areas for installation, since the ground area and the space on roofs and facades facing south are limited. Photovoltaic-thermal cogeneration systems may then be an excellent solution [66].

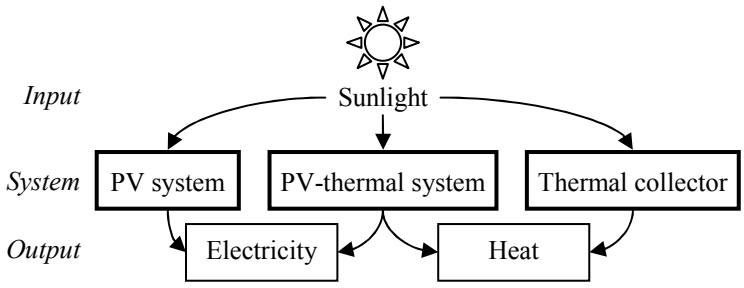

Figure 17: Comparison between photovoltaic (PV), photovoltaic-thermal and solar thermal systems.

The advantage of photovoltaic-thermal systems is their high total efficiency, η_{tot}, due to simultaneous heat and electricity production. The total efficiency of a photovoltaic-thermal system is given by the sum of the electrical and thermal efficiencies:

$$\eta_{tot} = \eta_{electrical} + \eta_{thermal} . \tag{29}$$

However, the thermal efficiency is not as high as for an optimised solar thermal system, since in a photovoltaic-thermal system, the extraction of electrical energy reduces the thermal efficiency. This is demonstrated in Figure 18, which shows the effect of connecting an electrical load to a photovoltaic-thermal module. Furthermore, in many applications, the "value" of the produced electrical energy is significantly higher than the "value" of the thermal energy. An energy value ratio can be introduced in Equation 29 to account for this [67].

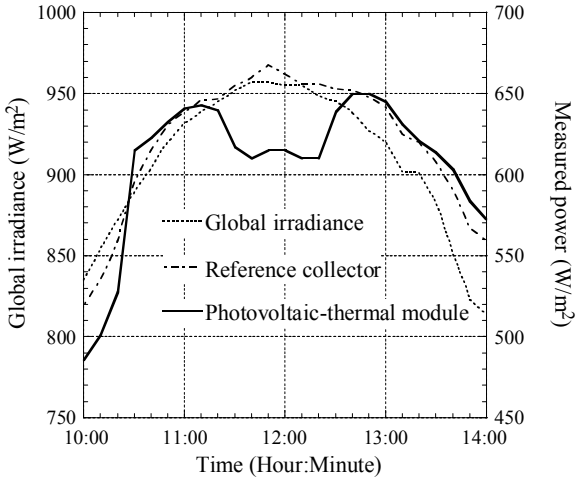

Figure 18: Global irradiance on a plane inclined at 45° to the south, thermal power from a reference collector and thermal power from a photovoltaic-thermal module, on the 15th August 2001. Between 11:15 and 12:20, a 60 W electrical load was connected to the photovoltaic-thermal module. Data from B. Karlsson, Vattenfall Utveckling AB.

There have been several studies, both theoretical and experimental, performed on photovoltaic-thermal systems and their applications [67-73]. As for photovoltaic systems, the total energy output of a photovoltaic-thermal system (the electrical plus the thermal output) depends on the irradiance, ambient temperature, wind speed, and operating temperature. For a photovoltaic-thermal system, the choice of cooling medium and the

efficiency of the heat transport from the cells to the cooling medium also influence system performance [74].

Figure 19 shows the energy balance of a building-integrated photovoltaic-thermal system that generates P_{PV} electrical power and Q_{out} thermal power. The electrical output is often prioritised in photovoltaic-thermal systems and the other system parameters are adapted accordingly [75]. Since the significant voltage drop in most photovoltaic cells at high operating temperatures puts constrains on the operating temperature, the water temperatures obtained in photovoltaic-thermal systems are often moderate. If a photovoltaic-thermal system is operated at moderate temperatures in order to maximise the electricity production, the warm water that is produced cannot be used directly as domestic hot water. However, a photovoltaic-thermal system can be useful for producing warm water for floor-heating and for pre-heating of domestic hot water.

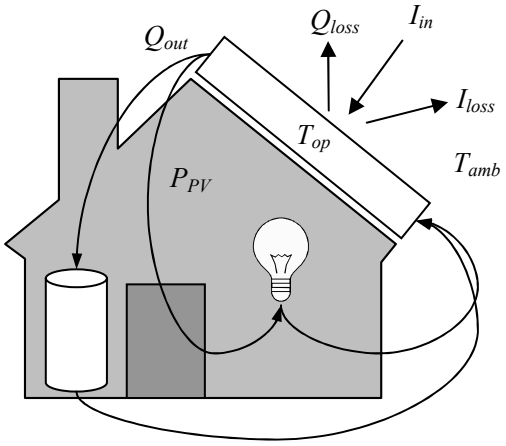

Figure 19: Energy balance of a photovoltaic-thermal system that generates P_{PV} electrical power and Q_{out} thermal power. The ambient temperature is T_{amb} and the total solar irradiance is I_{in}. The average operating temperature of the module is T_{op}. The optical losses are indicated by I_{loss} and the thermal losses by Q_{loss} [75].

There are also photovoltaic-thermal systems that utilise air as a coolant [76-80]. However, such systems have not been considered in this work, since domestic hot water and water for space heating were assumed to be more desirable than warm air for space heating, especially when the photovoltaic-thermal system can be incorporated in an existing heating system and combined with another thermal energy production unit, such as a pellet burner.

6. Solar concentrators

The current generated in a photovoltaic cell is, in principle, proportional to the light intensity on the cell. Thus, in order to produce more electricity from a given cell area it is possible to either increase the conversion efficiency of the cells or increase the light intensity. The high production cost of high-efficiency photovoltaic modules motivates the use of concentrators for increasing the irradiation on the photovoltaic modules, thus utilizing the expensive cell material more efficiently. Concentrator types range from inexpensive and reliable static booster reflectors to more advanced concentrating systems, such as multiple stage concentrators that track the sun continuously. Other examples of solar concentrators are dielectric Fresnel lenses, compound parabolic concentrators, and dish concentrators.

Figure 20 shows a schematic picture of a solar concentrator that concentrates radiation which is distributed over an aperture area, A_1, onto a smaller area, A_2. In most practical applications, the rays from the sun can be considered parallel when they reach the aperture.

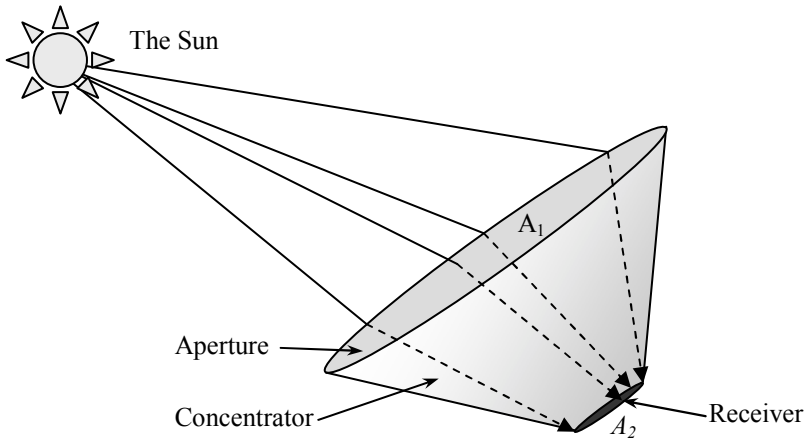

Figure 20: Schematic picture of a solar concentrator. All radiation that intercepts the aperture area, A_1, will reach the receiver area, A_2.

The geometrical concentration ratio, C_g, of a concentrating system is given by

$$C_g = \frac{A_1}{A_2}, \tag{30}$$

where A_1 is the aperture area of the concentrator and A_2 is the area onto which the radiation is concentrated. It follows from the second law of thermodynamics that the flux concentration, C_{opt}, of sunlight provided by any three-dimensional optical system must satisfy

$$C_{opt}^{3D} \leq \frac{n^2}{\sin^2 \delta_S}, \tag{31}$$

where δ_S is the angular half-width of the sun and n is the refractive index of the medium that surrounds the receiver area, A_2. This means that sunlight cannot be concentrated more than about 45 000 times by a three-dimensional concentrator [81]. For a two-dimensional system, the maximum concentration is given by

$$C_{opt}^{2D} \leq \frac{n}{\sin \delta_S}, \tag{32}$$

which results in a maximum theoretical concentration of about 220 times. Concentration of light can be achieved with imaging or non-imaging optical elements. While imaging optics is used to transform light in an orderly way, for example to a focal point by the use of a glass lens, non-imaging optics is used for transferring a radiation flux from one area to another where the paths of the individual light rays are of less importance [30]. If imaging concentrators are used for solar energy applications, they have to be able to move and follow the sun's movement across the sky. This concept allows very high concentration ratios to be used and photovoltaic modules for use with such concentrating devices have to be specially designed to allow high illumination levels [82].

With non-imaging optics, it is possible to design devices that concentrate all radiation from a certain angular region of the sky onto a receiver. This means that both the direct radiation (if the sun is in the specified angular region, i.e. within the so-called acceptance angle, θ_a, of the concentrating element) and a substantial part of the diffuse radiation will be transferred to the receiver [83]. This enables the design of concentrators that are static or, alternatively, concentrators of which the inclination is changed a few times per year.

Solar concentrators can also be classified as either point focusing or line focusing. Point focusing systems have circular symmetry and are generally used when high concentration ratios are required. Solar cells in highly concentrating elements see only a small angular interval of the sky, and the system must therefore track the sun. The two most common types of tracking are one-axis tracking, where the array tracks the sun from east to west, or from north to south and back again, during the day, and two-axis tracking, where the normal of the photovoltaic module points directly at the sun at all times. The choice of tracking mode is important in the design of the system. Often, the aim is to maximise output while keeping the concentrating system as simple as possible [84]. Point focus concentrators require two-axis tracking of the sun.

Line focus systems have cylindrical symmetry and are used when moderate concentration (15–30 times) is desired. Line-focusing concentrators require tracking around one axis only (if any). In Paper I and later in this summary, a semi-static, non-imaging, line-focusing compound parabolic concentrator (CPC) with adjustable inclination is considered. Figure 21 shows the three main types of concentrators which are studied in this thesis: a booster reflector, a CPC, and a semi-parabolic over edge reflector.

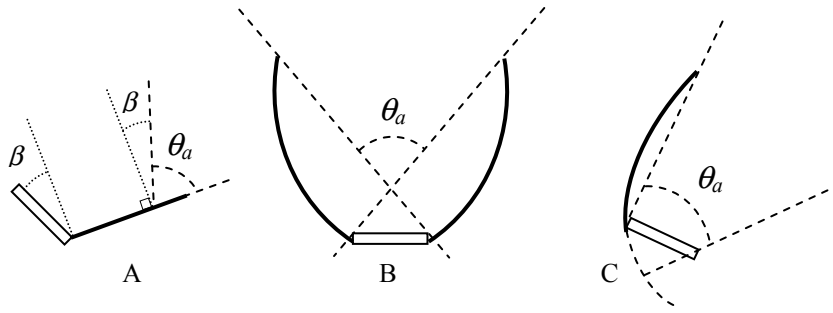

Figure 21: Schematic picture of different types of non-imaging concentrators: a planar booster reflector (A), a compound parabolic concentrator (B), and a parabolic over edge reflector (C). θ_a is the acceptance angle of the reflector, which is, however, not well defined in case A, where it depends on the position on the booster reflector in which the light is incident, and the angle β.

Although higher concentration ratios result in higher light intensities on the cells and a possibility of a lower cost per kWh produced, the necessity of greater initial investments for high-concentrating systems suggests that low-concentrating systems are a good, low-risk solution [85]. Previous studies have indicated that the investment cost per annually delivered kWh of

photovoltaic electricity can be significantly reduced by the use of low-concentrating reflectors [82, 86]. With low-concentrating systems (<5X) it is not necessary to track the sun, and thus facade-integration of the systems is possible, which is an important aspect for installations in urban areas.

6.1. Planar reflectors

The principle use of reflectors is to increase the solar flux on a receiver. One advantage of using planar reflectors in photovoltaic systems is that the irradiance distribution on the receiver will be more uniform as compared to when curved reflectors are used. However, the fundamental disadvantage of planar reflectors is the low concentration ratios obtained. Typically, the concentration ratios for systems with planar reflectors are about 1.5 [82].

At high latitudes, such as in Sweden, ground based solar collectors must be well separated in order to avoid shading due to the low solar altitude, and the distance between the collector rows is normally twice the collector height [46]. Under such conditions, it is advantageous to use booster reflectors between the collectors in a collector field, since instead of letting the solar radiation fall between the collector rows, it can be reflected onto the collectors and increase the collector field efficiency. This way the required ground and collector area can be decreased for a given annual heat production. In Sweden, the optimum tilt angle is approximately 45° from the horizontal plane for the solar collectors and approximately 20° for plane booster reflectors [87]. A solar collector thermal collector field with planar reflectors of corrugated lacquered aluminium is shown in Figure 22.

Figure 22: Solar collectors with planar reflectors of corrugated aluminium. Photo: B. Karlsson.

In Sweden, the annual output from photovoltaic panels can be increased by 20–25% by using fixed planar external reflectors [46]. With 2–8 annual adjustments of the reflector tilt, the annual irradiation increases by up to 40%, compared to a fixed photovoltaic module without reflectors.

Planar reflectors can also be utilised to reduce the seasonal variation in the output from a solar thermal or a photovoltaic system. Figure 23 shows a photograph of an over edge reflector that is used to increase the wintertime radiation on a photovoltaic module that powers control and monitoring equipment for electricity transmission lines. The use of the over edge reflector decreases the battery capacity needed to provide uninterrupted electricity supply. The reflector also protects the module from weather and wind, as well as it prevents snow from covering the module.

Figure 23: Testing of a crystalline silicon module with a planar over edge reflector of anodised aluminium, at Vattenfall Utveckling AB. Photo: M. Brogren.

6.2. Compound parabolic concentrators

According to the literature on solar concentrators, the compound parabolic concentrator (CPC) was invented independently in the United States by Hinterberger and Winston [88], in the Soviet Union by Baranov and Melnikov [89], and in Germany by Ploke [90]. It consists of parabolic reflectors that funnel the radiation from the aperture to the receiver. A CPC can have either cylindrical or circular geometry, although in this work only CPCs with cylindrical geometry are considered. The two halves of a CPC with cylindrical geometry belong to different parabolas, as expressed by the name compound parabolic concentrator. The optical axes of the two

parabolas are tilted an angle $\theta_a=2\theta_{a/2}$ with respect to each other, as illustrated in Figure 24. The angle $\theta_{a/2}$ is the acceptance half-angle of the concentrator. The significance of this angle is that all radiation with an angle of incidence, θ_t, to the optical axis of the CPC within the interval $-\theta_{a/2} \leq \theta_t \leq \theta_{a/2}$ is accepted by the concentrator and reflected onto the receiver, while radiation with $|\theta_t| > \theta_{a/2}$ is rejected by the concentrator [91]. The angular acceptance function of a CPC is also shown in Figure 24. Parametric representations of the CPC, in Cartesian and polar coordinates, can be found elsewhere [30].

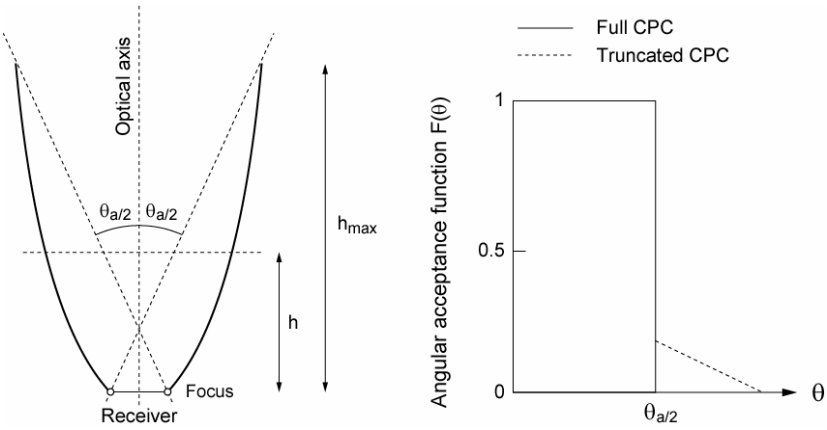

Figure 24: Compound parabolic concentrator, CPC, (left) and the acceptance function of a full and a truncated CPC (right).

The compound parabolic concentrator is the only type of concentrator that reaches the theoretical maximum concentration. For a CPC with cylindrical geometry and an acceptance half-angle of $\theta_{a/2}$, the geometrical concentration, C_g, is given by

$$C_g = \frac{1}{\sin\theta_{a/2}} \quad . \tag{33}$$

Truncation of the CPC is often a practical choice, since it can result in a substantial decrease in reflector area and material consumption, with only a small reduction in concentration [92]. If the upper part of the concentrator is cut away (by cutting through the dashed horizontal line at the height h in Figure 24), the geometrical concentration ratio, C_g, will decrease. On the other hand, a fraction of the radiation reaching the entrance aperture with angles of incidence greater than $\theta_{a/2}$ will reach the receiver directly, as indicated by the dashed line in the angular acceptance function in Figure 24.

A drawback with compound parabolic concentrators is that the irradiance distribution on the receiver is uneven. The parabolic reflectors focus radiation in a sharp line on the receiver in the bottom of the concentrator [84]. Owing to voltage drop and reduced fill-factor at elevated temperatures and resistive losses at high local currents, an uneven irradiance distribution causes power losses and may be critical for the electrical performance of a concentrating photovoltaic system [93]. If highly specular (perfectly smooth, non-scattering) reflectors without geometrical errors are used, there can be areas on the receiver where the irradiance is much higher than on other spots. In practice, however, due to imperfections in geometry and the non-unity reflectance of available reflector materials, the irradiance on the receiver is less uneven than would be the case for a perfect CPC [94]. Still, this implies that if CPCs are used for concentration of radiation onto photovoltaic cells, the design of the cells is critical in order to achieve good electrical performance.

In optical systems that minimise sun tracking to occasional seasonal adjustments, there is a trade-off between the geometrical concentration ratio and the angular interval of the sky over which the solar radiation is accepted. The CPC is well suited for use in such semi-fixed systems. Because of its wide angle of acceptance, the CPC can concentrate solar radiation up to a factor of ten without diurnal tracking of the sun [95]. If compound parabolic concentrators are designed to be fixed with a good year-round performance, an acceptance angle of θ_a>30° is needed, giving a concentration ratio of C_g=2 or less [96]. However, if the tilt angle of the concentrator is changed two or more times a year, the acceptance angle can be smaller, giving concentration ratios of up to C_g =4 [97], see section 6.4.

6.3. Semi-parabolic concentrators

A basic parabola is depicted in Figure 25. It can be described by

$$r = \frac{2f}{1+\cos\varphi} \tag{34}$$

where f is the focal length, r is the radius vector, and φ is the angle between the z axis and the radius vector [98]. Parabolic concentrators are based on the parabolic shape, and in a parabolic concentrator, the z axis in Figure 25 constitutes the optical axis. Parabolic concentrators can be either two- or three-dimensional. Three-dimensional concentrators have rotational symmetry around the optical axis, while two-dimensional concentrators have

translational symmetry. In a concentrating system that utilises a specular two-dimensional parabolic reflector, light that is incident parallel to the optical axis is concentrated on a line in the focus of the system, see Figure 25. In a three-dimensional system, the focus is point-like. If light is incident at an angle to the optical axis, but still within the acceptance angle, θ_a, of the parabola, it will be focused between the vertex and the focal point. For angles of incidence outside the acceptance interval, all radiation will be rejected.

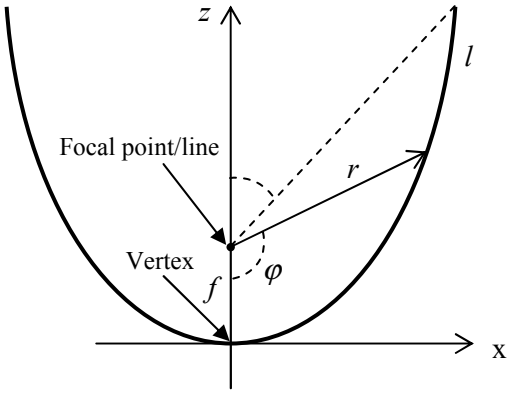

Figure 25: Parabola. The symbols are described in the text above.

A semi-parabolic concentrator utilises only half, or less than half, of the parabola in Figure 25. A schematic drawing of the semi-parabolic concentrator that was studied in Papers III, IV, and V is shown in Figure 26. The letter *h* is the height of the glazing and *a* denotes the width of the module plane. The inclination of the optical axis of the parabolic reflector is denoted by α. In the figure, *f* is the focal length, *F* is the focal point, θ_a is the angle between the vertical glazing and the optical axis, and γ is the angle between the optical axis and the module plane. The system geometry can be varied, for example by adjusting the angles α and γ. The geometrical concentration ratio, C_g, of the semi-parabolic concentrating system is defined as the ratio of *h* to *a*:

$$C_g = \frac{h}{a} = \frac{\cos^2\left(\frac{\gamma}{2}\right)}{\cos^2\left(\frac{\alpha+90}{2}\right)}. \tag{35}$$

All symbols are found in Figure 26. With α=25° and γ=45°, the resulting geometrical concentration ratio is 2.96. However, the maximum flux concentration for a concentrator with this geometry depends on the angle of incidence of the direct solar radiation, and the value given by Equation 35 have to be reduced by a cosine factor to take into account that light is not incident perpendicular to the glazing [99].

When used as concentrators in photovoltaic systems, parabolic reflectors, like the CPC, give a non-uniform illumination of the module that may be critical for its electrical performance [93].

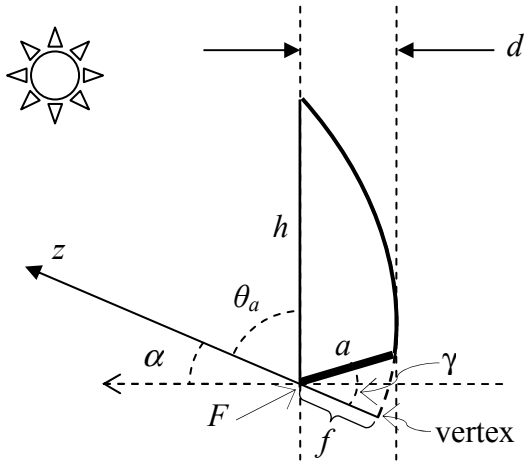

Figure 26: Semi-parabolic over edge reflector. The symbols are described in the text above.

Figure 27 shows a photograph of a 30 m^2 facade-integrated solar thermal collector with semi-parabolic over edge reflectors, similar to the one depicted in Figure 26, which has been operating continuously since 1999 [48].

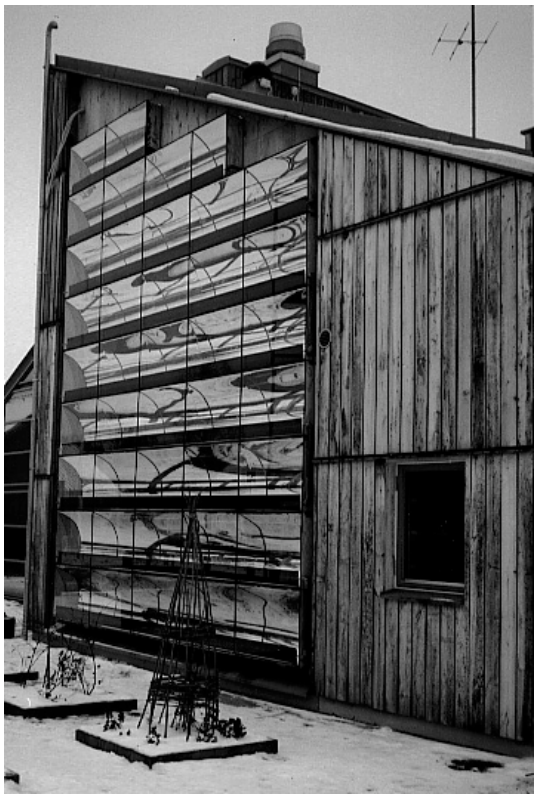

Figure 27: Facade-integrated solar thermal collectors with semi-parabolic over edge reflectors. Photo: B. Karlsson.

6.4. Design of static concentrators

If static concentrators are designed for use at high latitudes, there are some principal differences to take into account compared to if the concentrators are designed for lower latitudes. In southern Europe or at lower latitudes, both winter and summer irradiation gives significant contributions to the annual output of a solar energy system. At high latitudes, for example in the Scandinavian countries, the irradiation during summer is predominating and the winter irradiation is of little importance for the total solar heat or electricity production. Thus, the annual available irradiation at high latitudes is received from a small angular interval of the sky, compared to sites at lower latitudes. In practice, this means that the concentration ratio for static concentrating systems generally can be higher at high latitudes than at low latitudes [100]. For concentrators with seasonal adjustments of the tilt, the number of annual adjustments necessary is lower at higher latitudes.

The irradiation distribution in Sweden is suitable for utilisation of east-west oriented concentrating systems with no or seasonal adjustments of the reflector inclination, because the direct irradiation is very low for low south projection angles during wintertime, which was shown in section 4.3. This implies that systems with east-west oriented two-dimensional concentrating elements can be constructed with a geometrical concentration ratio of 2–3 without any need for sun tracking [44].

The south projection angle, which was introduced in section 4.3, is useful for the design of concentrators. For example, the mean irradiation distribution for Stockholm can be divided in seasonal periods with similar angular width of the distribution in a north-south vertical plane. All the four periods have the irradiation concentrated to an angular interval of $\theta_{NS}\approx 25°$. This means that if an east-west oriented concentrator, e. g. a CPC, is designed for a limited period of the year, or tilted four times per year, the acceptance half angle can be decreased to $\theta_{a/2}=12.5°$, and have a concentration ratio, $C_g=4$. In comparison, a fixed concentrator designed for year round performance would operate at $\theta_{NS}=20°–65°$ and require an acceptance half-angle, $\theta_{a/2}=22.5°$ and a corresponding concentration ratio, $C_g=2.5$ [44].

6.5. Optical efficiency of concentrating systems

The optical efficiency, η_{opt}, limits the electrical performance of a concentrating photovoltaic system. It relates the geometrical concentration ratio to the relative gain in irradiance on the photovoltaic cell area. The ratio of the irradiance on the cell with a concentrator to that without a concentrator is called the optical or flux concentration ratio, C_{opt}, and is given by

$$C_{opt} = \eta_{opt} C_g \,. \tag{36}$$

For a concentrating photovoltaic system, the total system efficiency, η_{system}, defined as the ratio of the electrical power, P_{out}, to the total irradiance on the aperture of the system, I_{tot}, is given by the product of the electrical efficiency of the cell or module, $\eta_{electrical}$, and the optical efficiency, according to

$$\eta_{system} = \frac{P_{out}}{I_{tot}} = \eta_{electrical}\,\eta_{opt} \,. \tag{37}$$

In the case of a photovoltaic-thermal system, the optical efficiency influences the thermal performance as well as the electrical.

The total efficiency of a concentrating solar energy system is to a high extent determined by the optical properties of the components, i.e., the absorptance of the solar cell or thermal absorber, the transmittance of the (optional) cover glazing, and the reflectance of the reflector. The average number of reflections, $\langle n \rangle$, in the reflector before the light reaches the cell surface is often used to calculate reflection losses. In the case where the concentrator consists of a reflector without glazing, the optical efficiency of the concentrator can sometimes be approximated by

$$\eta_{opt} = 1 - R^{\langle n \rangle}, \tag{38}$$

where R is the specular solar reflectance of the reflector. However, Equation 38 is an approximation and the situation is complex for parabolic reflectors, since the solar reflectance depends on the angle of incidence, which is different on different parts of the reflector, and the average number of reflections is different for different solar altitudes.

6.5.1 Models for incidence angle dependence of optical efficiency

The annual production of electricity or heat in a solar energy system depends on the incidence angle dependence of the optical efficiency, η_{opt}, of the system. The optical efficiency of various concentrating systems is assessed in several of the appended papers and in Chapter 10 of this thesis. An experimental characterisation of the angular dependence of the optical performance of a concentrating system requires time-consuming measurements. Therefore, models for the angular dependence of the optical efficiency are often utilised. For planar isotropic systems, the incidence angle dependence of the optical efficiency is often modelled by the function

$$\eta_{opt}(\theta_i) = \eta_n \left[1 - b_0 \left(\frac{1}{\cos \theta_i} - 1 \right) \right], \tag{39}$$

where θ_t is the angle of incidence, η_n is the optical efficiency at normal angle of incidence, and b_0 is the incidence angle modifier coefficient, which is a dimensionless parameter that is obtained from a curve fit to measurement data [33, 101]. Measurements of the angular behaviour of symmetric planar modules and collectors to obtain the parameter b_0 are not overly time-consuming. It should be pointed out, however, that Equation 39 is unphysical for high angles of incidence since it approaches minus infinity when the incidence angle approaches 90°, but it is nevertheless the function

that is most often used for modelling of the angular dependence of planar solar collectors.

Figure 28 shows a concentrating system with an east-west aligned parabolic over edge reflector. For asymmetrical concentrating systems, such as this, it is often convenient to define projection angles in relation to the normal of the glazing of the system. The projected transverse, θ_T, and longitudinal, θ_L, incidence angles are related to the true incidence angle, θ_i, by

$$\tan^2(\theta_i) = \tan^2(\theta_T) + \tan^2(\theta_L) . \tag{40}$$

The projected angles as well as the true incidence angle are shown in Figure 28.

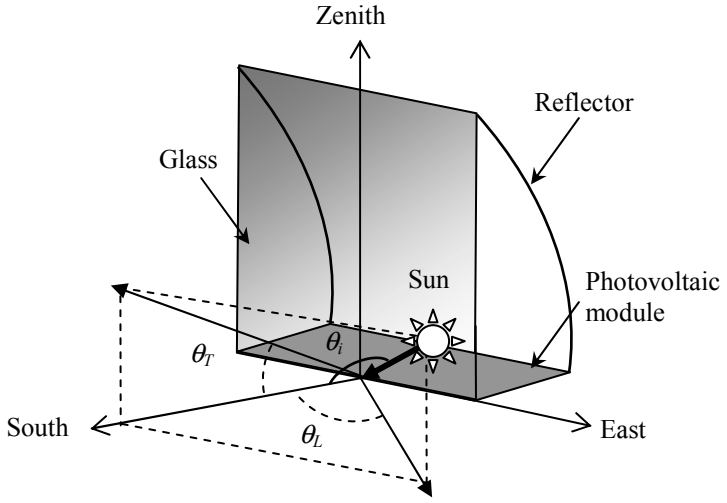

Figure 28: Definitions of the transverse and longitudinal projected incidence angles, θ_T and θ_L, of an east-west aligned concentrator with cylindrical symmetry. θ_i is the true incidence angle.

The system depicted in Figure 28 has cylindrical, or translational, symmetry. The b_0 model cannot be used for concentrating systems, which are asymmetrical about the surface normal, i.e. for which the incidence angle dependence is different in the transverse and the longitudinal directions. Sometimes, the angular dependence for such systems is modelled using a biaxial model:

$$\eta_{opt}(\theta_L, \theta_T) = f_L(\theta_L, 0)\, f_T(0, \theta_T) , \tag{41}$$

where θ_L and θ_T are the incidence angles in the transverse and the longitudinal planes of the concentrator [102]. The two main drawbacks with this model is that one of the functions f_L and f_T has to be normalised, in order not to account twice for the non-unity transmittance of glass at normal incidence, and that it is only correct when radiation is incident in either the transverse or the longitudinal plane. When radiation is incident in any other plane, the model tends to overestimate the optical efficiency for high angles of incidence, since the projected incidence angles are always smaller than the true incidence angle and the transmittance of glass decreases drastically at grazing angles of incidence. Figure 29 shows the solar altitude, the true incidence angle of the direct solar radiation against a vertical wall facing south, and the projected transverse and longitudinal incidence angles against the same wall, in Älvkarleby (60.5°N, 17.4°E), Sweden as functions of the time of the day on the 15th July (left) and on the 24th September (right). The sometimes large differences between the true and the projected incidence angles are clearly visible.

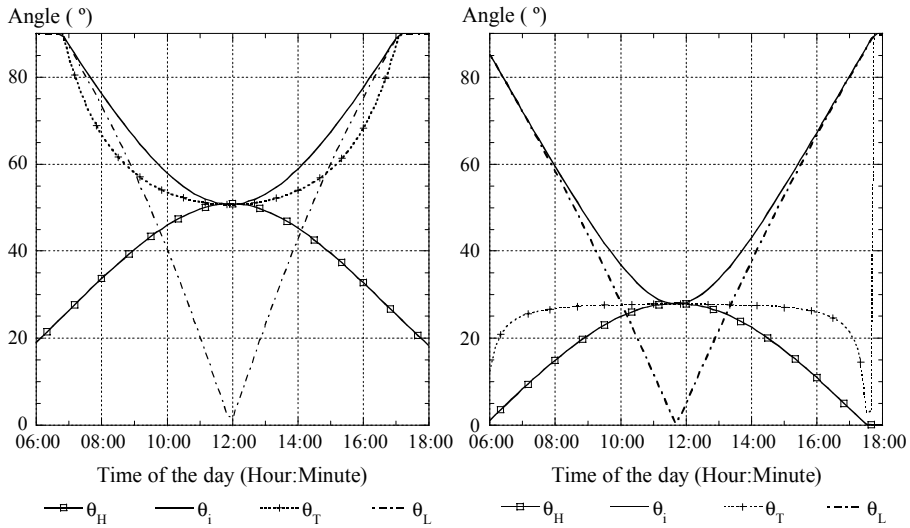

Figure 29: The solar altitude, θ_H, the true incidence angle of the direct solar radiation on a south wall, θ_i, and the projected transverse and longitudinal incidence angles, θ_T and θ_L, on the same wall, in Älvkarleby (60.5°N, 17.4°E), Sweden, as functions of the time of the day on 15th July (left) and 24th September (right).

When calculating the annual heat and electricity production of asymmetric concentrating solar energy systems it is appropriate to use a model that does not exhibit inherent over- or underestimations. Therefore a new biaxial model for the optical efficiency of asymmetric, as well as symmetric,

concentration systems is proposed in section 10.5. For east-west aligned concentrators with a relatively small acceptance angle, however, θ_T is always small and the difference between θ_t and θ_L, is often negligible.

When discussing the usefulness of projection angles for designing and predicting the performance of concentrating systems, it has to be pointed out, that when performing in-detail calculations on the system, such as ray-tracing, the true incidence angle should be used, since the optical properties of the materials depend on polarisation and change with the true incidence angle, and not with any of the projected incidence angles. The abovementioned south projection angle technique also assumes that the concentrating element has an infinite length in the east-west direction and it does not account for any end effects that are caused, for example, by gables on the concentrator. However, the projection angle concept is useful for the geometrical design of the system optics as well as for calculation of the required acceptance angle of a concentrating solar energy system.

6.6. Reflector materials for use in solar concentrators

In many solar energy applications, both solar thermal and photovoltaic, it is cost-effective to use reflectors to increase the irradiance on the receiver (the solar absorber or solar cell), and thereby the heat or electricity production [103, 104]. Reflectors for solar energy applications should fulfil a number of requirements:

- They should reflect as much as possible of the useful incident solar radiation onto the solar thermal absorbers or the photovoltaic cells.
- The reflector material and its support structure should be inexpensive compared to the solar cells or thermal absorbers onto which the reflector concentrates radiation.
- The high reflectance should be maintained during the entire lifetime of the solar collector or photovoltaic module, which is often longer than 20 years.
- If cleaning is necessary, the surface should be easily cleaned with inexpensive detergents, without damaging its optical properties.
- The construction should be mechanically strong to resist hard winds, snow loads, vibrations, etc.
- The reflector should preferably be of light weight and easy to mount.

- The reflector material should be environmentally benign and should not contain any hazardous compounds.
- The visual appearance of the reflector should be aesthetical, since solar concentrators are often large and must be placed fully visible on open spaces so that the concentrator aperture is not shaded by objects in the surroundings.

6.6.1 Optical requirements on reflectors

The optical requirement on reflector materials in solar thermal applications is high reflectance in the entire wavelength range of the solar spectrum (300–2 500 nm). For high-concentrating applications, such as high temperature concentrator solar collectors, the reflectance should be highly specular and light should not be scattered in other directions than the direction of the specular beam. This is crucial for obtaining high irradiance on, for instance, tubular absorbers.

In photovoltaic applications, photons with lower energy than the band gap of the solar cell, which corresponds to wavelengths longer than about 1 100 nm for a silicon cell, do not contribute to the photoelectric conversion but only to overheating. High cell temperatures reduce the output voltage and a high reflectance in the infrared is therefore counterproductive in photovoltaic applications.

In photovoltaic-thermal cogeneration systems, however, the reflectance should be as high as possible at all solar wavelengths, since the heat generated at wavelengths longer than the band gap wavelength, and non-converted absorbed radiation at all solar wavelengths is used for heat production.

Metals that are free electron-like and obey the Drude model [105] are suitable as reflectors for solar thermal applications, but not optimal for photovoltaics. Among the Drude metals, silver and aluminium are the best solar reflectors [32], with a solar hemispherical reflectance values of up to 97% and 92%, respectively. There are, however, no known metals that combine a low reflectance in the near-infrared with a high reflectance in the ultraviolet and the visible, which would make them especially suitable for photovoltaic applications. However, such a selective reflectance response can be obtained by an application of thin films on top of the reflecting metal, which are absorbing in the near-infrared, for example doped tin oxide [106, 107].

6.6.2 Durability of reflector materials

In order to prolong system lifetime and decrease the cost per kWh produced, the reflectors, as well as the modules and glazings, must be sturdy and durable in order to withstand many years of exposure to the outdoor environment. The high reflectance of the reflector material should be maintained during the entire lifetime of the solar collector or the photovoltaic module, which is 20–30 years, depending on type of system and performance criteria [108-110]. Loss of specular and total solar reflectivity can result from erosion or oxidation of the surface, dirt accumulation on the reflector, and action of cleaning agents [111], and while degradation caused by accumulation of dust on the reflecting surface is essentially reversible, surface oxidation is not [112].

Aluminium is the most abundant metal in the Earth's crust. It is inexpensive, has good mechanical properties, and is easy to recycle, but the poor long-term stability of the optical properties, especially the specular reflectance, is a serious drawback [108, 113, 114]. If the aluminium surface is not protected by an additional layer of, for instance, Al_2O_3, a polymer, or a lacquer, its optical performance degrades in a short time [115]. The most common way to protect aluminium from degradation is by anodisation. When direct current at sufficient voltage is passed through an electrolyte, often consisting of sulphuric acid dissolved in water, in which the aluminium is the anode, a layer of alumina (Al_2O_3) is formed on the surface of the aluminium, which protects the metal from further reaction [116]. The thickness of the alumina film on anodised aluminium reflectors is often a couple of microns. The addition of an alumina film reduces the total reflectance of aluminium by a couple of percent, see section 8.3.2.

The degradation of silver is essentially as rapid as that of aluminium [117]. Due to the limited corrosion resistance of the free electron-like metals, they are often used in back surface mirrors, evaporated on the back of a glass or a polymer that protects the metal from oxidation. Among the state-of-the art solar reflector materials are back surface silvered low-iron glass or polymethylmethacrylate (PMMA) [118]. However, glass mirrors tend to be brittle and heavy. Front surface mirrors, on the other hand, are often bendable and of light weight, but more susceptible to chemical attack [119]. The different types of reflectors are shown in figure Figure 47 in section 8.3.

Another way to obtain cost-effective, durable reflectors is to combine favourable properties of different materials into a reflector laminate. This concept was explored in Paper VIII, in which the optical properties and degradation of a polymer-aluminium-steel laminate were evaluated. This reflector combined the good mechanical properties of steel, the high solar

reflectance of aluminium, and the degradation protection of a plastic laminate. The technique of combining different materials by lamination is not new. For example, thin, flexible metal-polymer laminates can be purchased on rolls. Traditionally, these laminates are used within the packaging industry, but there are other applications as well. The combination of materials with different properties makes it possible to tailor the properties of the product for different applications. Since high reflectance is a property that is determined by the surface of the material, it can be created using thin foils (for example of aluminium). The substrate is then chosen to fulfil specific requirements on mechanical properties and a protective coating is used to prevent degradation of the reflective layer. Figure 30 shows a schematic picture of the fabrication of a reflector laminate. The lamination process will differ with the choice of materials in the laminate. If the substrate is a rigid steel sheet, it may be impossible too to use a roll process, and if the protective coating is a lacquer, spray painting may be utilised instead of lamination of the top layer.

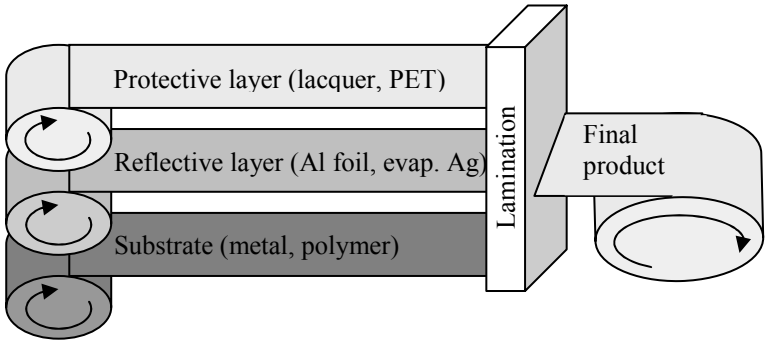

Figure 30: Schematic of the fabrication of a reflector laminate [120].

6.6.3 Cost of reflectors

In Sweden, a solar thermal collector delivers about 380 kWh per m^2 collector area and year, and the total system cost is approximately €200 per m^2 collector area. The increase in annual heat production has been found to be 30% when installing a booster reflector having a solar reflectance of only 63% in front of solar collectors [45]. This means that reflectors are cost-effective if the total cost of the reflector material, its support structure, and mounting does not exceed €60 per m^2 collector area. Reflectors with higher reflectance would give a larger increase in annular heat production and could thus be more expensive and still cost-effective. For photovoltaic systems, a higher reflector cost is acceptable than for solar collector systems, since photovoltaic modules are more expensive than solar thermal absorbers. For

tracking photovoltaic systems, which give a higher annual output per unit cell area than static systems, even higher mirror costs are acceptable, and often unavoidable, since the alignment of the mirror is crucial to the system performance. Costs for reflector maintenance, if applicable, should also be included in the life-cycle cost, although regular maintenance costs are generally not acceptable for solar collector systems, since this makes the generated thermal energy too expensive in comparison with heat produced from other energy sources. For photovoltaic systems, however, there might be economic room for certain maintenance costs, such as cleaning of the reflectors. In this investigation, costs as such have not been considered. However, with long term stable optical properties of the reflector materials, the economic life of a concentrating solar energy system can be prolonged.

When a complete concentrating system is designed, which includes absorbers or photovoltaic cells, reflectors, support structure, and protective glazing, there are many parameters influencing the optimisation process. For example, the optical and mechanical properties of the components may be matched to one another; the glazing and the support structure can be omitted if the reflector has long-term stable optical properties and high mechanical strength.

7. Experimental methods

This chapter describes the methods and instruments that have been used in this work to analyse the performance and degradation of components of photovoltaic and photovoltaic-thermal cogeneration systems. The tools that have been utilised for simulating, evaluating, and optimising system performance are also presented.

7.1. Materials characterisation

The efficiency of a solar energy system is to a large extent determined by the optical properties (transmittance, reflectance, and absorptance) of its components. The optical performance puts an upper limit upon the performance of the system. In solar energy research, it is therefore essential to perform optical characterization of system components. The properties of significance for a concentrating photovoltaic system are the absorptance of the solar cell, the reflectance of the reflector material, and the transmittance of the cover glazing (if applicable). In this work, the optical properties of components of concentrating photovoltaic and photovoltaic-thermal systems were studied using different techniques, which are described below.

7.1.1 Spectrophotometry

The spectral reflectance, transmittance, and absorptance of reflectors, glazings, and solar cells were measured using different spectrophotometers. Such instruments consist in principle of a light source, a grating monochromator, filters, and a detector. In addition, there are mirrors or lenses to guide the light from the light source via the sample to the detector.

The instrument most often used for optical measurements was a Lambda-900 UV/VIS/NIR spectrophotometer from Perkin Elmer, equipped with an integrating sphere. Figure 31 shows a photograph of the Lambda-900 spectrophotometer. With this instrument, the wavelength dependent diffuse and total reflectance and transmittance can be measured at near normal angle of incidence ($\theta_i \approx 8°$) in the wavelength interval 200–3 000 nm. However, at wavelengths, λ, below 250 nm and above 2 500 nm, the absorptance of the

Spectralon® coating on the sphere walls is significant, which reduces the signal and thus the accuracy of the measurements.

Figure 31: Lambda-900 spectrophotometer. The sample holder for reflectance measurements is shown to the right. Photo: M. Brogren.

The measured optical properties were most often recorded at every fifth nanometre between 300 nm and 2 500 nm. This wavelength interval is considered wide enough for optical characterisation, as it covers 98.5% of the total terrestrial solar power [121].

The diffuse reflectance is measured by letting the specularly reflected beam escape through a 3.4×3.4 cm^2 square port in the integrating sphere, while the total reflectance is measured with the port closed. The diameter of the integrating sphere is 15 cm. The large dimensions of the exit port in combination with the relatively small sphere radius results in an angular interval of ±6.5° within which the scattered radiation that exits the sphere in the corners of the port is defined as "specular". The measured diffuse reflectance is thus often underestimated by the instrument. On the other hand, the image of the light source on the sample is oblong, which results in an oval specularly reflected beam, of which the top and bottom parts almost hit the sphere wall instead of escaping through the exit aperture. Thus, light that is reflected with an angle of only a fraction of a degree (which might be called specularly reflected) may miss the exit aperture and be mistaken for diffuse reflectance.

The square shape of the exit aperture in combination with the oblong image of the light source on the sample, thus results in an averaging over an angular interval of ±6.5°, in which part of the reflected radiation will be measured as diffuse and part will be measured as specular. Hence, the geometry of the instrument makes the measured values of the specular and diffuse reflectance uncertain within a few percent. Especially when measuring anisotropically scattering samples, such as rolled metal sheets, the

uncertainty in the measured diffuse reflectance increases [122], and the orientation of the sample must be considered so that a significant part of the low-angle scattered light is not allowed to escape through openings in the sphere wall [122]. Figure 32 shows the interior of the integrating sphere and the reflected chromatic light from a rolled reflector that has the grooves from the rolling process oriented at about 45° with respect to the horizontal. The observed type of scattering is typical of a sample with a one-dimensional surface texture [34]. It is obvious that it is difficult to define the specular reflectance of this type of sample. Furthermore, the mounting of the sample in the exact way that is shown in the figure will allow for the largest fraction of reflected light to escape through the exit port if it was opened, and the diffuse reflectance of the sample would thus be underestimated.

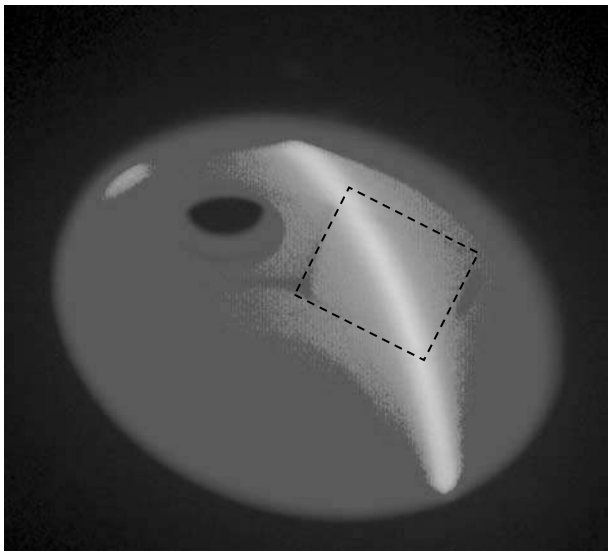

Figure 32: The interior of the integrating sphere during measurement of the total reflectance of a sample with a one-dimensional surface texture. The dashed line indicates the contour of the exit aperture. Photo: M. Brogren.

When the total and diffuse reflectance spectra have been measured, the wavelength dependent specular reflectance can be calculated from the measured total and diffuse reflectance spectra using

$$\rho_{spec}(\lambda) = \rho_{tot}(\lambda) - \rho_{diff}(\lambda) \,. \tag{42}$$

The circular entrance port to the integrating sphere of the Lambda-900 instrument and the sample holder for transmittance measurements is shown in Figure 33. This sample holder does not allow measurements on large

samples, nor can the angle of incidence be changed. The closed square shaped exit port for the specularly reflected beam is visible to the left of the entrance port.

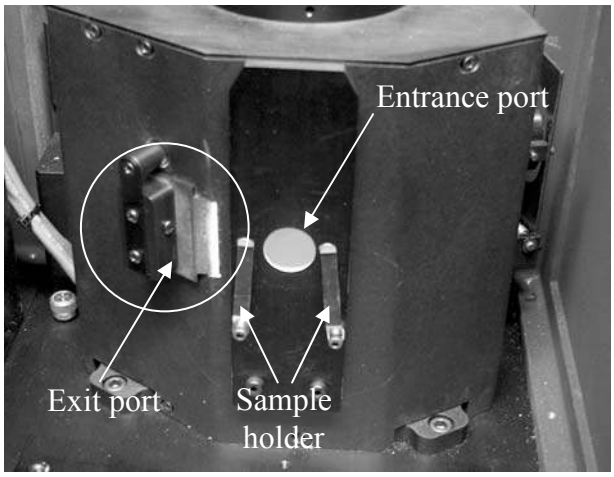

Figure 33: The entrance port of the integrating sphere, the sample holder for transmittance measurements, and the exit port for specularly reflected radiation. Photo: M. Brogren.

For large samples that could not be cut into small pieces that would fit in the sample holder of the Lambda-900 instrument, such as tempered glass, a single-beam spectrophotometer with a an integrating sphere was used. For example, this instrument was used to measure the spectral transmittance of a glazing at several different angles of incidence. This instrument was designed for measurements of reflectance and transmittance versus angle of incidence and, by using different configurations, specular or light scattering samples can be measured [123]. The special design of this instrument makes the specular reflectance measurements absolute, and no standard is required. For specular samples, where the loss of the diffuse signal is regarded as insignificant, the angular variation can therefore be determined with high precision.

The spectral reflectance of a photovoltaic cell was measured at several different angles of incidence in the single-beam spectrophotometer equipped with an integrating sphere. Since the metallic back contact of the silicon cell prohibits transmission at solar wavelengths, it is possible to obtain the cell absorptance from reflectance measurements only.

The infrared reflectance of polymer coated reflectors was measured using a double beam Perkin Elmer 983 Infrared Spectrophotometer in order to

characterise the coatings and compare their absorption in the infrared with characteristic spectra of known polymers.

7.1.2 Spectral averaging

The integrated total solar reflectance values, R_{tot}^{solar}, of reflector surfaces were calculated from measurement data using

$$R_{tot}^{solar} = \frac{\int_0^\infty \rho_{tot}(\lambda)\, I(\lambda)\, d\lambda}{\int_0^\infty I(\lambda)\, d\lambda}, \tag{43}$$

where $I(\lambda)$ denotes the wavelength dependent solar irradiance. The international reference solar spectra ISO 9845-1 for air mass 1.5 were used in the calculations [36]. The standard spectra include the global irradiance on the horizontal and the direct irradiance on a 37° inclined surface. Most often the global spectrum was used. Since the standardised solar spectrum does not contain data for all those wavelengths at which the reflectance measurements were performed, the reflectance was weighted by the solar irradiance at the wavelengths for which data were available in the solar spectrum. This procedure was followed, since the solar spectrum has several strong and narrow absorption bands, which makes it erroneous to interpolate the solar radiation data to fit the data points of the reflectance measurements. Thus, mathematically, the integrals in Equation 43 and the following equations were not calculated as continuous functions, but as summations over a finite number of wavelengths that are specified in the ISO 9845-1 standard.

The specular and the diffuse solar reflectance, R_{spec}^{solar} and R_{diff}^{solar}, were calculated by inserting $\rho_{spec}(\lambda)$ or $\rho_{diff}(\lambda)$ instead of $\rho_{tot}(\lambda)$ in Equation 43. The solar weighted transmittance was obtained by inserting the spectral transmittance instead of the spectral reflectance in Equation 43. The angular dependent solar weighted optical properties were obtained by measuring several reflectance spectra, at different angles of incidence, and using Equation 43 for each of the incidence angles. The solar weighted reflectance could then be plotted as a function of the angle of incidence.

For calculation of the weighted total and specular solar reflectance that is useful for photovoltaic conversion, R_{tot}^{PV} and R_{spec}^{PV}, the spectral response, S, of the specific solar cell that was used in the studied system was included in the calculations of the photovoltaic weighted reflectance values:

$$R_{tot,spec}^{PV} = \frac{\int_0^\infty \rho_{tot,spec}(\lambda)\ S(\lambda)\, I(\lambda)\, d\lambda}{\int_0^\infty S(\lambda)\, I(\lambda) d\lambda}. \tag{44}$$

For simplicity, and to be more generally applicable, the spectral response, S, was sometimes replaced by a step function, f_S, that was adjusted to the band gap wavelength, λ_{bg}, of the solar cell:

$$f_S(\lambda) = \begin{cases} 1 \text{ for } \lambda < \lambda_{\text{bg}} \\ 0 \text{ elsewhere} \end{cases}, \tag{45}$$

resulting in the expression

$$R_{tot,spec} = \frac{\int_0^{\lambda_{bg}} \rho_{tot,spec}(\lambda)\, I(\lambda)\, d\lambda}{\int_0^{\lambda_{bg}} I(\lambda) d\lambda} \tag{46}$$

for the calculation of the photovoltaic weighted reflectance values. One reason for using a step function instead of a true spectral response curve is that the spectral response varies significantly between different types of cells and if a specific response curve is used, the results will only be valid for that specific cell type.

It is possible to calculate the integrated values, T_{tot}^{PV}, T_{spec}^{PV}, R_{tot}^{PV}, and R_{spec}^{PV} at any given angle of incidence. However, this task is complex for the calculation of the weighted values of bent components, such as a parabolic reflector, since the radiation is incident on the surface at a wide range of incidence angles. In principle, the angular behaviour of the photovoltaic cell should also be included in photovoltaics weighted optical properties, but the photovoltaic cell is fairly insensitive to the incidence angle, as will be shown in section 8.1.

7.1.3 Light scattering measurements

The angular distribution of the scattered light influences the performance of solar energy components, such as reflectors and, to a smaller extent, cover glazings. Furthermore, a lot of information about the microscopic structure of a surface can be obtained from the angular distribution of the light that is scattered from the surface [124]. Measurements of light scattering are therefore useful for characterising the quality and degradation of surfaces. Light scattering is usually recorded using monochromatic laser light as a light source.

The spatial distribution of radiation scattered from reflector surfaces was measured using a custom-made angle resolved scatterometer [125]. In these measurements, light from a HeNe laser (λ=632.8 nm) is incident on the sample at an angle that can be altered by a stepper motor. A silicon detector, which is at a distance of 40 cm from the sample, can be moved in the hemisphere above the sample in the azimuth, χ, and zenith, ψ, directions. The angular resolution of the measurements is 1°. Figure 34 shows a schematic layout of the experimental setup to measure light scattering from a sample.

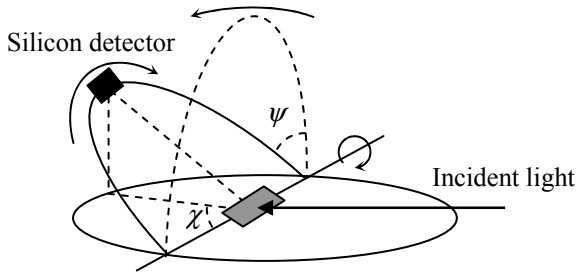

Figure 34: Experimental setup for measurement of scattered light from surfaces. The illuminated surface scatters light into the upper hemisphere and the detector sweeps the upper hemisphere with an angular resolution of 1° in the azimuth, χ, and zenith, ψ, directions.

7.1.4 Optical microscopy and profilometry

The surfaces of some reflector samples were inspected and photographed using an Olympus BX 60 optical microscope equipped with a Ikegami ICD-700PAC CCD color camera, which was connected to a computer for image analysis. The optical microscope is shown in Figure 35.

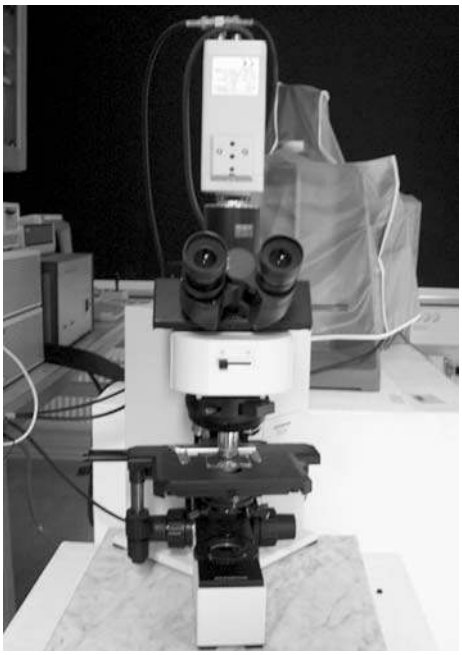

Figure 35: Optical microscope equipped with a CCD colour camera. Photo: M. Brogren.

The surface roughness of a reflector material largely determines the distribution of the light that is scattered from the reflector. It is therefore interesting to measure the surface profile. There are several methods for doing this, but in this work the surfaces of reflector samples were scanned using a profilometer, a Dektak V 200-Si from Veeco. This instrument utilises a sharp tip that is scanned across the surface, in contact with the material. The force on the tip can be adjusted to avoid scratching the surface, but for relatively hard surfaces, such as anodised aluminium, the maximum force of the instrument, which gives the most accurate surface profile, can be used.

In this work, the scans were performed over a 5 mm length of the surface and the root mean square surface roughness (RMS) was calculated. To eliminate the effect of possible bending of the sample upon the calculated surface roughness, a high pass filter was applied. The high pass filter was constructed by fitting a second order polynomial to measurement data and subtracting this polynomial before calculating the surface roughness.

7.2. Ageing of reflector materials

In order to predict the long-term optical efficiency of a concentrator, the initial optical properties of the reflector materials must be known and the degradation of the reflectance due to ageing of the material must be foreseeable. Lifetime tests are therefore eligible prior to application, to prove stability of the optical properties. In this work, several reflector materials, both commercially available and newly developed, that are intended for use in concentrating solar energy systems have been evaluated. In particular, the difference in specularity before and after ageing was investigated as the total and specular reflectance in combination determine the usefulness of the reflector materials in different concentrator applications.

7.2.1 Accelerated ageing in climatic test chamber

Testing in the real outdoor environment is time-consuming and therefore accelerated testing is often undertaken. In this work, samples of several reflector materials were tested in a climatic test chamber of type VCL 4033/MH from Heraeus-Vötsch. The test chamber is shown in Figure 36.

Figure 36: The climatic test chamber. Photo: K. Gelin.

The samples were aged for a total time of 2 000 hours, repeating 400 times the five-hour test cycle which is shown in Figure 36. The test cycle included two different levels of high temperature and two levels of humidity. The relative humidity varied between 50% and 85% and the temperature varied between 40°C and 80°C, resulting in an absolute humidity that is shown in Figure 37. During half of each cycle, the samples were exposed to irradiation

from a 2 kW metal-halogen lamp. The lamp was located in the middle of the ceiling of the chamber, at a distance of 60 cm from the grid upon which the samples were placed. The light intensity on the samples was 1 000 W/m^2, confined to the wavelength range 280 to 3 000 nm. In placing the samples in the test chamber, precaution was taken to expose the entire front surface of all samples uniformly to radiation; the samples were grouped together in the middle of the chamber with narrow gaps between them, where air could circulate.

The reflector samples were taken out and the total and diffuse reflectance was measured after 500 hours, after 1 000 hours, and after completed testing.

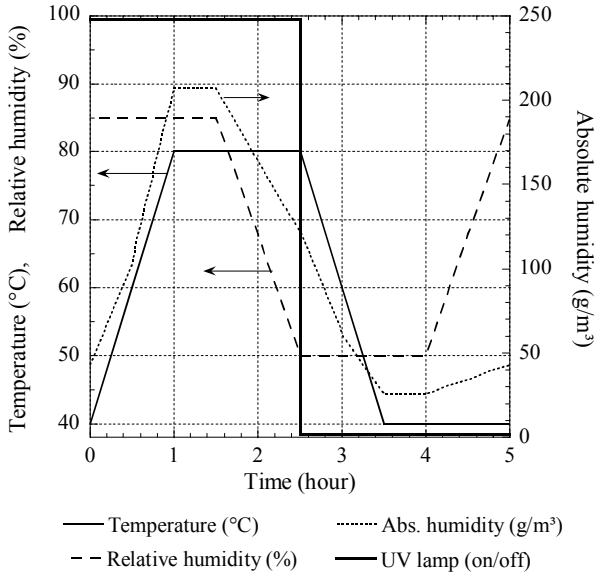

Figure 37: Test cycle for accelerated ageing of reflector materials. The relative humidity varies between 50% and 85%. The temperature varies between 40°C and 80°C. The resulting absolute humidity, as calculated from tabulated data, varies between 40 and 210 g/m^3.

7.2.2 Outdoor ageing

Samples of different reflector materials were also exposed outdoors in order to study degradation in real outdoor conditions and to enable a comparison of the degradation of the samples that was aged in the climatic test chamber and those that were aged in real ambient conditions. Apart from studying the degradation of the optical properties of the specific reflector materials, the

aim of the comparison was to draw conclusions about the applicability of accelerated ageing tests on different types of reflector materials.

Several samples, that were part of the International Energy Agency's Solar Heating and Cooling Programme's investigation of degradation of solar energy components, named Task 27, were tested outdoors. The samples were mounted with an inclination of 30° on a roof facing south at the company Vattenfall Utveckling AB's test facility in Älvkarleby (60.5°N, 17.4°E), Sweden. The total and specular reflectance of the samples were measured before they were put up and after they were taken down nine months or one year later. (The exposure time varied between different tests.) Furthermore, old reflector samples that had been mounted outdoors for almost 20 years were taken down, visually inspected, and their spectral reflectance was measured. The results of the ageing tests are presented in Chapter 8.

Figure 38: Reflector samples mounted for outdoor ageing at Vattenfall Utveckling AB's test facility in Älvkarleby. Photo: M. Brogren.

7.3. Measurements of the output from photovoltaic modules

The generated current and electrical power of concentrating photovoltaic and photovoltaic-thermal systems as a function of solar altitude angle and temperature were measured outdoors as well as indoors using large area solar simulator. In addition to global and direct irradiance, produced power, current, and output voltage, the generated heat and the water temperatures were continuously monitored for the photovoltaic-thermal systems. Current-voltage characteristics of various systems were measured using a variable

resistor or a custom-made current-voltage curve apparatus connected to a data logger.

7.3.1 Outdoor measurements

Since the short-circuit current is directly proportional to the total irradiance on the photovoltaic cell, the optical efficiency of the concentrating system can be obtained if the measured short-circuit current from the module in the concentrating system, I_{SC}^{with}, is divided by the measured short-circuit current from the module without concentration, $I_{SC}^{without}$, and the geometrical concentration ratio, C_g, according to

$$\eta_{opt} = \frac{1}{C_g} \frac{I_{SC}^{with}}{I_{SC}^{without}}. \tag{47}$$

Current-voltage characteristics for modules in concentrating systems were measured outdoors at different solar heights. Most of the measurements were performed with the systems in upright position, like in the leftmost photograph in Figure 39. Short-circuit currents as function of solar height were also measured using the setup showed on the photograph to the right in Figure 39. Here, the system is rotated 90° (it is placed with the left side down) and tilted 30° backwards in order to be able to measure system performance at (constructed) solar heights between -90˚ and 90˚. This type of experiment can only be performed close to the equinoxes, since only at these two times of the year, with the system tilted to 90° minus the latitude (60°N in the case of Uppsala), the sun will move in the plane that is normal to the module and the reflector and each hour will correspond to an angular movement of the sun of 15˚. It is thus possible to measure for example generated power at all solar heights during one single day.

During the outdoor measurements, the total irradiance was continuously measured in the south-facing vertical plane using a small calibrated solar cell and measurement data were normalised to an irradiance of 1 000 W/m^2.

For measurement of module mean temperature, the surface temperature was measured in several points on the front and the back of the module using a Fluke 80T-150 temperature probe. The module mean temperature was then calculated as the arithmetic mean of the temperature at those points.

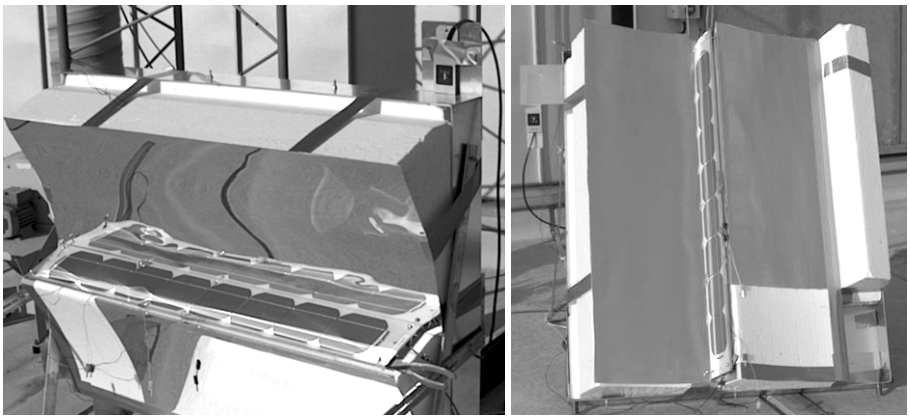

Figure 39: Experimental setup for outdoor measurements of short-circuit current as a function of solar height and current-voltage characteristics at different solar heights (left). Close to the equinox, the system was rotated 90° and tilted 30° backwards for simulation of all solar heights during a single day (right). Photo: M. Brogren.

7.3.2 Solar simulator

A large area solar simulator was used for analysis of various concentrating systems. The solar simulator is shown in Figure 40. The simulator has seven lamps with parabolic reflectors that give essentially parallel light. The solar height can be changed between 0° and 73.5°. Technical details of the solar simulator are given elsewhere [126]. In addition to measurements of short-circuit current characteristics, the solar simulator was used for measurements of the irradiance distribution on modules in a concentrating element for different solar heights. The irradiance was measured using a 3×3 mm^2 silicon detector that was moved in the plane of the module. A stationary identical cell was used as a reference.

The advantage of a solar simulator over the real sun is that in the simulator the solar height can be rapidly changed, which allows thorough characterisation of the optical efficiency of an asymmetrical concentrating system in a short time. If the same characterisation was to be performed outdoors under the real sun, it would take much longer. Furthermore, characterisation for solar heights higher than the available at the specific latitude would not be possible. However, there are some aspects that have to be considered when using a solar simulator: Firstly, the solar simulator that was used in this work gives a non-uniform illumination over the relatively large areas that were analysed. When the simulator is lifted to simulate higher solar azimuth angles, the illumination pattern will move across the studied

system. Therefore it is necessary to continuously measure the irradiation in the module plane in order to enable a correction for the uneven illumination.

The spectrum of the solar simulator is not identical to the ISO AM1.5 spectrum. However, the exact spectral distribution was not regarded as important, since the simulator was used mainly for comparative measurements. Furthermore, the lamps in the solar simulator flicker with the grid frequency (50 Hz). This was accounted for in the measurements, by comparing the probe result with a reference in real time. Given the disadvantages of the solar simulator, outdoor measurements are assumed to give more accurate results for system behaviour.

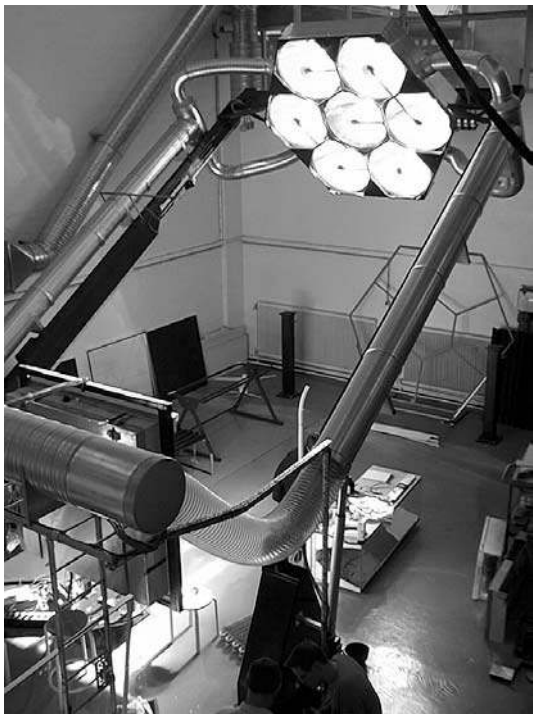

Figure 40: The large area solar simulator in Lund. Photo: J. Wennerberg.

7.4. Modelling, simulation and ray-tracing

Design of fixed concentrating systems is always a trade off between high concentration ratio and time of operation (acceptance angle interval). It is therefore important to carefully design concentrating systems and cells in order to obtain optimum performance. Modelling of the optical system, including the optical properties and the shape of the reflector, followed by

ray-tracing using a simulation program, and investigation of the resulting irradiance distribution on the photovoltaic cells, can be useful tools in the process of optimising system performance.

7.4.1 The MINSUN simulation program

With the MINSUN simulation program, the annual irradiation on an arbitrarily inclined surface can be calculated [127-129]. For example, the optical efficiency of a concentrating system as a function of solar altitude angle, that has been obtained from measurements of the produced short-circuit current, can be used to simulate the annually irradiated energy on the photovoltaic module. The annually produced electrical energy can then be estimated by multiplying the irradiation by the module efficiency.

The MINSUN program was originally developed for simulation of energy yield from flat plate thermal collectors. However, the program can also be utilised for simulation of electricity yield from photovoltaic modules of known nominal power, since it calculates the annual irradiation on a specified surface. The program was used to simulate the annual irradiation on the photovoltaic cell with angular dependent optical losses taken into consideration. MINSUN uses the incidence angle modifier, b_0, which was defined in Equation 39. There is also a possibility to use a biaxial incidence angle modifier. If a biaxial model is used, the program calculates the incidence angle dependent optical efficiency as a product of the incidence angle dependence in the north-south vertical plane and that in the east-west horizontal direction [40]:

$$\eta_{opt}(\theta_i) = g(\gamma_s)\, n(\theta_{NS})\,. \tag{48}$$

In Equation 48, g is a function of the azimuth angle, γ_s, and n is a function of the north-south projection angle, θ_{NS}. Input values are required for both $g(\gamma_s)$ and $n(\theta_{NS})$ for every tenth degree.

In Paper V, the biaxial model in Equation 48 was used to model the angular dependence of the optical efficiency of an east-west aligned concentrating system. In the paper, a b_0-function was utilised for modelling the azimuthal dependence. This approximation was justified by outdoor measurements, which showed that the incidence angle dependence of the concentrating system in the east-west direction was practically equal to the incidence angle dependence in the east-west direction of a flat vertical module [VI, xi]. The variation in the optical efficiency for incidence angles in the north-south vertical plane was calculated from measurements of short-circuit current as function of θ_{NS} for every tenth degree and used in the simulations.

In the calculations in Paper V, the efficiency of the photovoltaic module was set to 13%, but any value of the conversion efficiency could have been used. In Paper IX, the module efficiency was weighted by different fill-factor for different solar altitudes and reflector materials. The angular dependence of the solar cell can also be included in the calculations. However, this dependence is small, which was shown in Paper I.

7.4.2 The OptiCAD ray-tracing program

In Paper IV, modelling of low-concentrating photovoltaic systems with parabolic reflectors and investigation of the irradiance distribution on modules in such systems were performed using the ray-tracing program OptiCAD. One of the objectives was to develop a method for modelling and analysing the optical performance of concentrating systems.

OptiCAD is a commercially available computer program for the design and analysis of three-dimensional optical systems. It utilises a ray-tracing method that follows light in the forward direction, starting at the light source. The program may be used to simulate a variety of non-imaging optical systems and comprises possibilities to model parabolic and flat mirrors, parabolic and elliptical troughs, compound parabolic concentrators, and light sources as well as detectors, which makes it possible to calculate the irradiance on a plane. For all surfaces, the reflectance and absorptance may be specified. OptiCAD also includes models for several types of light scattering that can be applied to the reflecting surfaces.

Figure 41 shows a photovoltaic module (the 20° sloping surface) with a parabolic over edge reflector as it was modelled in OptiCAD. The parabolic reflector, consisting of anodised aluminium, was constructed as a polygonal object with approximately 450 sections constituting the reflective front surface of the parabola. A total reflectance of 83%, with a lambertian diffuse scattering of 2.1%, was assigned to the surface. (These reflectance values were taken from Paper I.) The ray-tracing was performed with a fixed reflectance value on the reflector, without regarding the angular or spectral variations. The solar altitude was 37.5° in the simulation that is shown in the figure. The traced rays are indicated by grey arrows. The high intensity in the middle of the module is clearly visible.

For calculations of the total energy incident on the module at different solar altitudes, which was used for estimation of the optical concentration ratio for different, a collimated beam of rays, distributed in the north-south vertical plane was used. For calculations of the irradiance distribution on the module, “energy bins” were distributed across the module. In order to account for the

half-angle of the solar disc of 0.27° [130], which gives a deviation from the simple case of perfectly parallel rays, the ray-tracing was performed at two different solar altitudes, separated by 0.54°, and the mean value of the irradiance on each energy bin was calculated.

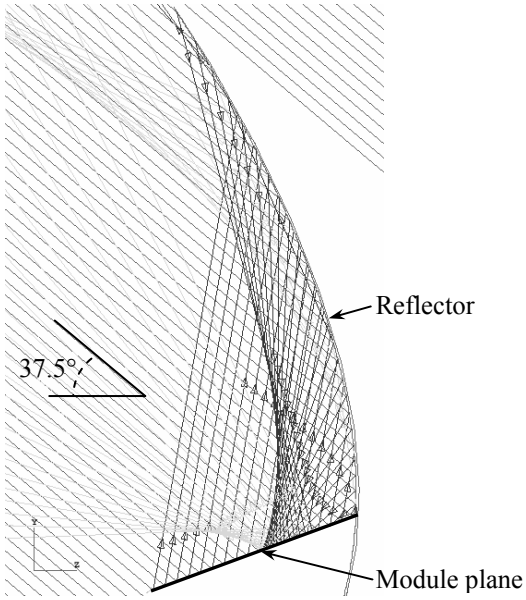

Figure 41: OptiCAD model of a concentrating element. The grey arrows indicate the directions of the traced rays. The solar altitude angle was 37.5° in this simulation.

7.4.3 Modelling of the optical properties of materials

Modelling, based on the Fresnel formalism in section 3.3, of the optical properties of various solar energy materials was performed in order to validate measurements and to obtain the thickness of the thin films. A Matlab Fresnel program was used in the modelling. The program can model the reflectance, transmittance, and absorbtance of a stack of maximum three films of arbitrary thickness on a glass substrate. The model assumes homogeneous films and ideal interfaces. Tabulated complex refractive index data in the wavelength interval $300<\lambda<2\ 500$ nm for various elements and compounds were used in the modelling.

8. Optical properties and degradation of system components

The efficiency of a concentrating photovoltaic or photovoltaic-thermal system is to a large extent determined by the optical properties of the system components, i.e. the cover glazing, the reflector, and the photovoltaic cells or the combined photovoltaic-thermal absorber. In this chapter, some results from the measurements of material properties of solar energy system components are presented. Measurements of the optical properties of reflectors were performed on fresh samples as well as on samples that had been aged outdoors and in a climatic test chamber. Reflector surfaces were analysed by profilometry and studied in an optical microscope in order to obtain a better understanding of what processes that govern surface degradation.

8.1. Photovoltaic cells

The spectral response is a measure of how well a solar cell converts solar radiation of different wavelengths into electricity [57]. It depends on the absorption and the band gap of the semiconductor material. The spectral response curve is therefore different for different solar cells. Figure 42 shows the solar spectrum together with the normalised spectral response curves of a copper-indium-gallium-diselenide (CIGS) cell and a mono-crystalline silicon cell of the same type as those that were used in the photovoltaic-thermal cogeneration system [I]. The spectral response of the silicon cell was measured by the Institute for Environment and Sustainability, which is part of the Joint Research Centre of the European Commission. The spectral response of the CIGS cell was calculated from quantum efficiency data[10]. Figure 42 shows that the CIGS cell converts solar radiation in the wavelength interval 360–1 350 nm into electricity and that the conversion is most efficient at around 1 000 nm, whereas the silicon cell converts radiation in the wavelength interval 300–1 150 nm and most efficiently at around 900 nm.

[10] J. Malmström at the Division of Solid State Electronics, Department of Engineering Sciences, Uppsala University, is acknowledged for spectral quantum efficiency data.

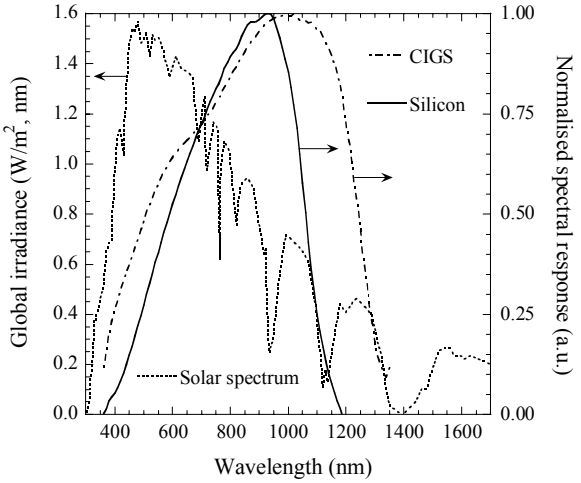

Figure 42: The global solar spectrum (ISO AM1.5) [36] and the normalised spectral response at near normal angle of incidence for a mono-crystalline silicon solar cell and a CIGS cell, in the wavelength interval 300–1 700 nm. The spectral response of the silicon cell was measured by the Institute for Environment and Sustainability of the European Commission and the spectral response of the CIGS module is courtesy of J. Malmström.

The total reflectance of the photovoltaic cell was measured using a single-beam integrating sphere designed for measurements at oblique angles of incidence [123]. The measurements were performed at incidence angles of 0°, 10°, 45°, 60°, and 75° as shown in Figure 43. Concern was taken to avoid measurements on the two metallic contacts on the front side of the cell. The band gap of silicon is clearly indicated by the increase in the reflectance spectra for wavelengths longer than 1 100 nm. At even longer wavelengths, where silicon is transparent, the metallic contact on the rear side of the silicon wafer also contributes to the reflectance, which increases accordingly.

The efficiency of a photovoltaic cell depends on the angle of incidence. In Paper I, the normalised optical angular solar cell efficiency, $\eta_{cell}(\theta_i)$, which is based on measurements of angular dependent cell absorptance, was formulated as a measure of how well a photovoltaic cell responds to solar radiation at non-normal angles of incidence compared to radiation at normal incidence. The normalised optical angular solar cell efficiency was calculated using

$$\eta_{cell}(\theta_i) = \frac{\int_{0.3}^{1.1} \alpha(\lambda, \theta_i)\, G(\lambda)\, S_n(\lambda)\, d\lambda}{\int_{0.3}^{1.1} \alpha(\lambda, \theta_i = 0°)\, G(\lambda)\, S_n(\lambda)\, d\lambda} \tag{49}$$

where θ_i is the angle of incidence, α is the measured absorptance, and S_n is the normalised spectral response of the cell. The normalised optical angular solar cell efficiency for a silicon cell is shown in Figure 44. The normalised optical angular efficiency is fairly flat and higher than 93% for incidence angles below 75°. This fact justifies omission of the angular behaviour of the photovoltaic cell in calculations of the angular dependence of the optical efficiency of concentrating systems.

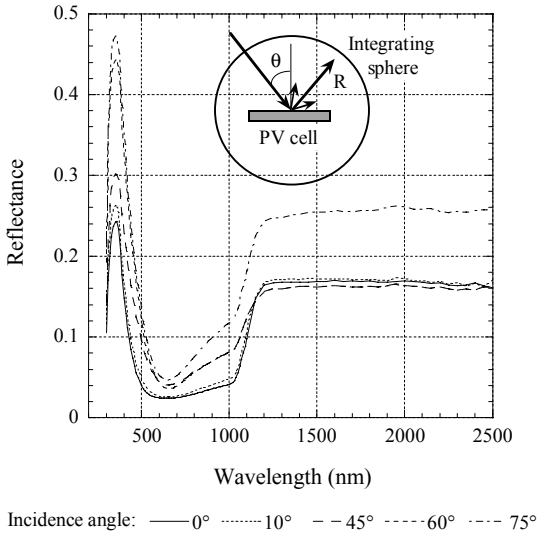

Figure 43: Angular dependent reflectance of a silicon photovoltaic cell, measured at the incidence angles of 0°, 10°, 45°, 60°, and 75° with a single beam integrating sphere.

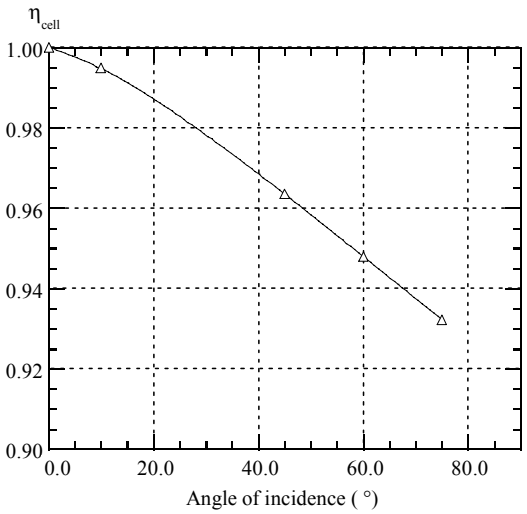

Figure 44: Normalised optical angular solar cell efficiency for the mono-crystalline silicon cell used in the concentrating photovoltaic-thermal system with compound parabolic concentrators.

8.2. Cover glazings

Due to its favourable optical and mechanical properties, glass is used as a protective cover over the active components (the absorber or photovoltaic cell and the reflectors, if such are used) in most solar energy applications. Glass is resistant to ageing outdoors and the solar weighted transmittance at normal angle of incidence is often above 90% for glass with low iron oxide content. Ordinary float glass contains a significant amount of iron oxide, which makes it absorbing thus unsuited for solar energy applications.

The transmittance of low-iron glass can be further increased by an anti-reflection treatment. An anti-reflection coating can be obtained by the deposition on both sides of the cover glazing of a thin dielectric film with an index of refraction, n_{AR}, that is given by

$$n_{AR} = \sqrt{n_{glass}}\ , \tag{50}$$

where n_{glass} is the index of refraction of the glass. Several different methods can be used for anti-reflection treatment of glass. For the glazing used in the photovoltaic-thermal cogeneration system [I], etching of the surface of the glass with fluosilicic acid was performed by Sunarc, Denmark [131]. It has been shown that this kind of anti-reflection treatment is stable outdoors for at

least seven years [132]. Figure 45 shows the wavelength dependent specular transmittance of the anti-reflection coated cover glass for different angles of incidence, measured with the absolute instrument. The solar weighted transmittance values for the different angles of incidence are indicated in the figure. The maximum in the transmittance is obtained at around 600 nm. Absorption due to non-negligible iron oxide content is the cause of the slight dip in the transmittance spectrum in the near-infrared.

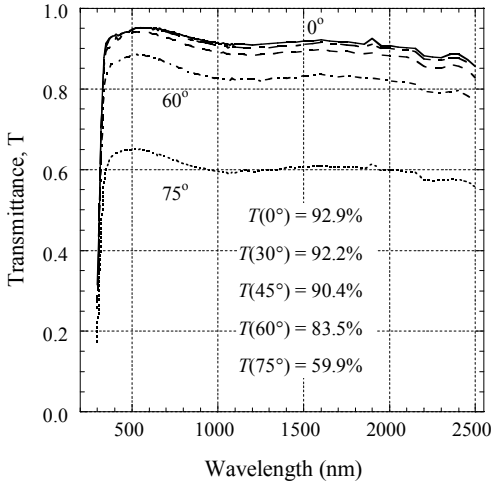

Figure 45: Spectral transmittance of anti-reflectance treated glass for different angles of incidence [I]. The corresponding integrated total solar transmittance values are also shown.

The transmittance of the glass, weighted by the solar spectrum and the spectral response of a spectral response, T_{PV}^{glass}, was determined to be 93% at near normal angle of incidence. The thus weighted transmittance as a function of the angle of incidence is shown in Figure 46. A comparison with an identical glass without an anti-reflection coating, gave that the anti-reflection treatment increased the solar photovoltaic weighted transmittance by about 4.4% for all angles of incidence [I].

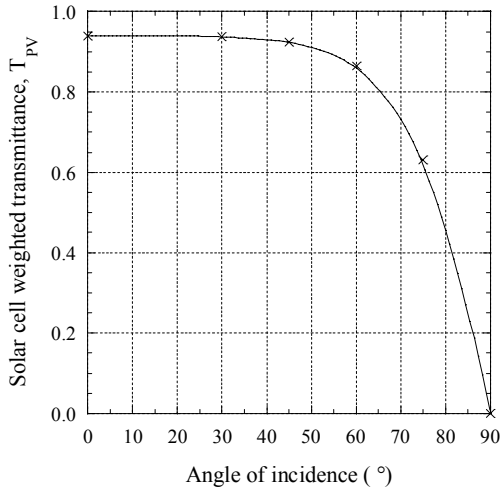

Figure 46: The transmittance of the anti-reflectance treated cover glass, weighted by the spectral response of the solar cell and the direct AM1.5 solar spectrum [I].

It is possible to further increase the solar transmittance of the anti-reflectance treated glass by improving the index matching between glass and film [133]. Since the increase in the delivered electrical energy is proportional to the irradiance on the photovoltaic module and thus to the increase in solar photovoltaic weighted transmittance of the glass, the currently used anti-reflection treatment increases the output from the photovoltaic module by 4.4% compared to an untreated glazing. The transmittance of the glazing could be increased by more than 6% in comparison with the uncoated case by using an optimized anti-reflection treatment [134].

8.3. Reflector materials

Figure 47 shows different types of reflector materials that have been studied in this work. There are two principally different types of reflectors: front surface mirrors and back surface mirrors. The latter, which are also called second surface mirrors, have a superstrate configuration, i.e. the structural part of the reflector is the front surface. The reflective layer of a second surface reflector consists of a sputtered, evaporated, sprayed, or otherwise deposited highly reflective material, most often silver or aluminium. The superstrate protects the front surface of the reflective layer. The back surface of the reflective layer is often protected from corrosion by a layer of paint or lacquer. In a front surface reflector, on the other hand, the reflective material

is often the structural material as well, as for metal sheet reflectors. However, if the reflective layer is a thin metal sheet or a foil it can be laminated on a substrate of, for example, rigid steel or a flexible polymer, whichever suits the application best. In a substrate configuration, it is also often necessary to protect the front surface of the reflective material from degradation. For aluminium sheet, this is most often done by anodisation, which results in a protective layer of alumina (Al_2O_3) on the surface, or by coating the surface with a layer of lacquer. Thin film coated reflectors, which use a combination of thin films with carefully chosen indices of refraction to enhance the reflectance of a metallic substrate by interference, are a variation of the substrate type of reflector. There are also all-polymer reflectors, i.e. reflectors that do not have a metallic substrate, which utilise interference in stacks of thin films for creating a high solar reflectance. However, these materials are newly developed, and to my knowledge not yet used in solar concentrator applications, and have not been studied in this thesis.

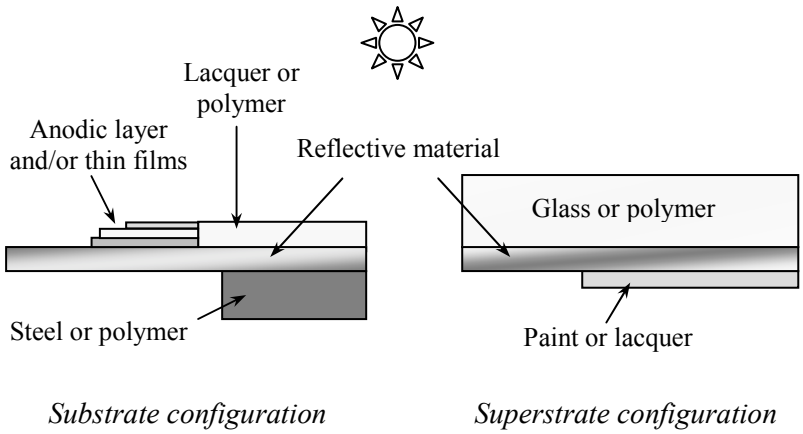

Figure 47: Reflector materials that have been studied in this work. To the left are front surface reflectors, based on a reflective metal sheet or foil. To the right are back surface mirrors, in which the reflective layer is deposited on the back surface of a protective glass or polymer.

8.3.1 Optical properties and degradation of reflectors

Papers VII–IX deal primarily with the optical properties and degradation of reflector materials. Unless stated otherwise, all optical measurements were performed with the same spectrophotometer (Lambda-900) and the same reference. The data for fresh and aged samples are thus comparable.

In Chapter 9, the performance of a photovoltaic-thermal system with compound parabolic concentrators is discussed. The reflector material that is

used in this photovoltaic-thermal system is anodised aluminium. The measured total solar reflectance of this reflector was determined to approximately 83% at an incidence angle of 60°, but the anodised aluminium was slightly scattering and the specular solar reflectance was roughly 81% [I]. In a later project, the total and specular solar weighted reflectance values at near normal angle of incidence of another sample of fresh anodised aluminium were found to be 88% and 87%, respectively [IIV]. The measured total and specular reflectance spectra of the latter type of anodised aluminium are shown in Figure 48, together with the ISO AM1.5 spectrum [36]. The interband transition of aluminium at approximately 860 nm is clearly visible in the figure, as well as the interference fringes caused by the aluminium oxide (Al_2O_3) layer. Modelling of the Fresnel reflectance of Al_2O_3 layers of varying thickness on an opaque aluminium substrate and a comparison between the simulated reflectance spectra and the interference structure of the measured reflectance spectrum indicated that the effective thickness of the anodic layer of this sample of anodised aluminium was about 0.8 µm. The modelled reflectance spectrum of a 0.8 µm Al_2O_3 film on aluminium is included in Figure 48. The solar weighted reflectance of the modelled reflector differs by less than 1% from the measured total reflectance.

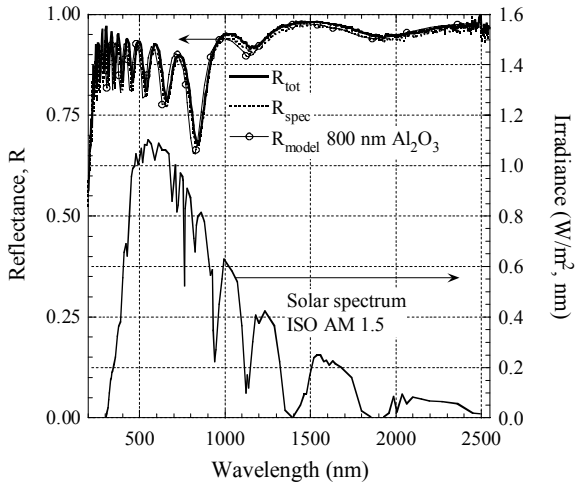

Figure 48: Measured total and specular spectral reflectance of anodised aluminium, the modelled reflectance spectrum for aluminium with an 800 nm layer of alumina, and the direct AM1.5 solar spectrum [IIV].

Figure 49 shows a photograph, taken with an optical microscope, of the surface of a fresh sample of anodised aluminium. Small surface defects are visible on the anodised aluminium. These defects may be starting points for

pit corrosion. The oblong defect to the left is approximately 50 μm long and 5–10 μm deep.

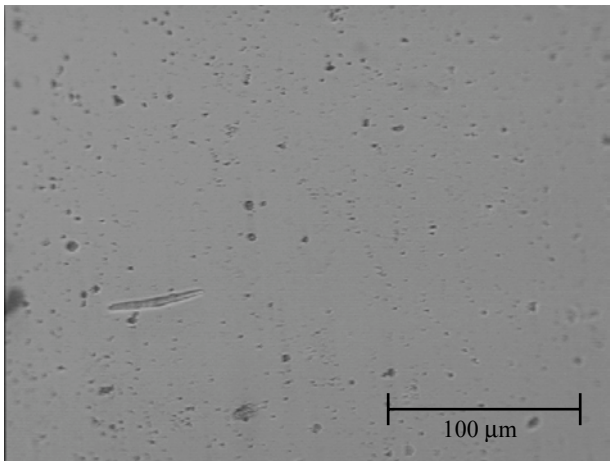

Figure 49: Photograph of a 320×240 μm^2 area of anodised aluminium. Photo: M. Brogren.

The specular properties of unprotected anodised aluminium has been found to deteriorate after a few years of outdoor ageing [108], but the behaviour under a protective cover glazing is better. After one and a half year of operation, the reflector in the concentrating photovoltaic-thermal system, which has a glazing, did not show any visible signs of ageing. However, after three years, there were visible signs of degradation and milky roses could be seen on the surface. The optical properties of a sample of anodised aluminium that had been mounted horizontally outdoors for 18 years were also investigated in this work. The surface of this reflector sample showed visible signs of degradation; it was fairly rough, with slightly brownish patches. Approximately 75% of the initially smooth surface, which resulted in a high initial specular reflectance, was corroded. A photograph of the surface of the aged anodised aluminium reflector, taken with an optical microscope, is shown in Figure 50. Figure 51 shows the surface roughness of a fresh sample of anodised aluminium and the sample of anodised aluminium that had been mounted outdoors for 18 years. The surface roughness was measured with a profilometer. The total scan length was 5 μm, but the figure shows only a part of the measured profiles. The measured surface roughness values were 50 nm for the fresh sample and 700 nm for the aged sample. Thus, the surface of the anodised aluminium that had been exposed outdoors for 18 years was more than an order of magnitude rougher than the surface of the unexposed anodised aluminium.

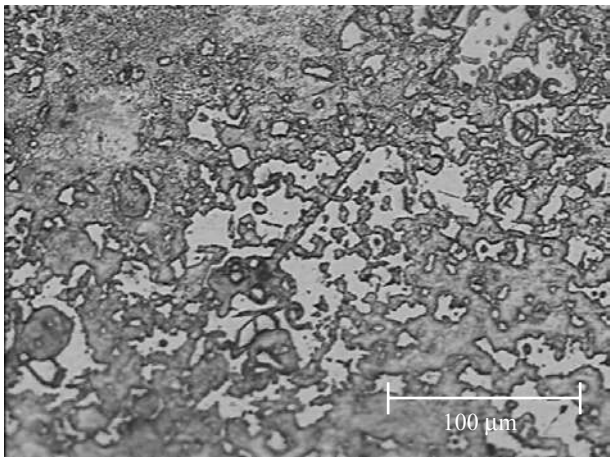

Figure 50: Photograph of a 320×240 µm^2 area of anodised aluminium that had been exposed outdoors for 18 years. Photo: M. Brogren.

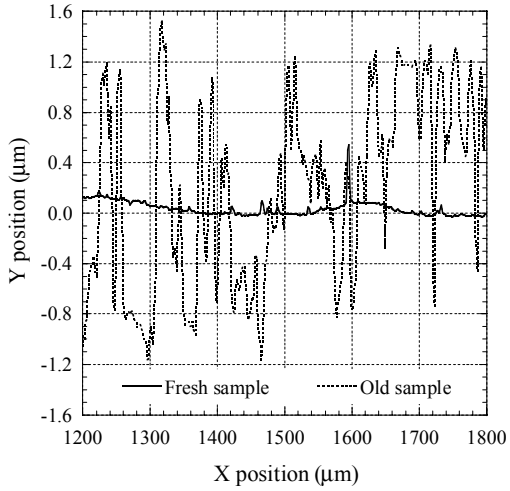

Figure 51: Surface profile of a fresh and an old sample of anodised aluminium, measured with a profilometer.

Figure 52 shows the measured total and specular reflectance of the anodised aluminium sample that had been aged outdoors for 18 years. The total solar weighted reflectance of this reflector was 77% but the specular reflectance was as low as 20%. The solar photovoltaics weighted values were even lower: 75% and 18%, respectively. The photograph and the reflectance spectrum show that unprotected anodised aluminium reflectors degrade severely when they are exposed outdoors for long periods.

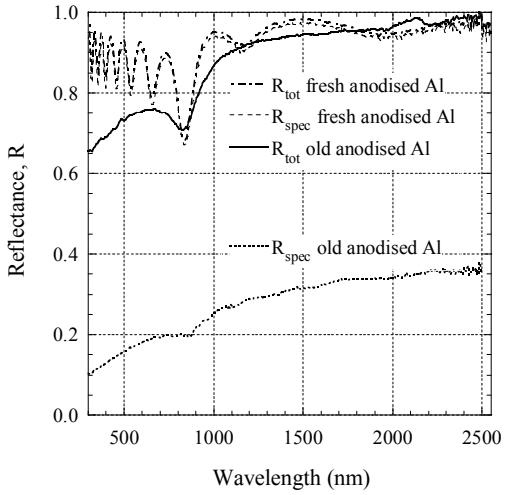

Figure 52: The total and specular reflectance of an old anodised aluminium reflector that had been exposed outdoors in Älvkarleby (60.5°N, 17.4°E) for 18 years. The total and specular reflectance spectra for fresh anodised aluminium are shown for comparison.

There are solar reflector materials which have considerably higher solar reflectance than anodised aluminium. Figure 53 shows the reflectance spectrum for a second surface silver mirror that reflects 90% of the solar radiation [VII]. The high reflectance in the visible and the infrared of the silver mirror is typical for a free electron-like material. The evaporated silver layer and the smooth glass surface make the silvered glass mirror almost completely specular. The reflective silver layer is deposited on the back of a 1.2 mm glass superstrate. The dip in the reflectance spectrum between 600 nm and 1 500 nm is due to absorption in the glass and indicates that the iron oxide content of this glass is not negligible. This absorption is the cause of the relatively low solar weighted reflectance, for a silver mirror. The silver mirror was highly specular, even after 2 000 hours in damp heat. The good durability of the optical properties of the second surface glass mirror is due to the glass that protects the front surface of the evaporated silver and a layer of paint that protects the back surface of the silver layer.

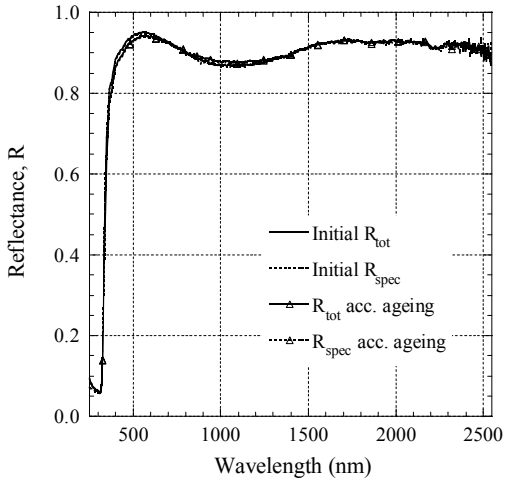

Figure 53: Total and specular reflectance of a second surface silver mirror, initially and after 2 000 hours of accelerated ageing [IIV].

Other highly reflective materials consist of multi-layer thin film stacks (usually of titania, which has a high index of refraction, and silica, which has a low index of refraction) on aluminium. Figure 54 shows the measured spectral total and specular reflectance of two thin film-coated aluminium based reflectors. A difference between the two reflectors is that one is coated by a lacquer. In contrast to Figure 48 and Figure 53, which are plotted with a linear wavelength axis, Figure 54 has a logarithmic wavelength scale. The reason for this is to show the characteristics of the material's reflectance in the solar wavelength range more clearly. The difference between the reflectance spectra of the two thin film-coated reflectors is that the material without a lacquer has a slightly shorter cut-off wavelength than the lacquered reflector, but a lower reflectance around 1 000 nm. These features reduce the solar reflectance to similar extents for the two reflector materials and the total solar weighted reflectance values are 89% for the uncoated thin film reflector and 90% for the thin film reflector with lacquer. The spectrum of the lacquered reflector has a clear interference structure, due to the layer of lacquer. The thickness of the lacquer was determined by Fresnel modelling to about 2 µm. While the anodised aluminium, the second surface silver mirror, and the uncoated thin film reflector have small (≤2%) diffuse components of the reflectance, the lacquer causes a diffuse solar reflectance of above 3% for this reflector material.

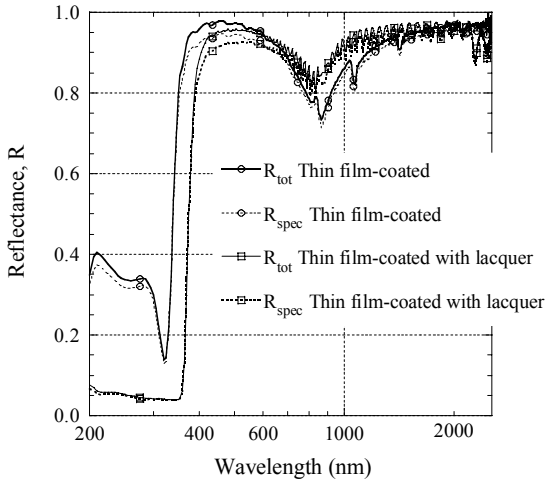

Figure 54: Measured total and diffuse reflectance spectra for two different thin film-coated aluminium based reflectors at near normal angle of incidence, plotted on a logarithmic wavelength scale.

The thin film-coated reflectors were degradation tested outdoors and in the climatic test chamber. While the unprotected thin film-coated reflector passed the accelerated testing fairly well [IIV], it showed a significant decrease in the specular reflectance after outdoor exposure, see Figure 55. Furthermore, interference fringes appeared in the diffuse reflectance. This indicates that there has been a change in the materials properties at one or both interfaces between the thin films and the aluminium substrate [135].

The angular optical properties of thin film coated materials that utilise interference to enhance the reflectance often vary strongly with the incidence angle. Since typical incidence angles in parabolic concentrators are high, Fresnel calculations were made to study the optical properties at high angles of incidence of a reflector consisting of an aluminium substrate coated with thin films of silica and titania. The optical constants of silica and titania that were used in the calculations were obtained from ellipsometric measurements [I]. It was found that by modifying the thickness of the outer layer of titania and of the inner layer of silica, it was possible to obtain higher reflectance values than for pure aluminium, even at glancing angles of incidence. This is illustrated in Figure 56, where the solar cell weighted reflectance has been calculated for the thin film-coated reflector material as a function of angle of incidence. Figure 56 also shows the solar photovoltaics weighted reflectance values of anodised aluminium and a back surface silver mirror, which were obtained by Fresnel calculations, as a function of incidence angle [I].

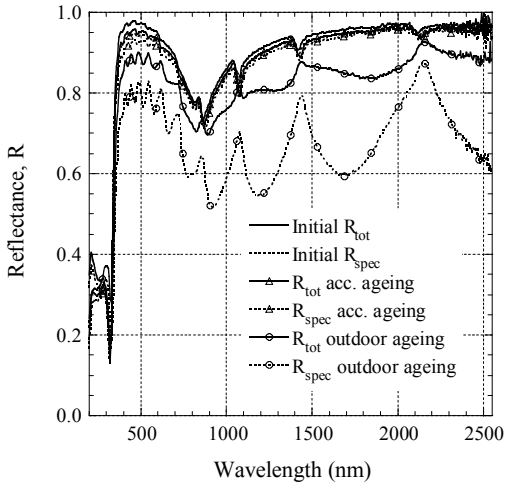

Figure 55: Measured total and specular reflectance of the thin film coated reflector without lacquer, initially, after outdoor ageing, and after 2000 hours of accelerated ageing in the climatic test chamber.

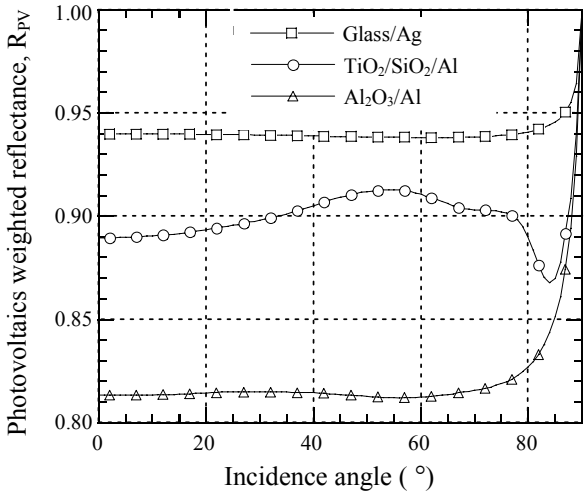

Figure 56: Comparison between the incidence angle dependent reflectance spectra of three different reflector materials: a second surface silver mirror (□), an optimised thin film-coated reflector (○), and anodised aluminium (Δ). The spectra are shown for unpolarised light [I].

Figure 57 shows measured total and speular reflectance of two flexible aluminium based reflector laminates. One consists of a reflective surface of aluminium that is evaporated on a polymethylmethacrylate (PMMA) foil that serves as surface protection. Beneath the evaporated aluminium there is a rolled aluminium foil and the PMMA/Al/Al sandwich is laminated on a flexible polyethylene terephthalate (PET) substrate. The reflective layer of the other reflector laminate is the same type of rolled aluminium foil as in the above mentioned reflector. This foil is laminated on a PET substrate and coated with a layer of lacquer. It is the protective PMMA foil on the first type of reflector that causes the cut-off at 400 nm in the reflectance spectra in Figure 57. The second type of reflector does not show this behaviour, since the lacquer that is used for protection of the reflective rolled aluminium foil is not as absorbing in the ultraviolet as the PMMA foil. The initial total reflectance, measured at near normal angle of incidence, was 85% for both reflectors. However, due to the grooves from the rolling process in the active reflector layer of the second type of reflector laminate, the specular reflectance of this reflector was only 58%, while it was 79% for the reflector with a reflective layer of evaporated aluminium.

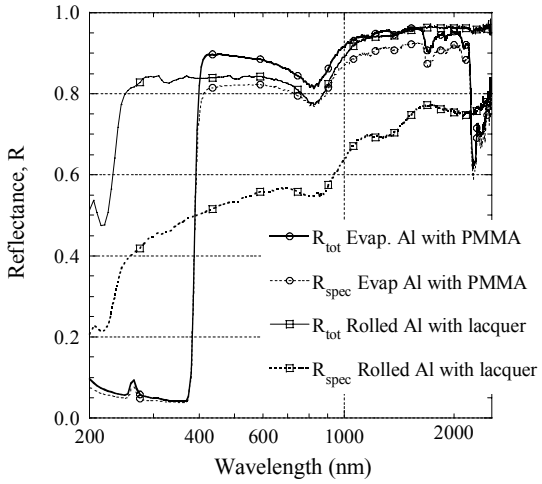

Figure 57: Measured initial total and diffuse reflectance for two flexible aluminium based reflector laminates. Note the logarithmic wavelength scale [VII].

Figure 58 shows a photograph of the surface of a fresh sample of the lacquered rolled aluminium reflector on a PET substrate. The grooves in Figure 58 originate from the rolling process and are approximately 5 μm wide. The grooves in the reflective surface make this reflector scatter light

anisotropically. The light scattering is higher in the direction perpendicular to the grooves. This can be seen Figure 59, which shows the scattered intensity in the perpendicular χ and ψ directions for a lacquered rolled reflector. The scattered intensity in the perpendicular χ and ψ directions for an anodised aluminium reflector is shown for comparison.

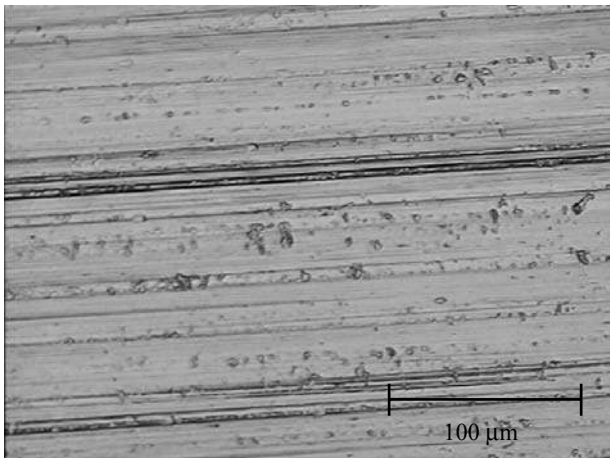

Figure 58: Photograph of a 320×240 µm^2 area of a lacquered rolled aluminium reflector on a flexible PET substrate. Photo: M. Brogren.

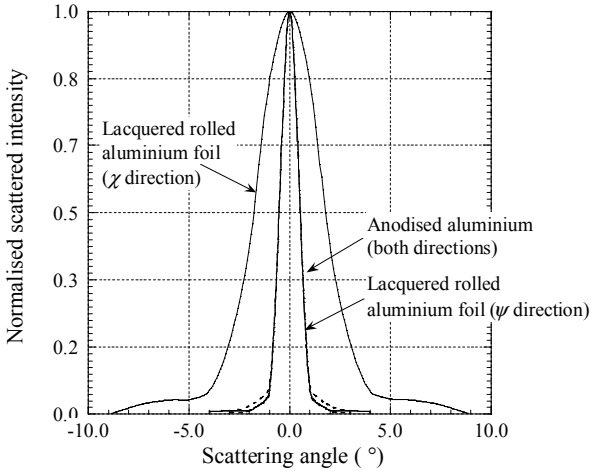

Figure 59: Scattered intensity in the χ and ψ directions for a lacquered rolled reflector and an anodised aluminium reflector. Note that there are three almost perfectly overlapping curves in the narrower of the bell curves [IX].

After 2 000 hours of accelerated ageing, the specular reflectance of the laminate with a reflective layer of evaporated aluminium had decreased to 7.5%, while the total reflectance was 82% [VII]. By visual inspection milky roses were found on the aluminium foil under the PMMA film. The lacquered reflector laminate withstood accelerated ageing better, probably due to a better contact between the lacquer and the foil, than between the PMMA and the thin reflective layer evaporated aluminium. The measured total and specular reflectance of the lacquered reflector after 2 000 hours of accelerated ageing were 82% and 51%, respectively. Nine months of outdoor exposure only degraded the reflectance of these two samples marginally [VII].

In Paper VIII, the optical properties and degradation of a polymer-aluminium-laminated steel reflector were investigated. The protective top layer of the laminate consists of PET on the back of which an aluminium film is evaporated. Beneath, there is a foil of rolled aluminium and another PET layer. The PET/Al/Al/PET-sandwich is then laminated on a steel substrate. A schematic of the lamination process for manufacturing this reflector material is shown in Figure 60.

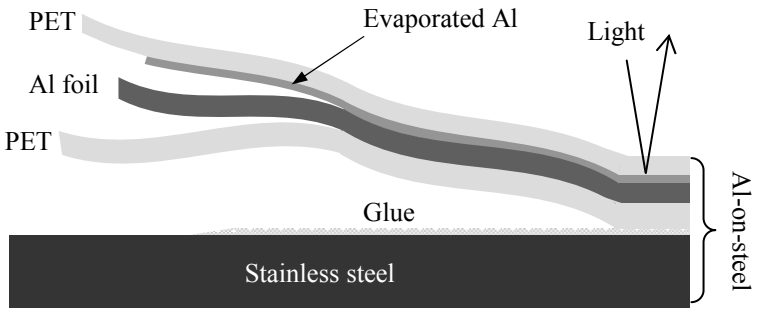

Figure 60: Manufacturing of a polymer-aluminium-laminated steel reflector. The arrow to the right depicts a light beam that is reflected at the interface between the top PET layer and the evaporated aluminium film.

Reflectance measurements on fresh Al-on-steel samples showed that the reflector had good optical properties for solar concentrator applications prior to ageing. It had an initial solar reflectance of 82% of which 77% was specular. The degradation of the reflector laminate was investigated by studying the changes in the total and diffuse reflectance spectra after accelerated and outdoor ageing. Reflectance measurements after more than one year of outdoor exposure indicated that the Al-on-steel reflector has good durability in an outdoor environment, probably because of the plastic coating that protects the evaporated aluminium foil from moisture and air pollutants. However, the total reflectance decreased significantly and the diffuse reflectance increased when the material was exposed to damp heat

and ultraviolet radiation in a climatic test chamber. Figure 61 shows the measured reflectance spectra.

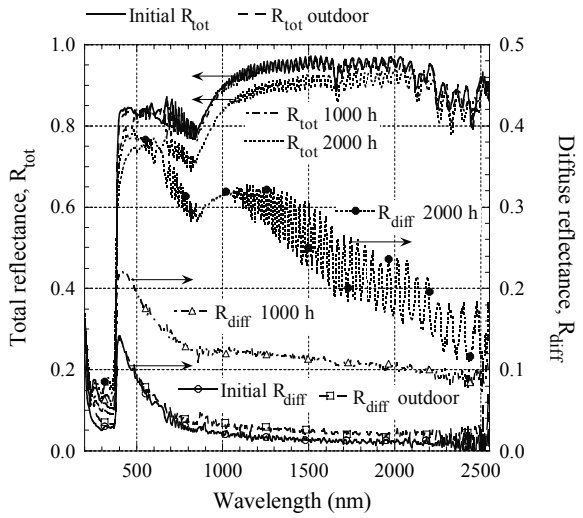

Figure 61: Total and diffuse reflectance of the polymer-aluminium-laminated steel reflector, initially as well as after accelerated and outdoor ageing.

The light scattering of the Al-on-steel reflector was measured in the χ and ψ directions prior to and after accelerated ageing. The results are shown in Figure 62. After accelerated ageing, the light scattering became anisotropic.

Measurement of the total and diffuse transmittance and reflectance of the isolated PET layer, after removing it from the steel substrate and etching away the aluminium, showed that increased diffusivity of the PET layer and absorption in this layer fully explained the degradation of the specular reflectance. Optical microscopy was used to further examine the surface of the reflector. Photographs of the reflector surface, before and after accelerated ageing, are shown in Figure 63. It was found that cracks in the PET layer caused the anisotropic scattering and that the PET coating did not withstand the accelerated testing. Thus, this material may not be suitable as an internal reflector or in other applications where it may be exposed to high temperatures. However, the good result in the outdoor test indicates that the Al-on-steel reflector has potential as a cost-effective reflector in low-concentrating solar thermal and photovoltaic applications.

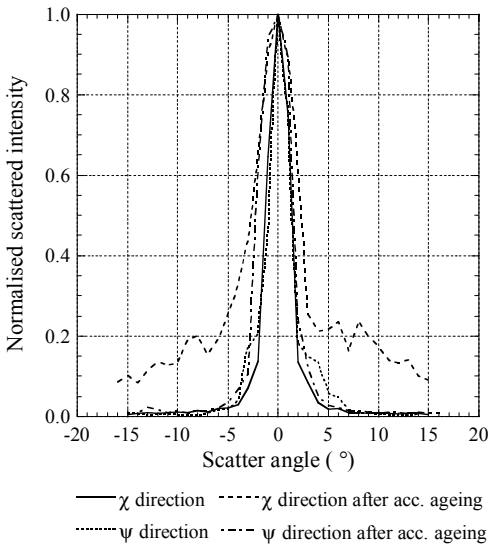

Figure 62: Light scattering from the Al-on-steel reflector in the χ and ψ directions prior to and after accelerated ageing.

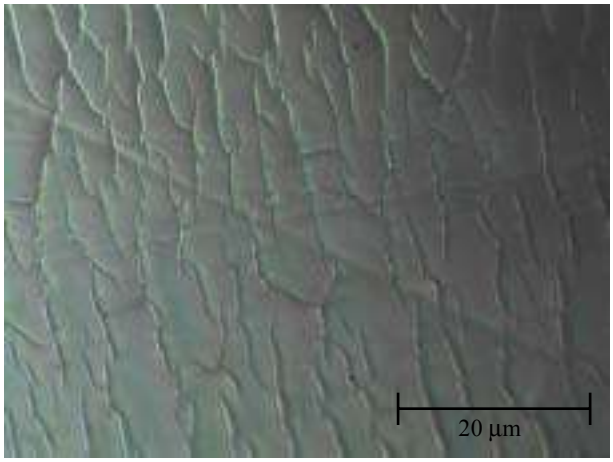

Figure 63: Photograph of a 64×48 μm^2 area of a polymer-aluminium-laminated steel reflector that was aged in the climatic test chamber for 2 000 hours. Photo: M. Brogren.

The degradation of the optical properties, which was found after outdoor ageing is not equal (and in some cases not even similar) to the degradation after accelerated ageing. Neither was the trend equal for the different types of samples. Anodised aluminium and thin film-coated reflectors showed more severe degradation after outdoor exposure than after exposure in the climatic test chamber, while laminated rolled aluminium and lacquered

reflectors degraded more in the test chamber than outdoors. The discrepancy between the results from outdoor and accelerated ageing is discussed in section 11.3 below.

8.3.2 The effect of anodisation on solar reflectance

The anodic layer of the anodised aluminium that was exposed outdoors for 18 years was almost completely destroyed. The initial thickness of the Al_2O_3 layer on this reflector is not known, but the thickness of the anodic layer of the reflector shown in the photograph in Figure 49 is about 800 nm. A thicker anodic layer would prolong the lifetime of the reflector, provided that it is not too thick. Because of the different materials properties, such as thermal expansion, of aluminium (Al) and Al_2O_3, there will be an optimal thickness, above which cracks in the protective layer, caused by tensile stresses at the interface, will cancel the advantage of a thicker anodic layer. In order to see how the thickness of the anodic layer influences the solar reflectance, aluminium reflectors with different thicknesses of the anodic layer were modelled and the resulting reflectance spectra were calculated. The thickness of the Al_2O_3 layer, as well as tabulated n and k data for Al_2O_3 and Al were used as input to the program. In the tabulated data, the extinction coefficient, k, for Al_2O_3 was zero for all wavelengths, resulting in zero absorption in the anodic layer. Figure 64 shows the calculated solar reflectance of anodised aluminium with different thickness of the Al_2O_3 layer.

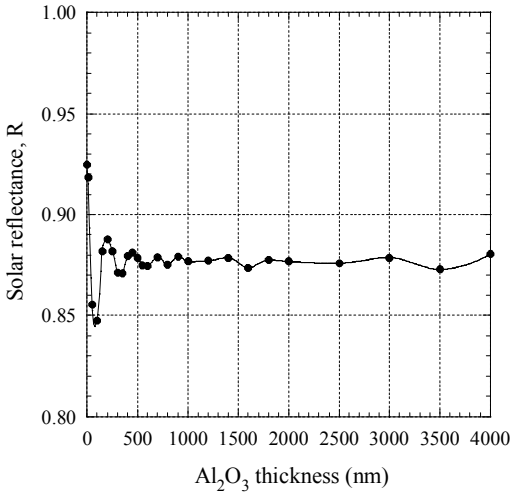

Figure 64: Calculated solar reflectance of anodised aluminium with different thickness of the Al_2O_3 layer. The solid line is an interpolation between the calculated data points (•).

There is no significant change in the solar reflectance when the thickness of the Al_2O_3 layer is varied between 150 nm and 4 000 nm. While the modelled reflectance of bare aluminium gives a total solar reflectance of 92.5%, the reflectance is 87–89% with an added anodic layer of 150–4 000 nm. However, from a corrosion prevention perspective, a thin (<500 nm) film is not recommended, and with a layer that is thinner than 150 nm, the anodic layer will enhance the dip in the reflectance spectrum of aluminium at 860 nm and the solar reflectance is below 85% for a 100 nm Al_2O_3 layer.

9. Performance of concentrating systems

This chapter summarises the evaluations of the optical efficiency and electrical (and thermal) performance of a photovoltaic-thermal cogeneration system with compound parabolic reflectors and of different types of concentrating systems for facade-integration of photovoltaic modules with parabolic over edge reflectors.

9.1. Photovoltaic-thermal system with CPCs

In a project, which was part of a Swedish building-integrated photovoltaics programme (the Elforsk projects SolEl 97–99 and SolEl 00–02), the objective was to halve the investment cost per annually delivered kWh of photovoltaic electricity, compared to a conventional flat plate system. Within this project, a water-cooled photovoltaic-thermal cogeneration system with compound parabolic concentrators was designed and constructed. It was mounted in Älvkarleby (60.5°N, 17.4°E), Sweden, at the end of July 1999 and has been in continuous operation since then. A photograph of the system is shown in Figure 65.

Figure 65: 4X concentrating photovoltaic-thermal system, which is installed in Älvkarleby (60.5°N, 17.4°E), Sweden. Photo: M. Brogren.

The system consists of three east-west aligned troughs. The geometric concentration ratio of the symmetrical compound parabolic concentrators is 4X and the acceptance half-angle is 12°. The total glazed aperture area of the system is 7.2 m² and the cell area is 1.5 m². The cells that are used are 10×10 cm^2 mono-crystalline silicon cells, which are designed for operation under one sun's illumination. In total, the system includes 144 cells, 48 in each trough. The cells are connected in series, in two separate current circuits. The nominal power of one circuit is 118 W. Hence, without concentrators the system has a nominal power of 236 W. The cells are laminated on a cooling fin, in which cooling-water is circulating.

The CPC troughs are made of anodised aluminium. They are truncated to a height of 0.45 m and extended 0.20 m to the east and the west of the photovoltaic modules, in order to avoid shading effects in the mornings and evenings. Where the cells are "missing" an approximately 20 cm long thermal absorber is placed instead. A photograph of the glazed gable of one of the CPC troughs is shown in Figure 66.

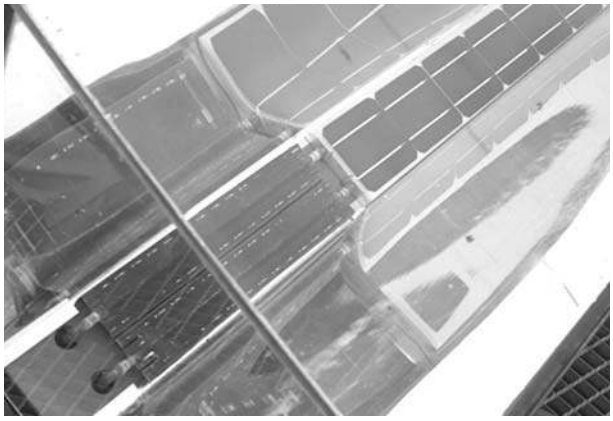

Figure 66: Crystalline silicon cells and thermal absorbers in a CPC trough. Cooling-water is flowing in copper pipes that are integrated in an aluminium fin on the back of the cells. Photo: M. Brogren.

The apertures of the troughs are covered with an anti-reflection treated glazing for protection of the reflectors and the modules and for reduction of heat losses [131, 132]. The generated heat and electricity of the photovoltaic-thermal system are continuously monitored.

The inclination angle of the CPC troughs can be varied using a hydraulic system. The irradiation distribution at the site and the chosen acceptance half-angle of 12° implies that the inclination angle have to be changed four times per year in order not to waste a significant amount of the solar radiation that is

available for electricity and heat production. The hydraulic system was constructed to facilitate measurements at different inclination angles and is, due to its high cost, not proposed to be a part of a future full-scale system.

The thermal power generated in the photovoltaic-thermal system was found to decrease with increasing water temperatures. This is due to thermal losses, which are a well known feature of solar thermal systems. In a photovoltaic-thermal system there is also a trade-off between water temperature and electrical power, since high cell temperatures cause a reduced output voltage. The loss in electrical power at high water temperatures thus limits the electrical performance of the photovoltaic-thermal system.

Figure 67 shows the thermal and electrical performance of the photovoltaic-thermal system during a clear day. The maximum output is 0.5 $kW_{electrical}$ and 3.5 $kW_{thermal}$, corresponding to an output per m^2 cell area of about 330 $W_{electrical}$ and 2.3 $kW_{thermal}$. Without concentrators, the electrical output from these cells would have been about 140 $W_{electrical}$ per m^2.

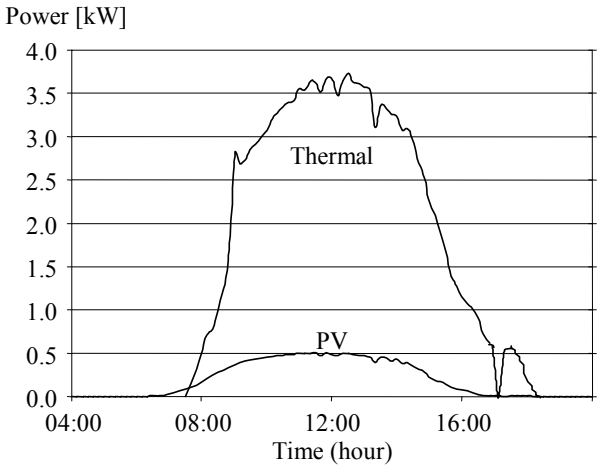

Figure 67: Electrical and thermal output from the photovoltaic-thermal system (1.5 m² cell area) during a clear August day. The cooling-water temperature was kept constant at 30°C.

Measurements showed that the open-circuit voltage of the two circuits decreased from 41 V to 37 V and the electrical efficiency per cell area decreased from 33% to 29.5% when the temperature was increased from 35°C to 65°C, as shown in Figure 68. The temperature coefficient for the electrical efficiency of the system is -0.12 percentage points per °C. This means that if the system is operated at 65°C instead of 25°C, the electrical power is 430 W instead of 500 W.

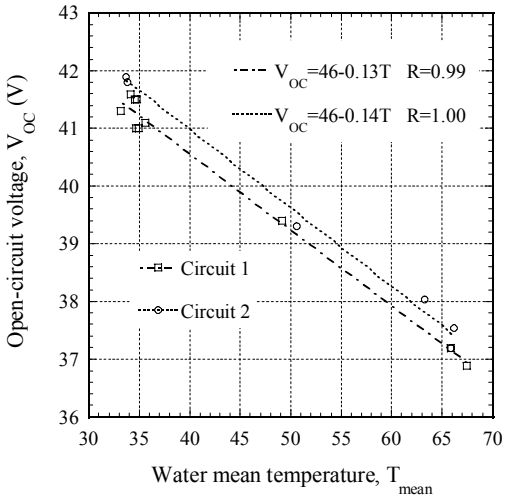

Figure 68: Open-circuit voltage as a function of water temperature for the two current circuits in the photovoltaic-thermal system.

Calculations using collected system data from the period July–December 1999 and meteorological data for an average year, showed that, with an inlet temperature of the cooling water of 50°C, the annually produced heat and electricity will be 225 kWh and 60 kWh per square metre glazed area, respectively. This corresponds to 900 kWh thermal and 236 kWh electrical energy per square metre cell area and year. Higher operating temperature reduces the produced heat and electricity. Figure 69 shows the calculated annual thermal and electrical outputs per square metre glazed area as functions of the inlet water temperature. The calculations are made under the assumption that the electrical efficiency of the system is 10% at 25°C, with a temperature coefficient of -0.5%/°C, and that the system is somewhat better insulated than it is at present.

As a comparison, a photovoltaic module of the same type, without reflectors, produces approximately 95 kWh electricity per square metre and year, and a standard solar collector delivers 450 kWh of heat at 50°C per square metre glazed area annually [136]. Thus, the annual electricity production in the concentrating system will be 2–2.5 times the production in a flat-plate module per square metre cell area, and in addition, the heat that is produced will be twice the heat that is produced in a solar thermal collector with the same absorber area.

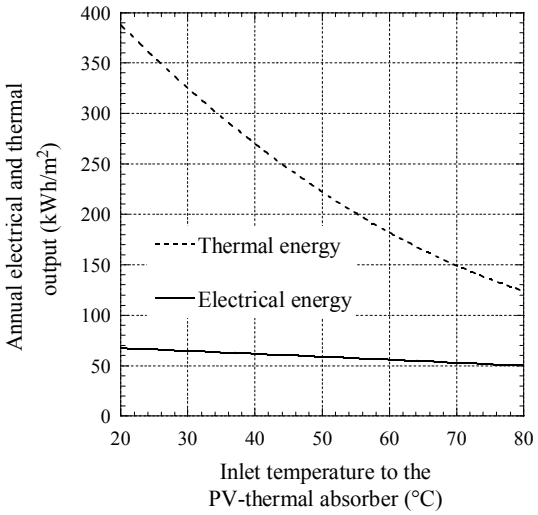

Figure 69: Calculated annually produced electrical and thermal energy per m^2 glazed area in an optimised photovoltaic-thermal hybrid as function of inlet water temperature[11].

The geometry of the compound parabolic concentrators has an observed impact on the electricity production in the photovoltaic-thermal system. In the concentrators, there is a pronounced focal line of high light intensity that traverses the string module, from north to south and back again, during the day. Such "hot spots", or lines of high local concentration, at incidence angles near $\pm\theta_{a/2}$ may cause severe problems for photovoltaic converters [137]. The non-uniform distribution of solar irradiance on the cell surface results in an uneven current distribution, which reduces electrical output and thus the effective concentration ratio. Tilting the compound parabolic concentrator shifts the position of the focal line. Therefore, the tilt angle has a significant impact on the electrical efficiency. For an efficiently cooled module with low series resistance, a maximum in the efficiency is expected when the focal line is in the middle of the photovoltaic cell, between the two conducting fingers, as indicated by the letter A in Figure 70. However, the left-hand graph in Figure 71 shows that the system experiences electrical losses at high irradiance. During the day monitored here, the tilt was adjusted so that the focal line was in the middle of the cell at noon. Nevertheless, there is a slight dip in the efficiency at noon. This is due to resistive losses and voltage drop at high irradiance.

[11] The calculation was performed by B. Perers.

The shift of the focal line is the cause of the two pronounced maxima in the right-hand graph in Figure 71. During the day shown here, the focal line was in the middle of the module (A in Figure 70) at 9:00 and 15:00 pm and in the southernmost area of the cell (indicated by the letter B in Figure 70) at noon. Thus, the system experienced a very asymmetrical illumination at noon, which caused a non-uniform current distribution in the cell and high resistive losses. This problem may be reduced by using slightly diffusing reflectors, which gives a more homogeneous irradiance on the cell surface [IX].

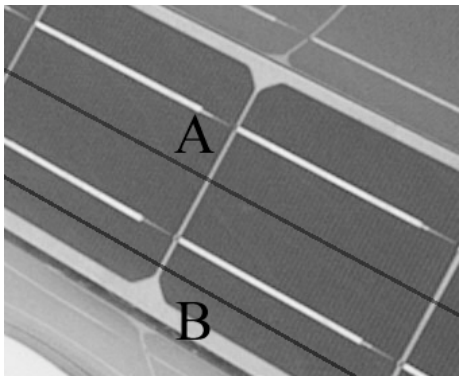

Figure 70: Photograph of a string module in the CPC photovoltaic-thermal system. The line A indicates the position of the focal line that gives optimal electrical performance. The focal line at B results in significant electrical losses. Photo: M. Brogren.

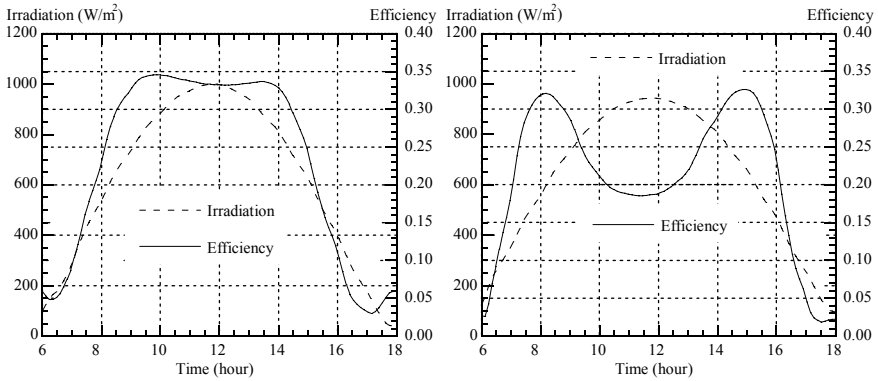

Figure 71: Electrical efficiency per cell area of the photovoltaic-thermal system for different inclination of the optical axis. In the rightmost diagram, the inclination of the CPC has been adjusted to give maximum efficiency during mornings and afternoons.

9.2. Concentrating photovoltaic systems for facade-integration

Integration of concentrating photovoltaic systems into vertical facades requires that the concentrating element has a relatively small depth and that the reflector is fixed. Since low concentration ratios eliminate the need for sun-tracking, it makes facade-integration of concentrating systems possible. Furthermore, a system intended for building-integration should preferably be modular and easy to install.

Concentrating systems with the above-mentioned features, which included photovoltaic modules and over edge parabolic reflectors were evaluated and optimised in Papers III, IV, and V. A prototype of such a system is shown in Figure 72. The system includes thermal insulation of expanded polystyrene (EPS) and is intended to substitute a part of a south-facing wall. It is designed for a commercially available CIGS based thin film module that measures 21×33 cm^2, including an aluminium framing. The thin film cells, which are connected in series, are oriented perpendicular to the focal line of the parabolic reflector. The reflector is made of the same type of anodised aluminium sheet of which the total solar reflectance at an incidence angle of 60° was determined to 83% in Paper I. The concentration ratio of the system is 3X. The height of each module and reflector segment is about 60 cm. The inclination of the optical axis of the parabolic reflector is 25°, which means that it accepts all radiation that is incident at south projection angles above 25°. The photovoltaic module is tilted forwards 20° relative to the horizontal plane and the angle between the module plane and the optical axis of the parabola is thus 45°.

At latitude 60°N, the direct solar radiation will be accepted by the concentrator from 15th March to 1st October. Radiation from all south projection angles will in fact reach the photovoltaic module. However, for south projection angles below 25° and above 70°, the parabola will not be effective, and radiation will reach the module directly. Furthermore, for solar altitudes below 25°, the radiation that reaches the module directly has an unfavourable angle of incidence.

Tests of the system were carried out both indoors using a large-area solar simulator and outdoors. The power and short-circuit current were measured as functions of solar altitude and compared with results obtained from modelling. The influence of the module temperature on the electrical performance was also assessed.

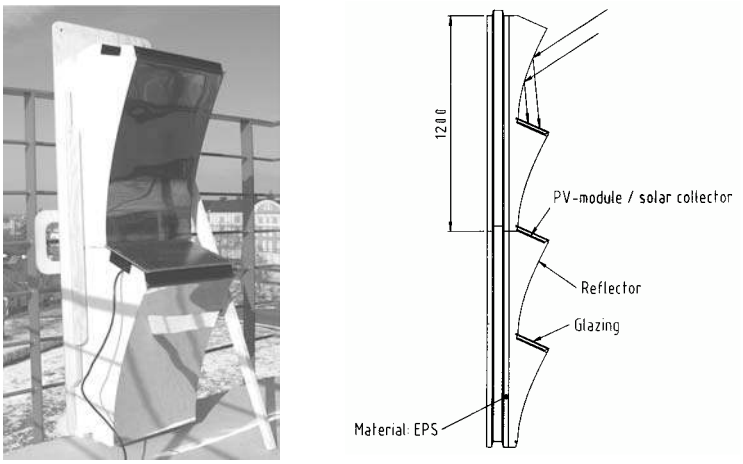

Figure 72: Photograph (left) and cross-section (right) of a 3X concentrating photovoltaic system including thermal insulation (EPS), parabolic reflectors and thin film photovoltaic modules. Photo: M. Brogren. The sketch is courtesy of Vattenfall Utveckling AB.

The optical efficiency of the concentrating system as a function of solar altitude was obtained as the ratio of the short-circuit current from the module in the concentrating system to the short-circuit current of the same module mounted vertically without the concentrator. A solar altitude angle of about 40° resulted in the highest short-circuit current and was thus found optimal for the optical performance of the parabolic over edge concentrator. The relative increase in maximum power by using the parabolic concentrator was also investigated. The ratio of the power with concentrators to the power without concentrators was 1.4 at a solar height of 40° and as high as 1.9 at high solar altitude angles.

Current-voltage characteristics for the CIGS module with the parabolic over edge reflector at different solar altitudes were compared to those of a vertical module without concentrators. In the measurements, the azimuth angle was 0°, and the solar altitude is thus equal to θ_{NS}. Figure 73 shows the measured power as function of voltage at a solar altitude of 40° for a vertical module and for the same module with a 3X concentrating parabolic over edge reflector. The measurements were performed both in the solar simulator and outdoors, as indicated in the figure labels. The higher open-circuit voltage, V_{OC}, in the indoor measurements is due to lower cell temperatures (because the module was only illuminated for a short time). The indoor measurements were performed at different solar altitudes. For θ_{NS}=20°, 40°, and 60°, the maximum power was 2.8 W, 7.3 W, and 4.8 W, respectively. It was found that the open-circuit voltage decreased with increasing temperature.

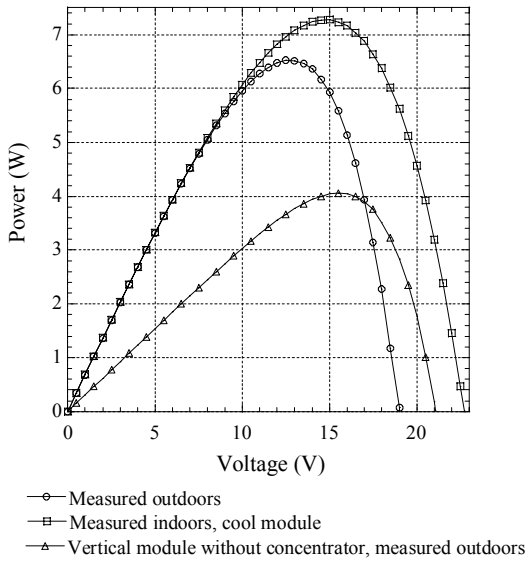

Figure 73: Power as a function of voltage at θ_{NS}=40 for a vertical module and for the same module with a 3X concentrating parabolic over edge reflector.

The efficiency of the thin film CIGS module was established outdoors under one sun's illumination to 11%. The module measured efficiency for 2.3 suns' effective illumination in the concentrating system at a solar altitude of 40° was 17% lower than the one sun efficiency. The observed decrease in efficiency corresponds to a decrease in module fill-factor from 0.6 to 0.5 in concentrated light. The reduction in fill-factor was believed to be due to high series resistance that causes high resistive losses, especially when the module is unevenly illuminated. The uneven irradiance on the module in the parabolic concentrator is shown in Figure 74, which shows photographs of a thin film module with a parabolic over edge reflector for different solar altitudes. The shift of the position of the focal band for different solar altitudes is also shown.

Approximately the same reduction in fill-factor was found for the mono-crystalline silicon string module in a concentrating system with essentially the same geometry, which was investigated in Paper IX, when a specular reflector of anodised aluminium was used. In Paper IX, it was also found that the use of a low-angle scattering reflector of lacquered rolled aluminium foil laminated on a flexible PET substrate resulted in a more homogeneous irradiance distribution on the modules, which had a significant positive effect on the fill-factor of the silicon module.

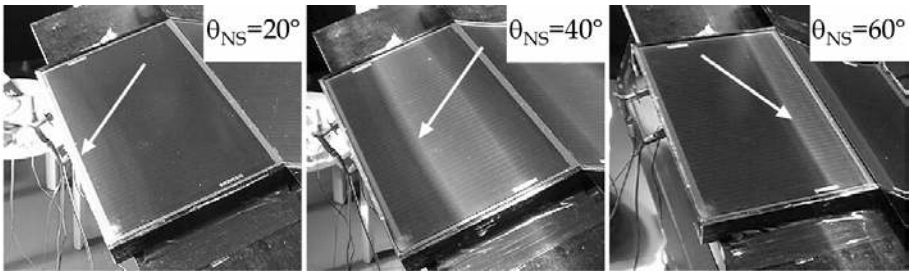

Figure 74: Photographs of a thin film module with a parabolic over edge reflector, which show the position of the focal band at different solar altitude angles. The irradiance is highest where the arrows point. Photo: M. Brogren.

Figure 75 shows the relative increase in electricity production for a module with a parabolic over edge reflector compared to a flat vertical module. If the relative gain as a function of south-projected incidence angle is weighted by the irradiation on a vertical wall at these projection angles, the annual increase in electricity production due to the concentrating system is obtained. In this way, the increase in electricity production was found to be 42% if the system is installed in Stockholm.

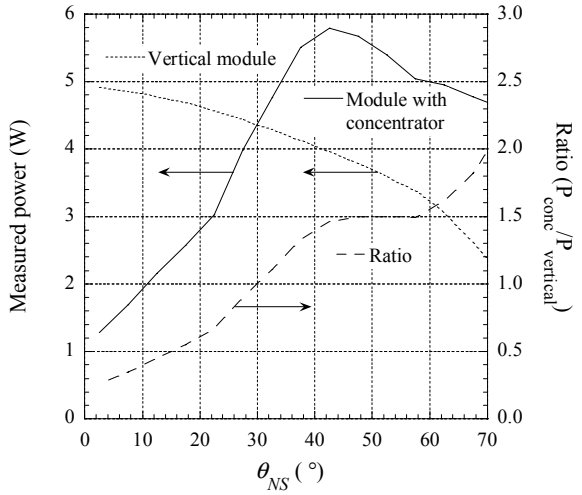

Figure 75: Measured power for the ST5 module in the parabolic concentrator, measured power for an identical, vertical module without concentrator, and the ratio of the measured power of the two modules as a function of south-projection angle θ_{NS}.

The characterisation of the concentrating system for facade-integration was made for the same, high irradiance at all solar heights. The high irradiance results in high module temperature, high local irradiance on the module, and high local currents. These factors reduce the fill-factor and the open-circuit voltage, resulting in a lower electrical power. However, when the module is operated outdoors in real sunlight, the irradiance will be lower for high south projection angles, because of the non-zero azimuth angle, and for low solar heights, during spring and autumn. Thus, under real operating conditions, the effects of over-heating, which was seen in the measurements, will be less severe due to the significant contribution of low intensity radiation to the annual irradiation. This means that the calculated annual electricity production of the system probably is an underestimation. Under real operating conditions, the increase in annual electricity production for a module with a 3X parabolic over edge parabolic reflector of anodised aluminium, compared to a vertical module, will probably be higher than the calculated 42%.

In order to keep costs low, the aim is to use off-the-shelf modules, such as the thin-film module discussed above, in the concentrating system for facade-integration. However, since the high temperatures obtained in the concentrating system significantly reduce the open-circuit voltage and the output power, it might be appropriate to use water-cooled photovoltaic-thermal hybrid string-modules in the facade-integrated system. Domestic hot water would then be an added value of the system. The facade-integrated concentrating solar thermal system in Figure 27 and the photovoltaic-thermal system with compound parabolic concentrators have both been operating since 1999 [vii], and these examples show that the technologies already exist, both for facade-integration of concentrating systems and for the photovoltaic-thermal concept.

The optical losses in the parabolic over edge reflector vary with the solar altitude, but are typically 20–25%. The losses are due both to imperfections in the geometry and the less than unity solar reflectance of the reflector material. In order to increase the optical efficiency, the use of e.g. second surface silver mirrors may be considered.

10. Optical efficiency and optimisation of system performance

This chapter summarises assessments of theoretical, measured, and modelled optical efficiency of various concentrating systems.

10.1. Theoretical optical efficiency

At normal angle of incidence, the theoretically expected optical efficiency, η_{opt}, of a compound parabolic concentrator (CPC) trough, is given by

$$\eta_{opt} = \frac{T_{glass}\left[a_{cell} + a_{reflector} \cdot R_{spec}{}^{\langle n \rangle}\right]\frac{I_b}{I_{tot}}}{a_{aperture}}, \tag{51}$$

where T_{glass} is the transmittance of the glazing, R_{spec} is the specular reflectance of the reflector, $\langle n \rangle$ is the average number of reflections in the reflector, I_{tot} is the global irradiance, and I_b is the direct irradiance. The respective areas, a_{cell}, $a_{reflector}$, and $a_{aperture}$ are shown in Figure 76. The cell absorptance does not appear in the expression for optical efficiency, since it is the same in a reference system without concentrators and glazing. The optical properties of the components of the 4X compound parabolic concentrator was evaluated in Paper I. Using this data, and with $\langle n \rangle$=1, Equation 51 gives

$$\eta_{opt} = \frac{0.94 \cdot (1 + 2.8 \cdot 0.81) \cdot 0.9}{4} = 0.69 .$$

The reason why the sum of the cell and reflector areas is 3.8 and not 4, is that the cell does not cover the full width of the aluminium profile. The profile is extended 1 cm on each side of the cell in the north-south direction, thus making the effective reflector area smaller. The factor 0.9, which is the ratio of the direct irradiance to the global irradiance, is only valid for a clear day with extremely dry air.

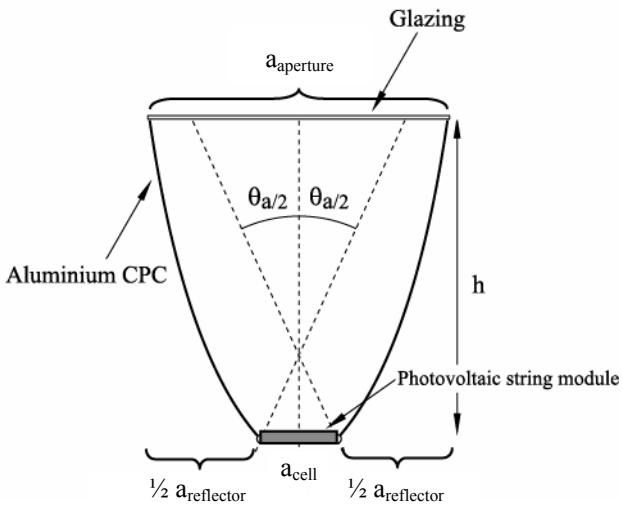

Figure 76: Cross-section of a CPC trough and definition of the dimensions that are used in the calculation of optical efficiency.

10.2. Measurements of the optical efficiency

The optical efficiency of a concentrating solar energy system depends on the optical properties of the components (glazing, reflector, and thermal absorber or photovoltaic cells). In the case of the photovoltaic-thermal system, the optical efficiency can be determined from measurements of the produced thermal power as well as from measurements of the short-circuit current.

10.2.1 Optical efficiency from thermal measurements

If the measured thermal power is compensated for thermal losses due to an operating temperature above the ambient, the measured thermal output can be used to determine the optical efficiency. Figure 77 shows the optical efficiency of the 4X concentrating photovoltaic-thermal system, determined from thermal measurements, as a function of the time of the day. The optical efficiency is shown relative the measured global and direct (beam) radiation. The measurements were performed close to the spring equinox, which means that one hour on the x-axis corresponds to a shift in the longitudinal incidence angle of 15°. Figure 77 shows a nearly constant optical efficiency over six hours, which corresponds to a shift in the incidence angle of 90°. Figure 77 gives a maximum optical efficiency of 0.65, while the theoretical optical efficiency is 0.71. The difference is explained by thermal losses due

to a limited fin-efficiency of the photovoltaic-thermal absorber and to reflector imperfections.

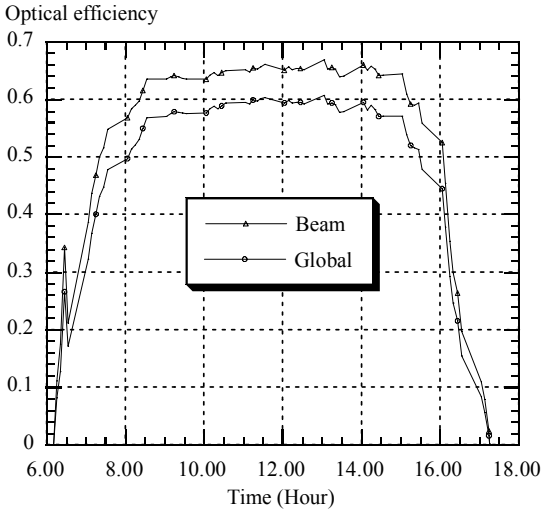

Figure 77: Optical efficiency as a function of the time of the day determined from thermal measurements on 6th April, 2000.

10.2.2 Optical efficiency from short-circuit current measurements

The optical efficiency of a concentrating photovoltaic system can also be determined from measurements of the short-circuit current, since this is proportional to the irradiance on the solar cells. Figure 78 shows a current-voltage curve for a string module in the 4X concentrating photovoltaic-thermal system at noon on a clear August day. The measured irradiance was 950 W/m^2 and the measured short-circuit current was 9.35 A. At standard test conditions, without concentration, the measured short-circuit current for the same module was 3.72 A. From these data, the optical efficiency for electricity production in the concentrating photovoltaic-thermal hybrid system was determined to 0.66 using Equation 47. This result agrees well with the theoretical optical efficiency and the optical efficiency determined from the thermal output.

The optical efficiency as a function of the transverse incidence angle was determined by turning the CPC troughs and monitoring the short-circuit current. Equation 47 was used to calculate the optical efficiency. The result is shown in Figure 79 together with the angular dependent theoretical optical efficiency, i.e. the acceptance function. The effects of the acceptance angle and truncation are visible in the theoretical as well as in the measured optical

efficiency. The measured efficiency decreases at angles close to the acceptance angle due to imperfections in reflector geometry and reflections in the conducting fingers on the cells. The decrease in optical efficiency due to a decreased glass transmittance is negligible due to the low incidence angles.

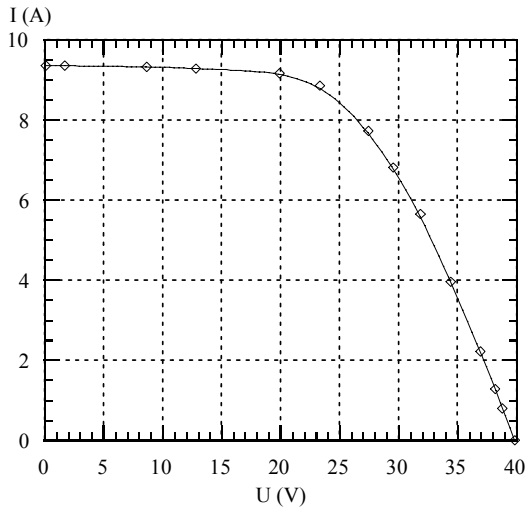

Figure 78: Current-voltage characteristic for a string module in the CPC at high irradiance normal to the glazing. The cooling-water temperature was 45°C and the ambient temperature was 20°C.

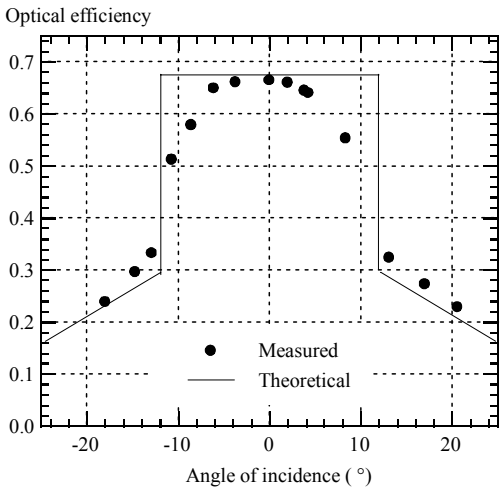

Figure 79: Theoretical optical efficiency of the CPC system as a function of transverse incidence angle and optical efficiency calculated from measured short-circuit currents.

The optical efficiency of the 4X concentrating photovoltaic-thermal system as a function of the time of the day was determined from measurements of the short-circuit current on a day close to the spring equinox, at which one hour corresponds to a shift in the longitudinal incidence angle of 15°. The result is shown in Figure 80.

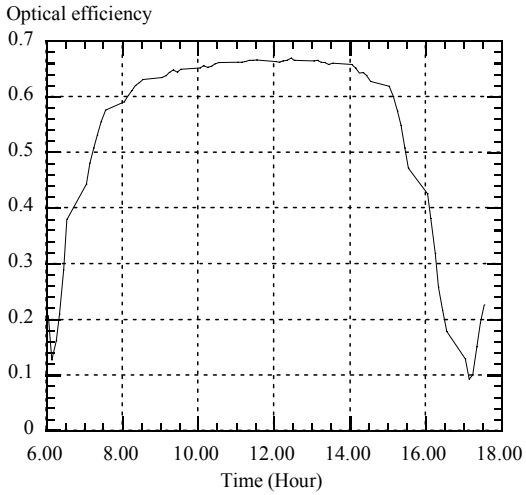

Figure 80: Angular dependent optical efficiency of the photovoltaic-thermal system as a function of the time of the day. Data from measurements of the short-circuit current on 6th April 2000.

There may be several explanations for the discrepancies between the measured short-circuit currents and the theoretical acceptance function. Firstly, the shape of the reflectors may not be a perfectly parabolic and the aluminium is slightly scattering. Secondly, the series resistance is not the same for all angles of incidence, since the position of the focal line is shifted across the module when the incidence angle is changed. At transverse angles of incidence close to the acceptance angle, one of the two front contacts will transport most of the generated current, as shown in section 9.1. Reflection in the conducting fingers when the angle of incidence is close to the acceptance angle may also contribute to the lower short-circuit current, i.e. to the rounded corners in the measured optical efficiency in comparison to the theoretical acceptance function in Figure 79. Furthermore, at angles of incidence, $|\theta_t|>12°$, the diffuse radiation contributes to the generated current, resulting in a measured short-circuit current that is higher than the theoretical.

10.3. Ray-tracing and comparison with measurements

The irradiance distribution on the mono-crystalline silicon cells in the modules in the 3X concentrating system for facade-integration was measured using a small photovoltaic cell. The measured irradiance at different solar altitudes was compared to the theoretical irradiance, which was found using ray-tracing.

Figure 81 shows the measured and calculated irradiance distributions on a module in the concentrating element for different south-projected solar altitudes, θ_{NS}. The diagrams are not normalized and thus only give a qualitative picture of the irradiance distribution. However, the relation between the peaks for different solar heights is quantitative. In the calculation, to the right, diffuse irradiation is neglected. The two peaks that are visible in both diagrams for high south projection angles result from double reflection in the parabolic reflector.

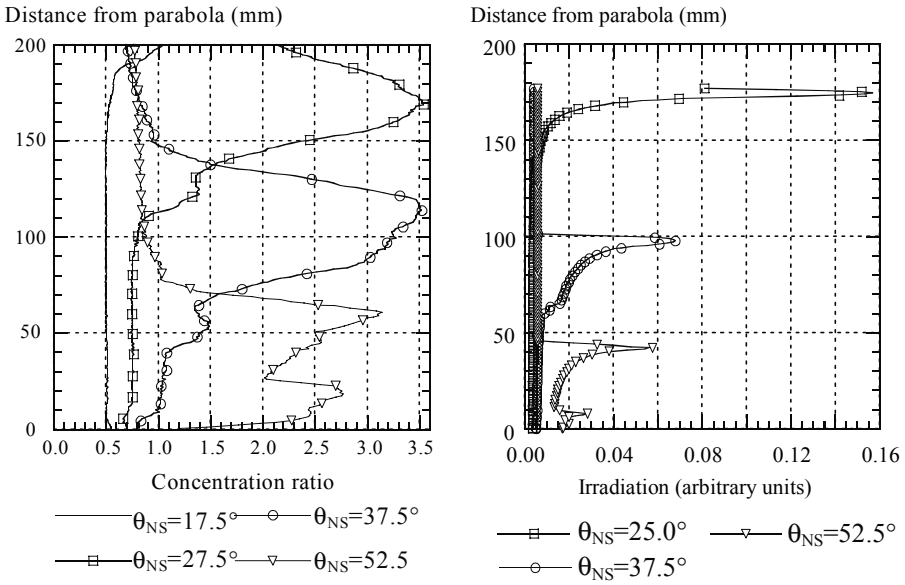

Figure 81: Measured (left) and simulated (right) energy distributions on a photovoltaic module in the over-edge parabolic concentrator at different projected solar heights, θ_{NS}.

The calculated total energy incident on a module as it was placed in the concentrating element and on a vertical module of the same size, was used to calculate the optical concentration ratio, C_{opt}, of the concentrating element. The comparison resulted in $C_{opt} \geq 2.6$ for $30° < \theta_{NS} < 50°$.

10.4. Optimisation of reflector geometries

The optical design of the 3X concentrating element for facade-integration was based on earlier experiences rather than on thorough modelling and calculations using i.e. ray-tracing. The lower acceptance angle of the system was 25°. However, Figure 13 shows that a lot of the annual irradiation is obtained for south-projected solar altitudes below 25º. In the original design of the system for facade-integration, this irradiation is not accepted by the parabolic mirror. Considering this, the concentrating element might be re-designed to accept irradiation at θ_{NS}<25º, by reducing the inclination of the optical axis of the parabolic reflector to 5º or 10º.

In order to optimise the geometry of the facade-integrated photovoltaic system with a static parabolic over edge reflector for maximum annual electricity production in southern Sweden, the annual electricity production was simulated for concentrating systems with different geometries. The parameters that were varied were the inclinations of the optical axis and the module plane, i.e. the α and γ angles. The simulations for different geometries were based on optical efficiencies obtained from short-circuit current measurements and performed using the MINSUN program. The optimisation was reported in Paper V. An illustration of how the system was altered is shown in Figure 82. With α=25° and γ=45° as in the original system, the acceptance angle, θ_a is 65° and the geometric concentration, C_g, is 2.96. The concentration ratio increases as the angle α is increased, because the height of the glazed aperture, h, relative to the module width, a, is increased. All symbols are found in Figure 26.

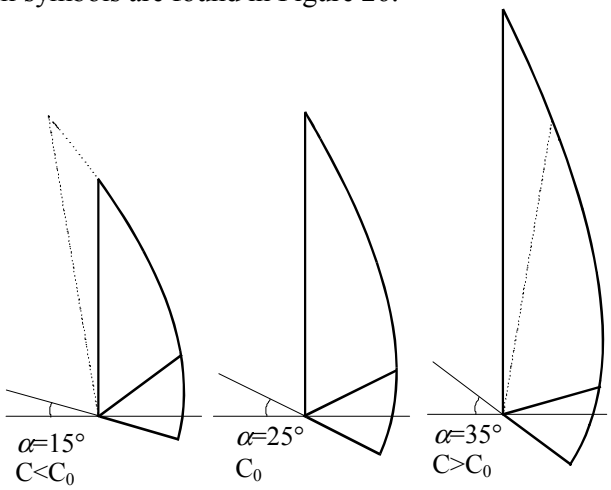

Figure 82: An illustration of how the geometry of the concentrating system with a parabolic reflector was altered.

Figure 83 shows the Geometries A and B. In geometry A, the angle γ is 10° and in geometry B, γ is 50°.

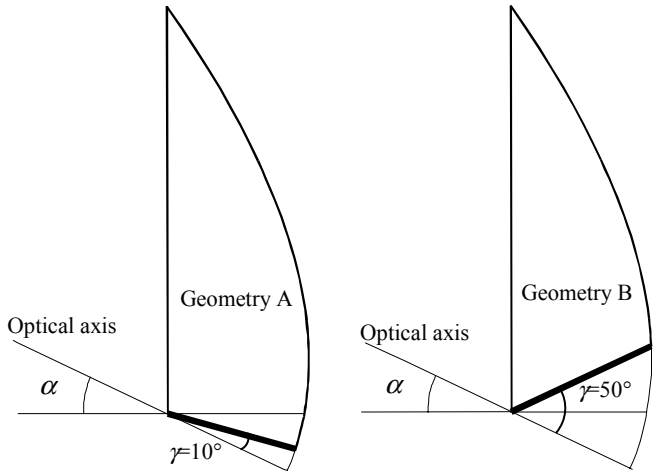

Figure 83: The geometries A and B, which were studied in Paper V.

The optical efficiency of these geometries and the original geometry, calculated from measurements of the short-circuit current as a function of altitude angle of the solar simulator are shown in Figure 84.

Figure 85 shows the simulated annual electricity production per module area as function of the inclination of the optical axis of the reflector for the different geometries. The maximum annual electricity production in the evaluated concentrating systems, if installed in Stockholm, Sweden, was calculated to 153 kWh/m² per solar cell area, using MINSUN and measurement data. This result was obtained for a system with C_g=6.8, an inclination of the optical axis, α=45°, and γ=10°. The calculated annual electricity production is 76% higher than that of a vertical reference module of the same size, which would produce 87 kWh per m^2 cell area. However, the obtained value of 153 kWh/m² per cell area may be somewhat unrealistic for building-integrated systems, since the electricity yield per glazed area is rather small and since the reflector would mainly be working during summertime, due to the high tilt angle of the optical axis. In the original design, which has an inclination of the optical axis of 25°, which results in a higher wintertime production on the expense of a lower summertime

production, the annual yield of the module in the concentrating system is 135 kWh per m^2 cell area (calculated from outdoor measurements).

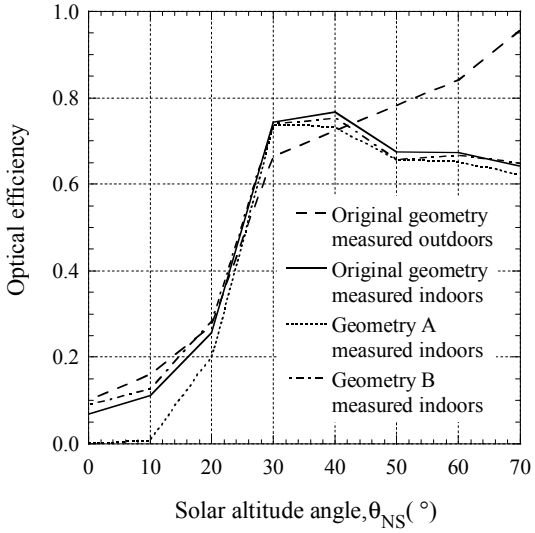

Figure 84: Optical efficiency of different geometries, calculated from measurements of short-circuit current as a function of solar altitude.

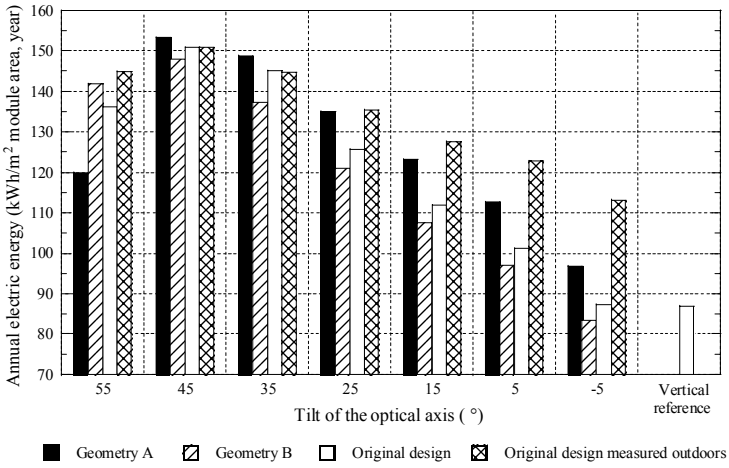

Figure 85: Simulated annual electricity production per module area as a function of the inclination of the optical axis of the parabolic reflector.

The conclusion is that the use of photovoltaic modules and parabolic aluminium reflectors in static, low-concentrating systems designed for building-integration has a potential to significantly increase the annual electricity production per cell area, compared to a planar vertical module

with the same cell type. Given the low cost of the highly reflective anodised aluminium mirrors and the insulation material, and in combination with a simple manufacturing process, the kind of systems evaluated in this work have a potential to reduce the cost of photovoltaic electricity.

10.5. The effect of light scattering on system performance

In Paper IX, the use of a low-angle scattering reflector in the 3X concentrating element for façade-integration was found to result in a higher module fill-factor. At high insolation, the positive effect on the fill-factor of the more even irradiance distribution on the module when partly diffuse reflectors were used was significant. The use of low-angle scattering reflectors in parabolic geometries also results in a smoother acceptance function. This is illustrated in Figure 86, which shows a photograph of a beam from a HeNe laser, reflected and scattered from a lacquered rolled aluminium reflector. The beam was incident on the parabolic concentrator with an angle of 24° over the horizontal. The dashed white line indicates the front edge of the photovoltaic module. A schematic of the experimental setup that was used to take the photograph is shown in Figure 87. The smoother acceptance function allows for some of the radiation that is incident at angles below the lower acceptance angle to be accepted by the system. This was found to be favourable in the 3X concentrating system with a parabolic over edge reflector, since the lower acceptance angle of that system is only 25° and a significant part of the annual irradiation can be found at south-projected incidence angles below 25°. However, the influence of this effect on annual electricity production has not been quantified and is probably only a few percent.

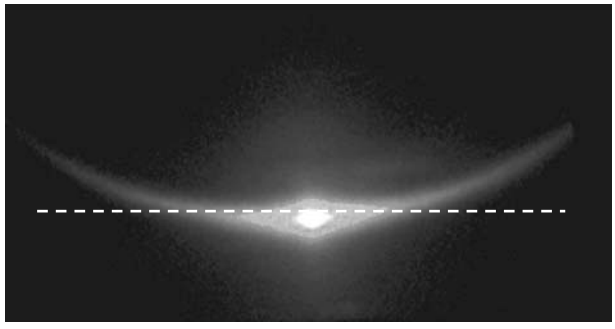

Figure 86: Image on the module plane of a laser beam that has been reflected in a parabolic mirror of lacquered rolled aluminium. The dashed white line indicates the front edge of the photovoltaic module. Photo: M. Brogren.

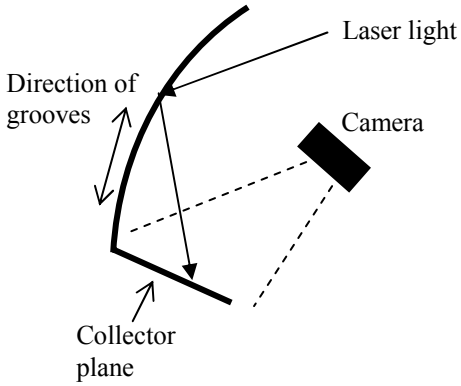

Figure 87: The setup that was used to take the photograph in Figure 86.

10.6. New model for incidence angle dependence

The model for the incidence angle dependence of the optical efficiency, which is described by Equation 41, is only correct when radiation is incident in either the *L* or the *T* plane, since the angular dependence of the glazing is accounted for in both functions f_L and f_T. When radiation is incident in another, arbitrary, plane, the model biaxial model described by Equation 41 is not valid, and tends to underestimate optical losses in the glazing. In Paper VI, a new method for calculating the angle dependence of photovoltaic systems with east-west aligned reflectors is proposed. The new model is similar to Equation 41, but it is valid for all angles of incidence. The model is given by

$$\eta_{opt} = f_L(\theta_i) \cdot R(\theta_T) \tag{52}$$

where $R_T(\theta_T)$ gives the influence of the reflector as a function of the projected transverse incidence angle and f_L gives the influence of the cover glass as a function of the true angle of incidence. The function f_L is assumed to be equal to the angular dependent transmittance of the glass that is used in the system. Measurements of the optical efficiency as a function of the transverse incidence angle were performed on a system without a glazing, and measurement data were used to formulate a numerical expression for $R_T(\theta_T)$ of the 3X concentrating system with a parabolic over edge reflector.

In order to study how well the proposed model describes real system performance, outdoor measurements were made on the 3X concentrating system. It was found that, in the east-west direction, the incidence angle

dependence of the optical efficiency of an east-west aligned concentrating system without a glazing is equal to that of a flat plate module. Thus it is only the angular dependence in the north-south plane that differs between the concentrating system and a vertical module.

Model predictions of the optical efficiency of a concentrating system without a glazing (f_L=1), using the numerical expression for $R_T(\theta_T)$ multiplied by the short-circuit current of a vertical reference module and the geometrical concentration ratio, were found to be well in accordance with measurements of the optical efficiency of such a system. Adding a glazing should, to a first approximation, only influence the function f_L. This indicates that the proposed model describes the angular dependence of the optical efficiency of an asymmetric concentrator better than the commonly used biaxial models [102]. The graphic representation of the proposed model for the incidence angle dependence of the optical efficiency of a 3X concentrating system with a parabolic over edge reflector and a glazing is shown in Figure 88.

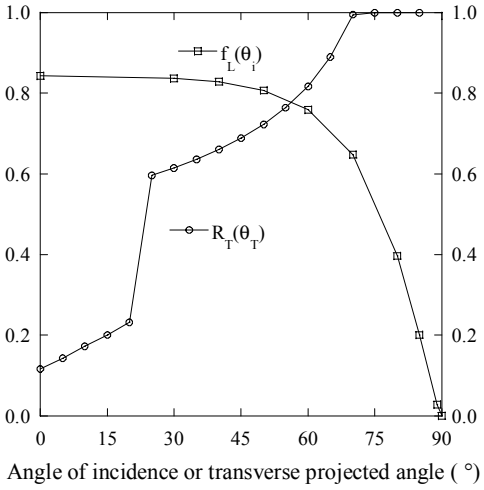

Figure 88: The factors f_L and R_T that determine the optical efficiency of a 3X concentrating photovoltaic system with a parabolic over edge reflector.

Effects of polarisation will occur when a glazing is introduced in the system, since the light that is transmitted trough the glass will be strongly polarised at high angles of incidence. The new model does not explicitly account for polarisation, but the problem is discussed in Paper VI. In the case where the reflector is essentially parallel to the glazing, like in the 3X concentrating system with a parabolic over edge reflector, polarisation will result in an optical efficiency that is lower than model predictions, due to the lower

reflectance of aluminium for p-polarised light. This is because the radiation transmitted trough the glass at high angles is partly polarised with a predominant p-polarised component and at high angles the reflectance of aluminium is lower for p-polarised than for s-polarised light.

11. Discussion

In this chapter, aspects of using photovoltaic cells and modules that are designed for one sun's illumination in concentrators are discussed, such as the effect on module performance of using diffuse versus specular solar reflectors. The validity of accelerated ageing tests and the difficulties to translate the results from accelerated testing into outdoor performance are elaborated on. The future potential for photovoltaic-thermal and building-integrated systems is discussed.

11.1. Solar cells and modules in concentrators

Photovoltaic systems that utilise concentrated light have several advantages. The primary reason for utilizing concentrators is the possibility of significantly reducing the cost of the generated electricity, provided that low-cost concentrators are available. Another advantage of concentrating systems is that highly efficient photovoltaic-thermal cogeneration systems, which produce both electrical and thermal energy is a possible, and probably a cost-effective, solution. The drawbacks of concentrating systems are, for example, that no practical optical system has negligible optical losses and that high cell temperatures and the series resistance of the photovoltaic modules may become a major problem. In this work, in which solar cells that are designed for one sun's illumination have been used, all these problems have been encountered.

Owing to the geometry of the reflectors in two-dimensional parabolic concentrators, the radiation is focused on a line or a narrow band across the cells. The results from simulations on a 3X concentrating semi-parabolic reflector in this work, showed that, in theory, the local irradiance on parts of the receiver can be up to 50 times higher than the irradiance without concentrators. In practice, the local irradiance on the receiver is rarely as high as this, due to for instance reflector imperfections. Still, this implies that when parabolic concentrators with cylindrical geometry are used for concentration of radiation onto photovoltaic cells, the design of the cells is critical in order to achieve a good electrical performance of the system. Commercially available modules, whether based on crystalline silicon or

thin film technology, are designed for standard operating conditions, i.e. one sun's illumination and convective cooling. When operated under high-intensity illumination in concentrating systems, the technical and physical requirements on the photovoltaic devices are different, both on the module and on the cell level. For any choice of photovoltaic technology it is therefore necessary to specifically address these issues when designing the concentrating system, in order to obtain cost-effective generation of photovoltaic electricity.

Conventional crystalline silicon photovoltaic cells can be used at elevated sunlight intensities. At constant temperature, the short circuit current increases proportionally to the irradiance, while the open circuit voltage increases logarithmically. The fill-factor remains constant, or would in theory even increase, provided the series resistance is negligible. In practice, however, the series resistance quickly dominates the cell behaviour, and increasing resistive losses at high light intensities are detrimental to system performance. High resistive losses were found, for example, in the study of the 4X CPC. An increased number of narrow, conducting grid fingers on the cell surface can decrease this problem, but at a higher cell cost and at the price of increased optical losses.

It is characteristic for photovoltaic modules with series connected cells that the cell with the lowest current output dictates the module performance. In the dark, a photovoltaic cell functions as a diode and efficiently blocks the current. Therefore, in the case when one or more cells are shaded, the module performance will be limited by the output of these cells. On the other hand, if the concentration of light onto one or more cells is higher than for the rest of the cells, this energy cannot be utilised in the system. For a line focus system, such as the compound parabolic concentrator, this implies that string modules, with only one row of cells that are series connected, as the one-row crystalline silicon modules in the 4X CPC, should be used. This requires, however, that the module is custom designed, which is associated with a higher cost.

The commercially available CIGS modules, which were used in the 3X concentrating system with a parabolic over edge reflector, were placed with the cells perpendicular to the line of focus in order to achieve equal irradiance on each cell. However, for this type of module, the location of the contacts in relation to the line of focus was crucial to performance. This indicates that the internal series resistance of the cells is high.

11.2. Diffuse versus specular solar reflectors

As discussed above, photovoltaic cells should be evenly illuminated, since it is the least illuminated cell that determines the performance of the entire system. Thus, for photovoltaic systems it may be advantageous to use reflectors that scatter the light to some extent. In Paper IX, the performance of a mono-crystalline silicon module in a 3X concentrating system utilising a specular reflector was compared with the performance of the same module utilising a partly diffuse reflector. It was found that, in particular at high insolation at incidence angles just above the acceptance angle, it is favourable for the electrical performance of the photovoltaic module to use a partly diffuse reflector to smooth the image of the sun on the surface of the module. However, the reflector material that was used in this investigation was lacquered rolled aluminium, which scattered light in an orderly fashion, at low angles in the direction perpendicular to the grooves from the rolling process, thus primarily in the module plane. This fact must be considered when the results of this work, implying that semi-diffuse reflectors can give an increase in power production compared to the use of entirely specular reflectors, are interpreted. Isotropically scattering reflectors or rolled metal reflectors with the grooves oriented parallel to the length of the module will give a different irradiance distribution on the module, and may result in significant optical losses if incident light is reflected out of the system and does not reach the module.

In many cases, ageing results in a more diffuse reflectance. This may not be detrimental to system performance if the diffuse radiation is scattered at low angles and in the direction parallel to the length of the module. When performing ageing tests, it is therefore useful to assess the spatial distribution of the diffuse reflectance before and after ageing, in addition to measure the total and specular reflectance.

11.3. Accelerated ageing tests versus outdoor ageing

The optical properties of anodized aluminium are often considered long-term stable, due to the protective aluminium oxide layer. This work has shown that this is not true for unprotected samples (without glazing or protective coatings or lacquer) in outdoor applications. However, during the relatively short time of a climatic test in a test chamber, not much happened to the reflectance of the anodised aluminium and it is therefore assumed that the process governing the degradation of the optical properties of anodised aluminium is slow and depends on time and exposure to pollutants in the atmosphere, rather than on temperature and humidity. This is explained by

the fact that even though the protective aluminium oxide coating renders the metal impervious to most acids, any chemicals that form a strong complex with aluminium ions, e.g., OH^- and Cl^- ions, might react with the oxide coating. Therefore, anodised aluminium will dissolve in hydrochloric acid and sodium hydroxide solutions, which are often found in precipitation in industrial regions. At the outdoor test site in Älvkarleby, the air pollution levels and the salinity in the air are moderate, since it is located 10 km from the nearest industry and 10 km from the sea, with brackish water. Environmental tests, with controlled concentrations of air pollutants, in a test chamber should therefore be conducted to investigate which reflector materials withstand outdoor exposure in areas with higher pollution levels. Alternatively, the samples could be mounted at the seashore or near different types of industries.

Laminated samples degraded more in the climatic test chamber than during outdoor exposure and the deterioration of this kind of reflectors is therefore believed to depend more on climatic conditions than on exposure time and pollutants. The temperatures and humidity levels that were used in the accelerated testing may be considered too high for testing of this kind of samples, and in combination with high ultraviolet radiation levels, the organic laminates corroded disproportionately faster in the test chamber compared to other types of reflector materials. On the other hand, cold Swedish winters impose significantly different climatic conditions on the reflector materials than the accelerated ageing test performed in this work. It might therefore be interesting to submit the materials to controlled freezing tests, in addition to damp heat testing.

During outdoor exposure, however, a lacquer or a plastic laminate protects the reflective surface from air pollutants, thus prolonging the lifetime of laminated reflectors compared to bare metal reflectors, such as anodised aluminium. Ultraviolet radiation should not have any influence on the degradation of anodised aluminium or other metallic solar mirrors, neither outdoors nor in a climatic test chamber.

In this work is has been shown that essentially different processes govern the degradation of the optical properties of different types of solar reflector materials, for example metals and plastic laminates, and that an understanding of the corrosion mechanisms for the tested materials is necessary to be able to interpret results from accelerated ageing correctly and translate them into expected technical lifetime under outdoor environmental conditions. The results of the ongoing IEA Solar Heating and Cooling Programme's Task 27, in which accelerated testing and outdoor testing in

different climates of several reflector materials is performed, will be a welcome contribution to the knowledge in this field.

11.4. Potential for photovoltaic-thermal systems and BIPV

The annual electricity production in the evaluated 4X concentrating photovoltaic-thermal cogeneration system is more than twice the production in conventional photovoltaic systems. However, the electricity production in photovoltaic-thermal systems decreases with increasing temperature of the cooling water. This implies that the water temperature should be kept as low as possible. On the other hand, the system should deliver domestic hot water or warm water for space heating. Thus, there is a trade-off between maximizing the electricity production and producing water of useful temperatures. However, the electricity to heat ratio in the 4X photovoltaic-thermal system of about 0.25–0.3, at an operating temperature of about 50°C, makes it appropriate for domestic use.

In the 3X concentrating system with a parabolic over edge reflector, the reflector is fitted in a pre-shaped support construction of inexpensive, polystyrene of light weight, which has the additional function of being a thermal insulation material. This is advantageous since the system is intended to be a multi-functional, integrated part of a building envelope. The inclination of the optical axis of the parabolic reflector and the tilt of the module plane can be adjusted and optimised for different geographical sites. Likewise, the depth and height of a single concentrating element can be varied. At a given concentration ratio, choosing larger or smaller dimensions may result in a more or less cost-effective system, since the material content and costs do not scale linearly with system size [138]. The dimensions of commercially available string modules, however, impose constraints on the design of the systems, since the idea is to keep costs down by using off-the-shelf components.

A conceived future solar energy building would use a combination of state-of-the-art solar architecture, low-emittance coated, double or triple-glazed windows, transparent insulation, a heat-exchanger coupled to the ventilation system, and energy-efficient appliances to reduce the consumption of heat and electricity. For this building, the obvious choice of energy system would be a combination of the two systems described above, i.e. a façade-integrated concentrating photovoltaic-thermal cogeneration system. Covering a 30 m^2 south façade with the proposed solar energy system would produce all the electricity and thermal energy needed for a family living in this solar-energy-efficient house.

12. Conclusions and outlook

The conclusions of this thesis are summarised under the headings Materials, Systems, and Modelling. An outlook concludes this chapter.

12.1. Materials

The present high cost of photovoltaic electricity is a strong motivation for developing inexpensive and reliable reflector materials. A significant reduction of investment cost per produced kWh of electricity can be achieved by using reflectors in photovoltaic systems. However, the conventional mono-crystalline silicon modules and the commercially available CIGS modules that have been tested are not optimal for these types of applications due to their sensitivity to non-uniform illumination and high temperature.

Optical measurements showed that glass mirrors, anodised aluminium, and thin film coated aluminium reflectors have good initial optical properties for solar energy applications. However, all tested reflector materials degraded noticeably (with the exception of a back surface glass mirror, which showed a very slight degradation) during outdoor and accelerated ageing. Especially some thin film-based reflectors, which were initially developed for indoor applications, are not well suited as solar reflectors. Furthermore, thin film reflectors have optical properties that are very sensitive to the angle of incidence, and this must be taken into account when thin film based reflectors are used in concentrators with parabolic geometries.

A low-angle scattering reflector consisting of a lacquered rolled aluminium foil laminated onto a flexible polymer sheet, and a rigid polymer-aluminium-steel laminate are both newly developed solar reflectors, which show potential for being cost-effective in low-concentrating photovoltaic systems. This indicates that the development of reflector materials especially aimed at the solar energy applications is paying.

Accelerated ageing tests are in principle inevitable in the development of new reflector materials, since outdoor testing takes too long time. However,

one of the conclusions from the ageing tests, which were conducted in this thesis, is that a thorough understanding of the corrosion mechanisms of the specific reflector materials that are studied is necessary in order to interpret results from accelerated ageing correctly and translate them into operating lifetimes outdoors.

When studying the optical properties and degradation of reflector materials it is essential not only to measure the total and specular reflectance, but also to assess the angular distribution of the light that is scattered from the reflector, since this influences the performance of the reflector in a solar energy system.

12.2. Systems

The photovoltaic wall element that was studied in this work should be a technically attractive alternative for building-integration at high latitudes. Calculations indicated that, annually, the 3X concentrating system for facade-integration of CIGS modules and specular parabolic reflectors will produce at least 40% more electricity per cell unit area than a vertically mounted module without reflectors. Low-angle scattering reflectors and photovoltaic modules optimised for use in low-concentrating systems would increase system efficiency further. Efficient cooling of the photovoltaic modules may be needed to keep the output voltage at a reasonably high level. A water-cooled photovoltaic-thermal hybrid system might then be an appropriate solution. Examples have shown that the technology already exists, both for facade-integration of concentrating solar energy systems and for solar cogeneration.

With a reported annual output per cell area of 250 kWh/m² electrical energy and 800 kWh/m² of heat, the photovoltaic-thermal hybrid with compound parabolic concentrators is a promising concept for cogeneration of heat and electricity [vii]. The expected low cost per delivered energy unit is a strong argument for development of concentrating photovoltaic-thermal hybrids. The investment cost for a hybrid system would be around €220 per m² glazed area or €1 per annually delivered kWh, electricity and heat included. This corresponds to €0.05 per kWh heat and €0.20 per kWh electricity, which is significantly below the cost of photovoltaic electricity today.

Using numerical data from optical measurements of the components, the optical efficiency of the concentrating photovoltaic-thermal system with compound parabolic concentrators was determined to 0.7, which is in agreement with the optical efficiency that was obtained from thermal and electrical measurements. The optical efficiency is limited by the relatively

low reflectance of the anodised aluminium reflector for wavelengths shorter than the band gap wavelength of silicon. A reflector with higher reflectance, e.g. a silvered glass mirror or a thin film interference coated aluminium mirror, would increase the optical efficiency. However, the long-term durability of thin film mirrors has not been fully demonstrated and glass mirrors are often heavy and brittle. Furthermore, due to the more even irradiance distribution on the cells, which is obtained with a lacquered rolled reflector laminate, this type of reflector might be the most cost-effective choice. An optimised broad-band anti-reflection coating on the glazing would also increase the optical efficiency. Together, an optimised anti-reflection coating and better reflectors could increase the maximum electrical power by 20%.

12.3. Modelling

Modelling of concentrating systems, including the geometry and optical properties of the reflectors, and calculation of the optical efficiency as a function of the solar height, showed to be useful tools in the design and optimisation of concentrating systems. Ray-tracing and investigation of the resulting irradiance distribution on the photovoltaic cells also provided a means to better understand the losses in the concentrating photovoltaic systems. Furthermore, measurements of the optical efficiency as a function of the south projection angle can be used in combination with angular resolved irradiation data for a specific location to calculate the annual electricity production from different types of concentrating systems. A proposed design process that was undertaken in Paper V was to model and simulate systems with different concentration ratios, module tilt, and inclination of the optical axis, in order to maximise the electrical energy annually produced in the system at a given location.

The angular dependence of concentrating solar energy systems is often complex and approximate models have to be used to calculate the annual electricity and heat production. In this work, a biaxial model for the angular dependence of the optical efficiency of asymmetric concentrators was proposed that accounts for optical losses in a cover glass more accurately than previously utilised models. Model predictions of the produced short-circuit currents were compared with measurements and a good agreement was found. In general, performing both modelling and measurements on the same type of concentrating systems made it possible to validate the models and extrapolate the results of the measurements, and it was thus mutually beneficial. Some of the reported experimental methods have to our knowledge not been published previously, such as utilising the special conditions at the equinoxes to study the angular dependence of the optical efficiency.

12.4. Suggestions for further work

Important characteristics of photovoltaic systems with parabolic reflectors are that the cell temperature is often elevated and that the image of the sun is not uniformly intense over the whole surface of the photovoltaic module. As was seen in the evaluation of the various concentrating systems, this may be critical for the electrical performance and cause high power losses, due to voltage drop and resistive losses. These negative effects may be reduced by using slightly diffusing mirrors and cells with low series resistance, as well as by cooling. In this context, the development of a low-angle scattering reflector material, optimised for low-concentrating photovoltaic applications would be interesting, as well as the development of reflector geometries for static operation that are optimised to give a more even irradiance on the photovoltaic modules at those solar altitudes at which the solar radiation, on average, is most intense, i.e. at noon in the summer. Selective solar mirrors is another interesting approach to reduce overheating of the photovoltaic cells, which is already subject to research, and this type of reflectors may be especially useful for concentrating photovoltaic systems in warm climates.

To interpret the results from accelerated ageing tests and translate those into outdoor operating lifetimes is a challenging task. It is evident that accelerated ageing tests have to be tailored for the type of reflector material that is tested. The design and evaluation of test schemes for different types of reflectors (for example divided into categories like back surface mirrors, polymer laminates, and bare metal reflectors) would be a welcome contribution to solar concentrator research.[12]

In this work, concentrating photovoltaic systems for building-integration were optimised with respect to annual electricity production per cell area. However, the glazing, insulation, and other auxiliary components of such system are not for free, although they are inexpensive in comparison to the photovoltaic modules. Therefore, the costs of the various components should also be included in system optimisation.

The use of a cover glass in front of the reflectors and cells causes high optical losses, especially at glancing incidence. If the reflectors and modules have good durability, the glazing may not be necessary. If a glazing must be used, due to a poor outdoor stability of the other components, a selective glazing that only transmits radiation at those wavelength that are useful for photovoltaic conversion would be an interesting approach. An anti-

[12] Work is in progress in this field within the International Energy Agency's Solar Heating and Cooling Programme.

reflectance coating optimised for a narrow wavelength interval would increase the transmittance for the useful wavelengths.

The work presented in this thesis concerns the optical, electrical, and thermal performance of low-concentrating photovoltaic and photovoltaic-thermal systems, aiming at improved system performance. At a higher system level, further work should be done to clarify the potential role of these systems in the local, national, and global energy systems. Such an analysis could deal with the competitiveness of the systems on various niche and mass markets, as well as the compatibility with other existing and emerging energy systems. Potential environmental effects should also be assessed. For example, life cycle analyses (including calculations of lifetime CO_2 emissions and energy payback-times) of the systems that are evaluated in this thesis should be made.

The transformation of the global energy system that is expected and needed in the near future places many demands on society and in particular on the energy sector. There is an urgent need for research in this area in order to understand the extensive connections and interdependencies between different forms of energy. Owing to the variety of energy use, new systemic approaches must be developed. The aim should be not only to master the technology, but also to acquire an understanding of how this technology is affected by regulations, decision-making processes, and different actors' interests. A socio-technical research approach is especially useful for the understanding and development of the emerging renewable energy technologies, where the relations between actors are still uncertain and technical, structural, and organisational frameworks are not yet established. Specifically, the role that energy policy, industry, universities, and individuals have for the development and widespread utilisation of solar energy technologies should be assessed.

13. Sammanfattning på svenska

Användningen av el och värme är en grundpelare i det industrialiserade samhället. Den snabbt växande världsbefolkningen och den industriella utvecklingen i utvecklingsländerna innebär en dramatiskt ökande efterfrågan på energi. Produktion av el och värme i kol-, olje- eller gaseldade kraftverk ger upphov till utsläpp av koldioxid som i sin tur bidrar till en ökad växthuseffekt, vilket på sikt kan leda till ett ändrat klimat. För att undvika klimatpåverkan är det önskvärt att minska användningen av el och värme som producerats från fossila, icke förnybara energislag. Det finns flera sätt att åstadkomma detta. Det naturligaste – och ofta det billigaste – sättet är att minska energianvändningen genom energieffektivisering. Detta behöver inte innebära en sänkning av levnadsstandarden utan kan ske med hjälp av smarta tekniska lösningar, såsom lågenergilampor och energieffektiva fönster. I vissa fall kan det dock vara mer kostnadseffektivt att ersätta el- eller värmeproduktion från icke förnybara energikällor med produktion från förnybara källor, d v s källor som inte ger några koldioxidutsläpp. Dessutom vore det önskvärt att den ökande efterfrågan på energi i utvecklingsländerna, där många människor idag inte har tillgång till el eller annan kommersiell energi överhuvudtaget, redan från början kunde tillgodoses från förnyelsebara källor så att energisystemevolutionen i dessa länder inte behövde ta omvägen via icke förnybara energislag.

Till förnybar energi räknas alla energislag som baseras på solenergi, samt geotermisk och tidvattenenergi. Till de solbaserade energislagen hör bland annat vindkraft, vattenkraft och biobränslen, samt direkt utnyttjande av solstrålningen. Utnyttjande av solenergi kan ske på olika sätt. Man brukar dela in de tekniska systemen för att omvandla solenergi till el eller värme i passiva och aktiva tekniker. Passivt utnyttjande av solenergi kan innebära att låta solen skina in genom stora söderfönster eller värma upp en mörk fasad så att behovet av tillförd värme minskar. Omvandlingen av solenergi till värme i solfångare eller el i solceller är exempel på aktiva solenergitekniker.

Denna avhandling handlar om solcellssystem, samt om kombinerade solel-solvärmesystem. I en solcell omvandlas solljus till elektrisk energi. Förutsatt att den el som används i tillverkningen av solcellen och dess kringutrustning har producerats från förnyelsebara energislag ger solcellsel inga utsläpp av

koldioxid. Idag tillverkas de flesta solceller av halvledarmaterialet kisel, som är det näst vanligaste ämnet i jordskorpan efter syre. Kontakterna som ansluts till halvledaren, där energiomvandlingen sker, består ofta av aluminium, som är det tredje vanligaste ämnet i jordskorpan. Det råder alltså ingen brist på råvaror för att tillverka solceller.

Det största hindret för storskalig elproduktion från solceller är att solcellsmodulerna, som är de större, praktiskt användbara elproduktions-enheterna, är dyra. Detta beror huvudsakligen på att tillverkningsprocessen är kostsam. Tillverkningen av solceller och moduler sker i liten skala eftersom marknaden för solceller fortfarande är liten. Det finns idag ungefär 2 MW solcellseffekt installerad i världen, vilket motsvarar två kärnkraftreaktorer av svensk standarstorlek. Ett annat problem – och en möjlighet, vilket vi skall återkomma till senare – med solcellsel är att strömmen som genereras i en solcell är, i princip, proportionell mot solstrålningen som träffar solcellen. Detta innebär att el bara kan produceras när solen skiner. För att kunna säkerställa en oavbruten tillgång på el behövs därför någon form av energilager. Om solcellsanläggningen är ansluten till elnätet kan detta användas som lager genom att man kan spara vatten i vattenkraftdammar eller bränsle i kraftverk när solcellerna producerar el. Om solcellssystemet inte är anslutet till elnätet, utan är ett så kallat fristående system, behövs energilager i form av t ex batterier eller en elektrolysör som använder solcellselen för att producera vätgas som sedan kan användas i en bränslecell.

Det faktum att strömmen från en solcell är proportionell mot ljuset som faller på cellen innebär också en möjlighet att sänka kostnaden för solcellsel, genom att öka ljusintensiteten på solcellen. Syftet med denna avhandling är att undersöka hur man kan öka utbytet från en given yta (dyr) solcell genom att använda olika typer av (billiga) speglar för att koncentrera solljus från en stor öppningsyta på solcellsytan. I de bilagda artiklarna har olika reflektorgeometrier studerats (främst paraboliska reflektorer) liksom olika typer av reflektormaterial. De paraboliska reflektorernas geometri och solcellernas placering i koncentratorerna har optimerats för att ge en så hög elproduktion per solcellsyta som möjligt.

Ett koncentrerande system kan ses som en tratt som fångar in solljuset och kanaliserar det till solcellen. Systemets koncentrationsfaktor är kvoten mellan öppningsarean och solcellsarean. Ett koncentrerande systems optiska verkningsgrad avgör hur mycket av den solstrålning som når koncentratorns öppning som slutligen hamnar på solcellsytan. Den optiska verkningsgraden beror på de optiska egenskaperna hos täckglaset och reflektorn. Reflektorer för användning i solcellssystem bör ha hög reflektans, det vill säga en god förmåga att reflektera solljuset i den del av solspektrum som kan utnyttjas i

solcellen. De fotoner, d v s energikvanta i ljuset, som har längre våglängd än den våglängd som motsvarar halvledarmaterialets bandgap kan inte utnyttjas för elproduktion, utan bidrar i stället till uppvärmning av solcellen. En hög celltemperatur gör att cellspänningen sjunker och därmed minskar solcellens elektriska effekt. Om det är vindstilla och starkt solsken kan uppvärmning av en solcell ske även då den inte omges av reflektorer, men med reflektorer kan celltemperaturen bli så hög att den dramatiskt reducerar cellens verkningsgrad, och den positiva effekten av koncentratorn uteblir. Ett sätt att minimera detta problem är att kyla solcellen. Kylning kan ske passivt, med hjälp av kylflänsar, men ett mer elegant sätt är att använda ett kylmedium som cirkuleras i ett slutet system på baksidan av solcellerna. På detta sätt kan den termiska energin tillvaratas och användas för uppvärmning eller för att förvärma tappvarmvatten. I ett par av de bilagda artiklarna har el- och värmeproduktionen i kombinerade solel-solvärmesystem med koncentratorer av anodiserat aluminium studerats och olika faktorers inverkan på den optiska verkningsgraden och energiutbytet har kvantifierats. I en av artiklarna utvärderades ett vattenkylt solcellssystem med paraboliska reflektorer som koncentrerar ljuset fyra gånger (se bilden) och det årliga el- och värmeutbytet beräknades från mätdata. Beräkningarna visade att systemet skulle producera 800 kWh värme med en temperatur av +50°C, samt 250 kWh el per kvadratmeter solcellsyta och år. Det beräknade elektriska utbytet är 2,5 gånger det maximala utbytet från en solcell utan koncentratorer. De ingående komponenterna (solceller, täckglas och reflektorer) har även undersöks separat, med avseende på deras optiska egenskaper, d v s deras förmåga att absorbera, transmittera och reflektera solljus. Beräkningar visade att en reflektor med högre solreflektans och ett täckglas med optimerad anti-reflexbehandling skulle kunna öka det årliga utbytet med 20 %.

Ett “solkraftvärmeverk” med vattenkylda kiselsolceller, paraboliska reflektorer och täckglas, som ger både el och värme. Systemet finns hos Vattenfall Utveckling AB i Älvkarleby. Professor Björn Karlsson syns i bakgrunden. Foto: Maria Brogren.

I detta arbete undersöktes de optiska egenskaperna hos glas och solceller, och framförallt hos olika typer av reflektormaterial, medelst spektrofotometri, vinkelupplösta ljusspridningsmätningar, teoretisk modellering av tunna skikt, ljusmikroskopi och ytprofilmätningar. Då uppmätta reflektanskurvor viktas med solspektrum fås den totala solreflektansen. Reflektormaterialets solreflektans påverkar i hög grad det koncentrerande systemets optiska verkningsgrad. De reflektormaterial som studerats i avhandlingen är:

- silverspeglar, där det reflekterande skiktet belagts på baksidan av ett planglas
- reflektorer av aluminiumplåt med olika tjocka skikt av aluminiumoxid
- reflektorer av metall med olika skyddsskikt, såsom plastfilmer och lack
- reflektorer av metall med tunna skikt av olika oxider, som utnyttjar interferens för att ge en högre reflektans än metallen i sig
- reflektorlaminat, där det reflekterande skiktet laminerats mellan ett substrat, som utgör det bärande materialet, och ett skyddsskikt

Speglande paraboliska reflektorer ger en inhomogen ljusbild på solcellerna. Den ojämna belysningen leder till lokalt höga temperaturer och strömmar där belysningen är störst. Detta minskar solcellsmodulens verkningsgrad och leder därför till effektförluster. Ett sätt att reducera effekterna av ojämn belysning är, vilket berörts ovan, genom effektiv kylning av solcellerna. Ett annat sätt är att använda svagt diffuserande reflektorer, t ex av valsad aluminiumfolie som laminerats på ett flexibelt plastsubstrat, som ger en jämnare ljusbild på solcellerna. I avhandlingen har effekten av den ojämna belysningen på solceller i lågkoncentrerande system med paraboliska reflektorer studerats och utbytet från system med reflektorer med olika andel diffus reflektans har jämförts. Det visade sig att verkningsgraden är avsevärt högre för ett system med diffuserande reflektorer, särskilt vid hög instrålning, och att den jämnare ljusbilden kan kompensera för en lägre total reflektans hos reflektormaterialet.

Byggnadsintegrering av solcellsmoduler är ett annat sätt att minska kostnaderna för solel genom att man kan undvika kostnader för byggnadsmaterial (t ex fasadbeklädnad) och stativ för solcellerna. Olika typer av koncentrerande solcellssystem avsedda för byggnadsintegrering studerades i avhandlingen. Systemen bestod av solcellsmoduler, paraboliska överkantsreflektorer och isolering. Tanken med isoleringen var att systemen skulle utgöra kompletta byggnadselement som snabbt kunde byggas ihop till en vägg och enkelt anslutas till elnätet. Det årliga utbytet från systemen beräknades med hjälp av uppmätta producerade strömmar för olika solhöjder, vilket gav den optiska verkningsgraden som funktion av solhöjden.

Mätningarna gjordes både utomhus och i en stor solsimulator inomhus. Beräkningarna visade att om ett solcellssystem med paraboliska överkants-reflektorer som koncentrerar solljuset tre gånger monterades i rakt söderläge på en fasad i Stockholm skulle det årligen ge 40 % mer el än en likadan modul utan reflektor. En kvadratmeterstor solcellsmodul kostar ca 5 000 kr. Förutsatt att det extra material som behövs (aluminiumplåt och frigolit som utgör formen och isolering) kostar mindre än 2 000 kr per kvadratmeter använd solcellsyta, inklusive eventuella extra arbetskostnader, är det koncentrerande väggelementet alltså kostnadseffektivt.

Livslängden för en solcellsmodul är över 20 år. För att man skall slippa byta ut reflektorerna i förtid måste dessas livslängd vara minst lika lång. I detta arbete studerades åldring av reflektormaterial och förändringen av de optiska egenskaperna mättes både efter exponering utomhus och efter det att reflektormaterialen åldrats i en klimatkammare som accelererar åldrings-processen. I klimatkammaren varierades temperaturen mellan +40°C och +85°C och luftfuktigheten mellan 50 % och 85 %. Variationerna skedde i femtimmarscykler för att simulera dygnsvariationer och en stark sollampa var tänd under halva ”dygnet”. Testcykeln upprepades 400 gånger i följd. Efter 100, 200 och 400 cykler togs proverna ut och deras totala och speglande reflektans mättes. Reflektormaterialens ytprofiler uppmättes också och ytan studerades i mikroskop. De accelererade testerna jämfördes med resultat från 9–12,5 månaders utomhusåldring. Det visade sig att olika typer av reflektorer klarade de olika testerna olika bra. Vissa av de laminerade reflektorerna klarade inte de höga temperaturerna i klimatkammaren, medan aluminiumreflektorer utan skyddande lack blev diffusa efter utomhusåldring. Reflektorer i vilka den initialt höga solreflektansen baserades på interferens i tunna skikt försämrades markant vid utomhusåldring. En slutsats av resultaten från åldringstesten är att det är svårt att förutsäga reflektormaterialens livslängd utomhus på grundval av resultat från accelererad åldring och att man måste utforma accelererade tester utifrån den typ av material som skall testas.

Sammanfattningsvis kan konstateras att paraboliska reflektorer kan öka det årliga utbytet från solceller avsevärt. I kombinerade solel-solvärmesystem med koncentratorer fås dessutom termisk energi som kan användas för t ex uppvärmningsändamål. Ett reflektormaterial med hög solreflektans, som bör tåla åldring utomhus, är viktigt för systemets optiska verkningsgrad. Billiga, delvis diffusa, reflektorlaminat befanns öka elutbytet jämfört med helt speglande reflektorer och byggnadsintegrering av system med paraboliska reflektorer av sådant material är ett intressant alternativ för att ge billigare solel. Åldringstest av reflektorer visade sig dock vara en komplex fråga, till vilken det finns anledning att återkomma för att säkra kvaliteten hos koncentrerande solcellssystem.

References

[1] Ingelstam, L. *Implementing solar – Reflexions on how to conquer the system* in *ISES 2003*. Göteborg, Sweden, 2003.

[2] Goldemberg, J., ed. *World Energy Assessment*. Energy and the challenge of sustainability. United Nations Development Programme, 2000.

[3] Johansson, T.B. and J. Goldemberg, eds. *Energy for sustainable development: a policy agenda*, United Nations Development Programme, 2002.

[4] *Key world energy statistics 2003*, International Energy Agency, 2003.

[5] *World Energy Outlook*, International Energy Agency, 2002.

[6] Mahlman, J.D., *Mathematical Modeling of Greenhouse Warming*, in *Energy and the environment*, B. Abeles, A.J. Jacobson, and P. Sheng, Editors. World Scientific Publishing Co. Pte. Ltd.: Singapore, 1992.

[7] Intergovernmental Panel on Climate Change *(http://www.ipcc.ch)*, 2001.

[8] Sims, R.E.H., *Renewable energy: a response to climate change.* Solar Energy, 2004. **76**: p. 9-17.

[9] Azar, C. and H. Rodhe, *Targets for Stabilization of Atmospheric CO_2.* Science, 1997. **276**: p. 1818-1819.

[10] Eliasson, B., *Working Together on Global Climate Problems.* IEEE Power Engineering Review, 2001(March): p. 4, 5, 15.

[11] Notari, P., *Progress in Solar Energy Technologies and Applications*, The American Solar Energy Society, 1994.

[12] Lawand, T.A., *The Potential of Renewable Energy*, in *Solar Energy Conversion*, A.E. Dixon and J.D. Leslie, Editors. University of Waterloo, Pergamon Press: Ontario, Canada, 1978.

[13] *News release No 100/2002 23 August 2002*, Eurostat, 2002.

[14] *BP Statistical Review of World Energy (http://bp.com/bpstats)*, 1998.

[15] *Stand-alone PV power systems (off-grid) (http://www.iea-pvps.org)* International Energy Agency Photovoltaic Power Systems Programme, 2002.

[16] Adams, W.G. and R.E. Day. *The action of light on selenium* in *Royal Society*. London, 1877.

[17] Chapin, D.M., C.S. Fuller, and G.L. Pearson, *A New Silicon p-n Junction Photocell for Converting Solar Radiation into Electrical Power. J. Appl. Phys*, 1954. **25**: p. 676.

[18] *Nuclear reactor*, (*http://en.wikipedia.org/wiki/Nuclear_reactor#History),* Wikipedia, the free encyclopedia, 2003.

[19] Sayigh, A.A.M., *Photovoltaic and solar radiation*, in *Generating electricity from the sun*, F.C. Treble, Editor. BPCC Wheatons Ltd: Exeter, 1991.

[20] *International Statistics (http://www.iea-pvps.org),* International Energy Agency Photovoltaic Power Systems Programme, 2002.

[21] Rever, B., *Grid-tied market for photovoltaics – a new source emerges.* Renewable energy world, 2001. **4**(4): p. 176-189.

[22] *Trends in photovoltaic applications in selected IEA countries between 1992 and 2002 (http://www.iea-pvps.org)*, International Energy Agency Photovoltaic Power Systems Programme, 2003.

[23] Winter, C.-J., *High-temperature solar energy utilization after 15 years R&D: kick-off for the third generation of technologies.* Solar Energy Materials, 1991. **24**: p. 26-39.

[24] Tanaka, T., *Solar thermal power generation systems on commercial basis in USA (abstract).* Journal of the Electrical Engineers of Japan, 1992. **112**(3): p. 176-182.

[25] Hubbard, H.M., *The Real Cost of Energy.* Scientific American, 1991. **264**(4): p. 18-23.

[26] Reddy, A.K.N., *Energy and Social Issues*, in *Energy and the Challenge of Sustainability*, J. Goldemberg, Editor. United Nations Development Programme: New York, 2000.

[27] Solar Electric Light Fund *(http://www.self.org),* 2002.

[28] *Deployment issues (http://www.iea-pvps.org)*, International Energy Agency Photovoltaic Power Systems Programme, 2002.

[29] Bates, J.R. and A.R. Wilshaw. *Survey of Stand-alone Photovoltaic Programmes and Applications in Developing Countries* in *16th European Photovoltaic Solar Energy Conference, 1-5 May*. 2000. Glasgow, United Kingdom.

[30] Welford, W.T. and R. Winston, *High collection non-imaging optics*. San Diego: Academic Press, 1989.

[31] Halliday, D. and R. Resnick, *Fundamentals of Physics*. 3 ed. New York, USA: John Wiley & Sons, Inc., 1988.

[32] Granqvist, C.G., *Solar Energy Materials.* Advanced Materials, 2003. **15**(21): p. 1789-1803.

[33] Duffie, J.A. and W.A. Beckman, *Solar Engineering of Thermal Processes*. 1 ed. New York: John Wiley & Sons, Inc., 1980.

[34] Stover, J.C., *Introduction to Light Scatter*, in *Optical Scattering*, J.C. Stover, Editor. SPIE Optical Engineering Press: Bellingham, 1995.

[35] Perers, B., *The solar resource in cold climates*, in *Photovoltaics in cold climates*, M. Ross and J. Royer, Editors. James & James Ltd, 1999.

[36] *ISO 9845-1 Solar energy – Reference solar spectral irradiance at the ground at different receiving conditions. Part 1: Direct normal and hemispherical solar irradiance for air mass 1.5*, 1992.

[37] Sayigh, A.A.M., *Characteristics of Solar Radiation*, in *Solar Energy Conversion*, A.E. Dixon and J.D. Leslie, Editors. University of Waterloo, Pergamon Press: Ontario, Canada, 1978.

[38] Granqvist, C.G. and V. Wittwer, *Materials for solar energy conversion.* Solar Energy Materials and Solar Cells, 1998. **54**: p. 39-48.

[39] Sayigh, A.A.M., *Basics of Solar Energy*, in *Solar Energy Conversion*, A.E. Dixon and J.D. Leslie, Editors. University of Waterloo, Pergamon Press: Ontario, Canada, 1978.

[40] Duffie, J.A. and W.A. Beckman, *Solar Engineering of Thermal Processes*. 2 ed., New York: John Wiley & Sons, Inc., 1991.

[41] Meinel, A. and M. Meinel, *Applied Solar Energy – an Introduction*, Philippines: Addison-Wesley Publishing Company, Inc., 1976.

[42] Rönnelid, M. and B. Karlsson, *Irradiation distribution diagrams and their use for estimating collectable energy.* Solar Energy, 1997. **61**(3): p. 191-201.

[43] *Meteonorm 5.0 Global Meteorological Database for Solar Energy and Applied Meteorology*, Meteotest, 2003.

[44] Rönnelid, M., *Optical Design of Stationary Solar Concentrators for High Latitudes*, Doctoral Thesis from the Faculty of Science and Technology at Uppsala University, Uppsala, 1998.

[45] Karlsson, B., B. Perers, and U. Henfridsson. *Östhammar Hospital- Hot Water Production from a minor Solar Collector Field with Reflectors* in *ISES 1995 in search of the sun*. Harare, Zimbabwe, 1995.

[46] Rönnelid, M. and B. Karlsson, *The use of corrugated booster reflectors for solar collector fields.* Solar Energy, 1999. **65**(6): p. 343-351.

[47] Karlsson, B. and G. Wilson. *MaReCo – A Large Assymetric CPC for High Latitudes* in *ISES 1999 Solar World Congress*, Jerusalem, 1999.

[48] Karlsson, B. and G. Wilson. *MaReCo design for horizontal, vertical or tilted installation* in *EuroSun 2000*. Copenhagen, Denmark, 2000.

[49] Karlsson, B., S. Larsson, G. Wilson, and A. Andersson. *MaReCo for large systems* in *Eurosun 2000*. Copenhagen, Denmark, 2000.

[50] Kittel, C., *Introduction to Solid State Physics*. 5 ed. New York: John Wiley & Sons, Inc., 1976.

[51] Ashcroft, N.W. and N.D. Mermin, *Solid State Physics*. New York: Holt, Rinehart & Winston, 1976.

[52] Nordling, C. and J. Österman, *Physics handbook*. 4 ed. Lund: Studentlitteratur, 1987.

[53] Dixon, A.E., *Review of Solid State Physics*, in *Solar Energy Conversion*, A.E. Dixon and J.D. Leslie, Editors. University of Waterloo, Pergamon Press: Ontario, Canada, 1978.

[54] Green, M.A., *Solar Cells – Operating Principles, Technology and System Applications*. University of New South Wales, Australia, 1992.

[55] Fahrenbruch, A.L. and R.H. Bube, *Fundamentals of Solar Cells*. New York: Academic Press, Inc, 1983.

[56] Beeforth, T.H. and H.J. Goldsmid, *Physics of solid state devices*, London, UK: Pion Limited, 1970.

[57] Green, M.A., *Silicon Solar cells – Advanced Principles & Practice*. 1 ed., Centre for Photovoltaic Devices and Systems, University of New South Wales, Sydney, 1995.

[58] Green, M.A., *Photovoltaics: technology overview.* Energy Policy, 2000. **28**(14): p. 989-998.

[59] Wenham, S.R., M.A. Green, and M.E. Watt, *Applied Photovoltaics*. 1 ed. Sidney: Centre for Photovoltaic Devices and Systems, University of New South Wales, 1994.

[60] Green, M.A., *Crystalline and thin-film silicon cells: state of the art and future potential.* Solar Energy, 2003. **74**: p. 181-192.

[61] Goetzberger, A., C. Hebling, and H.-W. Schock, *Photovoltaics materials, history, status and outlook.* Materials Science and Engineering, 2003. **R**(40): p. 1-46.

[62] Sigurd, D., *Solceller för energiproduktion*, in *Energiomvandling – Kosmos 1982*, U. Litzén, Editor. 1982, Svenska Fysikersamfundet: Stockholm, Sweden. p. 127-146.

[63] Green, M.A., *Recent developments in photovoltaics.* Solar Energy, 2003. **76**(1-3): p. 3-8.

[64] Green, M.A., *Photovoltaics principles.* Physica E, 2002. **14**: p. 11-17.

[65] Rönnelid, M., B. Perers, B. Karlsson, and P. Krohn. *Cooling of PV modules with low-concentrating CPC reflectors* in *ISES Solar World Congress*. Jerusalem, 1999.

[66] Bakker, M., K.J. Strootman, and M.J.M. Jong. *PVT panels: fully renewable and competitive* in *PV for Europe*. Rome, Italy, 2002.

[67] Coventry, J.S., K. Lovegrove, *Development of an appraoch to compare the 'value' of electrical and thermal output from a domestic PV/Thermal concentrator system*. Solar Energy, 2003. **75**(1): p.63-75.

[68] Prakash, *Transient analysis of a photovoltaic-thermal solar collector for co-generation of electricity and hot air/water.* Energy Conversion and Management, 1994. **35**(11): p. 967-972.

[69] Kern, E.C.J. and M.C. Russel. *Combined photovoltaic and thermal hybrid collector systems* in *13th IEEE Photovoltaics Specialists*. Washington DC, USA, 1978.

[70] Hendrie, S.D. *Evaluation of combined photovoltaic/thermal collectors* in *ISES Int. Congress*. Atlanta, USA, 1979.

[71] Florschuetz, L.W., *Extension of the Hottel-Whillier model to the analysis of combined photovoltaic/thermal flat plate collectors.* Solar Energy, 1979. **22**: p. 361-366.

[72] Raghuraman, P., *Analytical predictions of liquid and air photovoltaic/thermal flat plate collector performance.* Journal of Solar Energy Engineering, 1981. **103**: p. 291-298.

[73] Rahman, S., M.A. Khallat, and B.H. Chowdhury, *A discussion on the diversity in the applications of photovoltaic systems.* IEEE-Transactions-on-Energy-Conversion. vol.3, no.4; Dec. 1988;, 1988: p. 738-46.

[74] Tripanagnostopoulos, Y., T. Nousia, M. Souliotis, and P. Yianoulis, *Hybrid photovoltaic/thermal solar systems.* Solar Energy, 2002. **72**(3): p. 217-234.

[75] Böer, K.W. and G. Tamm, *Solar conversion under consideration of energy and entropy.* Solar Energy, 2003. **74**: p. 525-528.

[76] Bhargava, A.K., H.P. Garg, and R.K. Agarwal, *Study of a hybrid solar system - solar air heater combined with solar cells.* Energy Convers. Mgmt., 1991. **31**: p. 471-479.

[77] Bazilian, M.D., F. Leenders, and B.G.C. Van der Ree, *Photovoltaic cogeneration in the built environment.* Solar Energy, 2001. **71**(1): p. 57-69.

[78] Bazilian, M.D., H. Kamalanathan, and D.K. Prasad. *Thermographic analysis of a building integrated photovoltaic system.* Renewable Energy, 2002. **26**(3): p. 449-461.

[79] Bazilian, M.D. and D. Prasad, *Modelling of a photovoltaic heat recovery system and its role in a design decision support tool for building professionals.* Renewable Energy, 2002. **27**(1): p. 57-68.

[80] Elazari, A. *Building Integrated Multi pv/t/a Solar System* in *EuroSun*. Copenhagen, Denmark, 2000.

[81] Rabl, A., *Comparison of Solar Concentrators.* Solar Energy, 1976. **18**: p. 93-111.

[82] Rönnelid, M., B. Karlsson, P. Krohn, and J. Wennerberg, *Booster Reflectors for PV Modules in Sweden.* Progress in Photovoltaics: Research and Applications, 2000. **8**: p. 279-291.

[83] Luque, A., *Static concentrators: a venture to meet the low cost target in photovoltaics.* Solar cells, 1984. **12**: p. 141-145.

[84] Meinel, A.B., *Concentrating Collectors*, in *Solar Energy Engineering*, A.A.M. Sayigh, Editor. Academic Press: New york. p. 183-216, 1977.

[85] Benítez, P., R. Mohedano, and J.C. Miñano. *DSMTS: A novel linear PV concentrator* in *26th PVSC*. Anaheim, California, USA: IEEE, 1997.

[86] Spante, L., M. Andersson, B. Perers, P. Krohn, A. Helgesson, B. Karlsson, C. Setterwall *et al.*, *SOLEL 97–99 – Ett Branschgemensamt FoU-program Årsrapport 1997 (in Swedish),* Elforsk AB, 1998.

[87] Perers, B., B. Karlsson, and M. Bergkvist, *Intensity distribution in the collector plane from stuctured booster reflectors with rolling grooves and corrugations.* Solar Energy, 1994. **53**(2): p. 215-226.

[88] Hinterberger, H. and R. Winston, *Efficient Light Coupler for Threshold Cerenkov Counters.* Review of Scientific Instruments, 1966. **37**: p. 1094-5.

[89] Baranov, V.K. and G.K. Melnikov, Soviet Journal of Optical Technology, 1966. **33**: p. 408.

[90] Ploke, M., *Lichtführungseinrichtungen mit starker Konzentrationswirkung.* Optik, 1967. **25**.

[91] Rabl, A., *Optical and Thermal Properties of Compound Parabolic Concentrators.* Solar Energy, 1976. **18**: p. 497.

[92] McIntire, W.R., *Truncation of nonimaging cusp concentrators.* Solar Energy, 1979. **23**: p. 351-355.

[93] Luque, A., G. Sala, and J.C. Arboiro, *Electric and thermal model for non-uniformly illuminated concentration cells.* Solar Energy materials & Solar Cells, 1998. **51**: p. 269-290.

[94] Karlsson, B., P. Krohn, B. Perers, and M. Rönnelid, *Solar Cells with Reflectors – Resultat 1997 (in Swedish)*, Vattenfall Utveckling AB: Älvkarleby, Sweden, 1997.

[95] Winston. *Development of the compound parabolic collector for photo-thermal and photo-voltaic applications* in *Society of Photo-Optical Instrumentation Engineers*. 1975.

[96] Carvalho, M.J., M. Collares-Pereira, J.M. Gordon, and A. Rabl, *Truncation of CPC Solar Collectors and its Effect on Energy Collection.* Solar Energy, 1985. **35**(5): p. 393-399.

[97] Rönnelid, M., B. Perers, P. Krohn, L. Spante, and B. Karlsson. *Experimental Performance of a String Module in a CPC Reflector Cavity* in *2nd (European) WCPEC, European Commission*. Vienna, 1998.

[98] Baum, H.P., M.E. Blanco, E. Gomez-Leal, and J.M. Gordon, *Optimal configurations of asymmetric CPC solar collectors with planar receivers.* Solar Energy, 1986. **36**(2): p. 187-189.

[99] Mills, D.R. and J.E. Giutronich, *Asymmetrical non-imaging cylindrical solar concentrators.* Solar Energy, 1978. **20**: p. 45-55.

[100] Rönnelid, M., B. Karlsson, and J.M. Gordon. *The Impact of High Latitudes on the Optical Design of Solar Systems* in *EuroSun '96*. Freiburg, 1996.

[101] Souka, A.F. and H.H. Safwat, *Optimum orientations for the double exposure flat-plate collector and its reflectors.* Solar Energy, 1966. **10**: p. 170-174.

[102] McIntire, W.R., *Factored approximations for biaxial incident angle modifiers.* Solar Energy, 1982. **29**(4): p. 315-322.

[103] Whitfield, G.R., R.W. Bentley, and J.D. Burton, *Increasing the cost-effectiveness of small solar photovoltaic pumping systems.* Renewable Energy, 1995. **6**(5-6): p. 469-475.

[104] Swanson, R.M., *The Promise of Concentrators.* Progress in Photovoltaics: Research and Applications, 2000. **8**(Millennium Special Issue): p. 93-111.

[105] Drude, P., *Lehrbuch der Optik*. Leipzig: Verlag von S. Hirzel, 1900.

[106] Mwamburi, M., E. Wäckelgård, and A. Roos, *Preparation of solar selective SnOx:F coated aluminium reflector surfaces.* Thin Solid Films, 2000. **374**: p. 1-9.

[107] Mwamburi, M., B. Karlsson, and R.T. Kivaisi. *Transparent Conductor Coated Aluminium Reflectors for PV Applications* in *North Sun 97*. Helsingfors, Finland, 1997.

[108] Nostell, P., A. Roos, and B. Karlsson, *Ageing of solar booster reflector materials.* Solar Energy Materials & Solar Cells, 1998. **54**: p. 235-246.

[109] Koehl, M., *Durability of solar energy materials.* Renewable energy, 2001. **24**: p. 597-607.

[110] Shaner, W.W. and H.S. Wilson, *Cost of paraboloidal collectors for solar to thermal electric conversion.* Solar Energy, 1975. **17**: p. 351-358.

[111] Duffie, J.A., *New materials in solar energy utilization.* Solar Energy, 1962. **6**(3): p. 114-118.

[112] Morris, V.L., *Cleaning agents and techniques for concentrating solar collectors.* Solar Energy Materials, 1980. **3**: p. 35-55.

[113] Wedepohl, K.H., *The composition of the continental crust.* Geochemica and Cosmochimica, 1995. **59**(7): p. 1217-1232.

[114] Fend, T., G. Jorgensen, and H. Kuster, *Applicability of highly reflective aluminium coil for solar concentrators.* Solar Energy, 2000. **68**(4): p. 361-370.

[115] Bouquet, F.L., R.G. Helms, and C.R. Maag, *Recent advances in long-lived mirrors for terrestrial and space applications.* Solar Energy Materials, 1987. **16**: p. 423-433.

[116] Brace, A.W. and P.G. Sheeasby, *The technology of anodizing aluminium*. 2 ed. Gloucestershire, England: Technicopy Ltd, 1979.

[117] Czanderna, A.W., *Stability of interfaces in solar energy materials.* Solar Energy Materials, 1981. **5**: p. 349-377.

[118] Schissel, P., G. Jorgensen, C. Kennedy, and R. Goggin, *Silvered-PMMA reflectors.* Solar Energy Materials and Solar Cells, 1994. **33**: p. 183-197.

[119] Roos, A., C.G. Ribbing, and B. Karlsson, *Stainless steel solar mirrors – A material feasibility study.* Solar Energy Materials, 1989. **18**: p. 233-240.

[120] Öhman, R., *Reflektormaterial från flexibla laminat – mot kostnadseffektiva reflektormaterial (in Swedish)*, Skultuna Flexible AB, Skultuna, 2000.

[121] *E 892, Standard Tables for Terrestrial Direct Normal Solar Spectral Irradiance for Air Mass 1.5: Table 1.* ASTM, 1992.

[122] Roos, A., *Use of an integrating sphere in solar energy research.* Solar Energy Materials & Solar Cells, 1993. **30**(1): p. 77-94.

[123] Nostell, P., A. Roos, and D. Rönnow, *Single-beam integrating sphere spectrophotometer for reflectance and transmittance measurements versus angle of incidence in the solar wavelength range on diffuse and specular samples.* Review of scientific instruments, 1999. **70**(5): p. 2481-2494.

[124] Rönnow, D., *Elastic Light Scattering by Thin Films*, Doctoral Thesis from the Faculty of Science and Technology at Uppsala University, Uppsala, 1996.

[125] Rönnelid, M., M. Adsten, T. Lindström, P. Nostell, and E. Wäckelgård, *Optical scattering from rough-rolled aluminum surfaces.* Applied Optics, 2001. **40**.

[126] Håkansson, H. and B. Fredlund. *A new solar simulation facility for calorimetric measurements on windows and shading devices* in *5th Symposium on Building Physics in the Nordic Countries*. Gothenburg, 1999.

[127] Chant, V.G. and R. Håkansson, *The MINSUN simulation and optimisation program. Application and users guide*, International Energy Agency, Solar Heating and Cooling Programme, Task VII: Ottawa, 1985.

[128] Adsten, M., *Solar Termal Collectors at High Latitudes – Design and Performance of Non-Tracking Concentrators*, Doctoral Thesis from the Faculty of Science and Technology at Uppsala University, Uppsala, 2002.

[129] Perers, B., *Dynamic method for solar collector array testing and evaluation with standard database and simulation programs.* Solar Energy, 1993. **50**(6): p. 517-526.

[130] Bühler, C., *Nichtabbildende Optik für Diffuslichtnutzung und Sonnenschutz*, in *Fakultät für Physik*. Albert-Ludwigs-Universität: Freiburg, 1999.

[131] Thomsen, S.M., *Low-reflection films produced on glass in a liquid fluosilcic acid bath.* RCA Review, 1951: p. 143-149.

[132] Chinyama, G.K., A. Roos, and B. Karlsson, *Stability of antireflection coatings for large area glazing.* Solar Energy, 1993. **50**(2): p. 105-.

[133] Nostell, P., *Preparation and optical characterisation of antireflection coatings and reflector materials for solar energy systems*, Doctoral Thesis from the Faculty of Science and Technology at Uppsala University, Uppsala, 2000.

[134] Nostell, P., A. Roos, and B. Karlsson, *Optical and mechanical properties of sol-gel antireflective films for solar energy applications.* Thin Solid Films, 1999. **351**.

[135] Roos, A. and D. Rönnow, *Diffuse Reflectance and Transmittance Spectra of an Interference Layer: 1. Model Formulation and Properties.* Applied Optics, 1994. **33**: p. 7908-7917.

[136] Hellström, B., M. Adsten, P. Nostell, E. Wäckelgård, and B. Karlsson. *The impact of optical and thermal properties on the performance of flat plate solar collectors* in *EuroSun 2000*. Copenhagen, Denmark, 2000.

[137] Tabor, *Comment – The CPC concept.* Solar Energy, 1984. **33**(6): p. 629-630.

[138] Whitfield, G.R., R.W. Bentley, and A.G. Atkins. *Optimising the optical component size of PV concentrators* in *PV for Europe*. Rome, Italy, 2002.

Acta Universitatis Upsaliensis

Comprehensive Summaries of Uppsala Dissertations from the Faculty of Science and Technology

Editor: The Dean of the Faculty of Science and Technology

A doctoral dissertation from the Faculty of Science and Technology, Uppsala University, is usually a summary of a number of papers. A few copies of the complete dissertation are kept at major Swedish research libraries, while the summary alone is distributed internationally through the series *Comprehensive Summaries of Uppsala Dissertations from the Faculty of Science and Technology*. (Prior to October, 1993, the series was published under the title "Comprehensive Summaries of Uppsala Dissertations from the Faculty of Science".)

Distribution:
Uppsala University Library
Box 510, SE-751 20 Uppsala, Sweden
www.uu.se, acta@ub.uu.se

ISSN 1104-232X
ISBN 91-554-5867-X